Masterarbeit

Titel der Masterarbeit

Landscape evolution north of the Sonnblick (Salzburg) during the Alpine Lateglacial

verfasst von
Mathias Bichler B.Sc.

gemeinsam mit
Martin Reindl B.Sc.

angestrebter akademischer Grad
Master of Science (M.Sc.)

Wien, 2013

Studienkennzahl lt. Studienblatt:	A 066 815
Studienrichtung lt. Studienblatt:	Masterstudium Erdwissenschaften
Betreut von:	Hermann Häusler, Ao. Univ. Prof. Dr.

Contents

1. Preface [Reindl]

The *Hoher Sonnblick* or *Rauriser Sonnblick* in the Hohe Tauern alpine range in the Austrian province of Salzburg has a long history of scientific research. The summit area houses the highest meteorological Observatory in Austria (3106m asl), operated by the Zentralanstalt für Meteorologie und Geodynamik (ZAMG). This observatory was opened in 1886 and since then has an uninterrupted record of climatic data in an alpine environment. Every year 40 to 50 projects work on or around the alpine area of the Sonnblick and the glacier which plays such a big role in the valley head of the Hüttwinkl valley, the Goldbergkees. These projects center on the topics of environmental research like atmospherics chemistry, atmospheric physics, precipitation chemistry, avalanche research, climate research, and glacial research, but rarely geomorphology and Quaternary studies.

In 2010, Ao. Univ. Prof. Dr. Hermann Häusler from the University of Vienna and Dr. Wolfgang Schöner of the ZAMG planned to research and date the diverse landforms (moraine ridges and landslides) in the area of Kolm-Saigurn, the head of the Hüttwinkl valley. With this spirit in mind, a field trip from the University of Vienna, under the supervision of Ao. Univ. Prof. Dr. Hermann Häusler and Dr. Jürgen Reitner of the Geological Survey of Austria (*Geologische Bundesanstalt* - GBA) was undertaken to explore the unique geomorphologic features. It was during this field trip, where the idea was born to investigate the full chronology of events during the Lateglacial ice decay. The GBA showed great interest in mapping the area part of the recently mapped *Blatt 154, Rauris*, being part of the Austrian geological map. This initial idea was then formulated and transformed into a project, where this document marks the final report. The goal was to clarify the time-stratigraphic position of the multiple identified glacial-deposits (moraines, boulders).

During the beginning stages of this project it became clear that not only the sediment evidence from earlier glaciers played a vital role in the history of this specific valley head, but also numerous landslides left their traces. As the field work revealed temporal unique relationships of cross-cutting landscape elements, a solid relative chronology of the processes was given. It was worth trying to establish an absolute chronology for all major events with the help of ^{10}Be exposure dating from boulders and bedrock and with the help of ^{14}C dating of base-layers from peat-bogs.

This document now represents the synthesis of our work, where we try to shed some light on the surface dynamics and document the special geomorphologic and Quaternary features and settings that make up the area north of the Hoher Sonnblick in the head of the Hüttwinkl valley.

Our decision to write one master thesis was based on numerous reasons. While the initial extent of the area might have justified a single thesis, the amount of work involved with sampling and preparation, especially the ^{10}Be method, was just too much to guarantee a successful outcome. During the course of our work it became apparent that the synergy when working as a team on these samples was very high. In addition, the relationship of the features high up on the mountain in the forefront of the glaciers as well as the landslides in the lower parts of the valley are inextricably connected with each other. It were these facts that lead to our (Mathias Bichler and Martin Reindl) decision to produce chapters individually and merge them in one common document.

2. The Study Area [Reindl/Bichler]

2.1. Overview [Reindl]

The Rauristal is a northward trending tributary valley of the Salzach valley in the Goldberg Mountains in the Austrian province of Salzburg, centered at 47°14′ N and 13°0′ E, about 60 km southwest of the city of Salzburg (Figure 2.1). To the south, the Rauristal splits in to the southwest trending Seidlwinkl valley and the south trending Hüttwinkl valley. The valleyhead of the Hüttwinkl valley with the basin of Kolm-Saigurn marks the primary research area of this study with the Goldbergkees (Hoher Sonnblick) and Pilatuskees (Hocharn) glaciers (Figure 2.2). During most of the recent summers, the annual ELA (Equilibrium Line Altitude) was higher than the highest points of the Goldbergkees and Pilatuskees, which is at 3254 m on the summit of the Hocharn, which is rather typical for similar oriented glaciers in the surrounding area.

Mining of gold and other valuable minerals has a long history in the valley, starting in the 14th century and peaking in the 15th and 16th century. During the 19th century, Ignaz Rojacher revived the gold mining activities. In 1886, under difficult conditions, he constructed the world-wide first, and by that time, highest meteorological observatory on the summit of the Hoher Sonnblick and laid the foundation for extensive and diverse research in this area. Nobel Prize recipient Viktor Franz Hess was studying the effects of cosmic rays in the observatory for short periods of time (Federmann, 2003), laying the foundation for methods we today know as dating with terrestrial in-situ cosmogenic nuclides, like ^{10}Be.

Presently, the westerlies are an important source of moisture and precipitation for the Alps, especially in the northern regions. Low-pressure systems in the Mediterranean are important for prolonged spells of cold and wet conditions, particularly along the southern fringe of the Alps. Annual precipitation along the northern and southern fringes are rather similar. Air temperatures are presently rather mild and usually similar to those from sites outside of the Alps at similar altitudes. Summer temperatures at the ELA of the Alpine glaciers are usually positive, and therefore most of the Alpine glaciers are

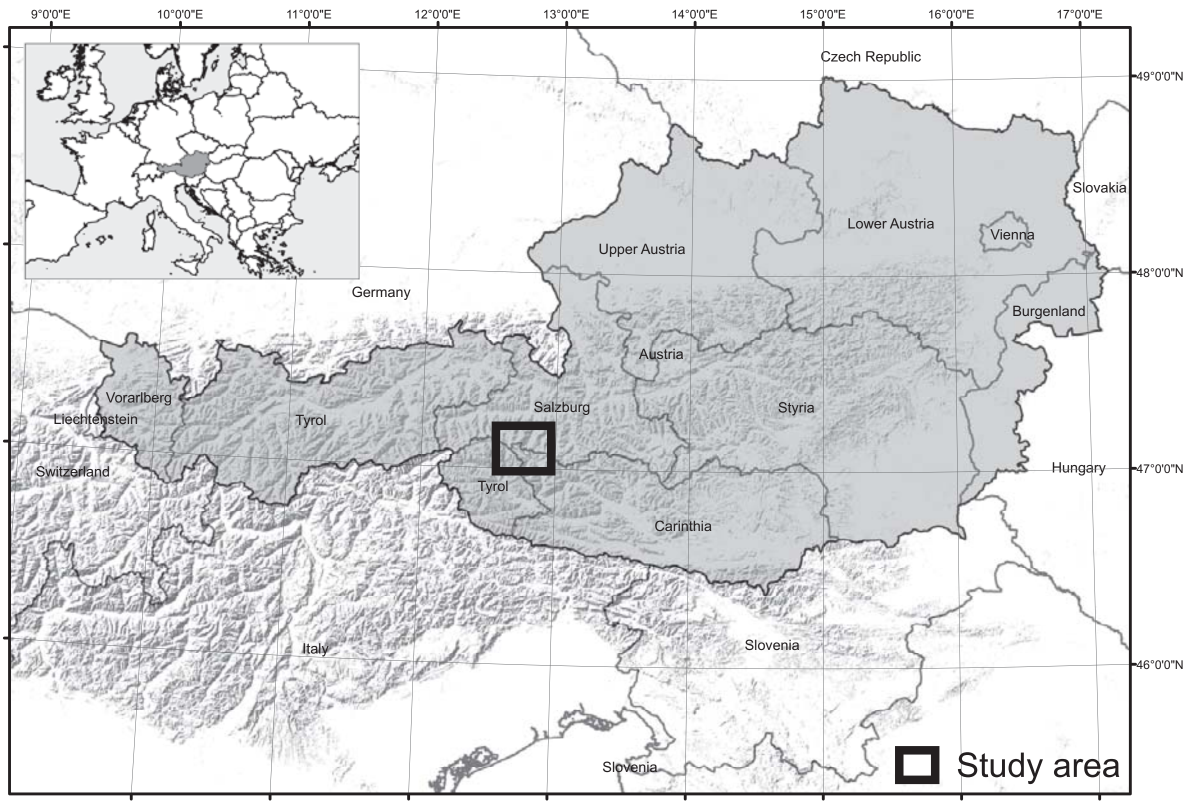

Figure 2.1.: Topographic map of Austria, marking the location of the study area in the province Salzburg, in close proximity to the alpine main ridge of the Hohe Tauern, and the provinces of Tirol and Carinthia. The map is a compilation of free Digital Elevation Model (DEM) data from the United States Geological Survey (USGS) and topographic data part of the ArcGIS suite by ESRI.

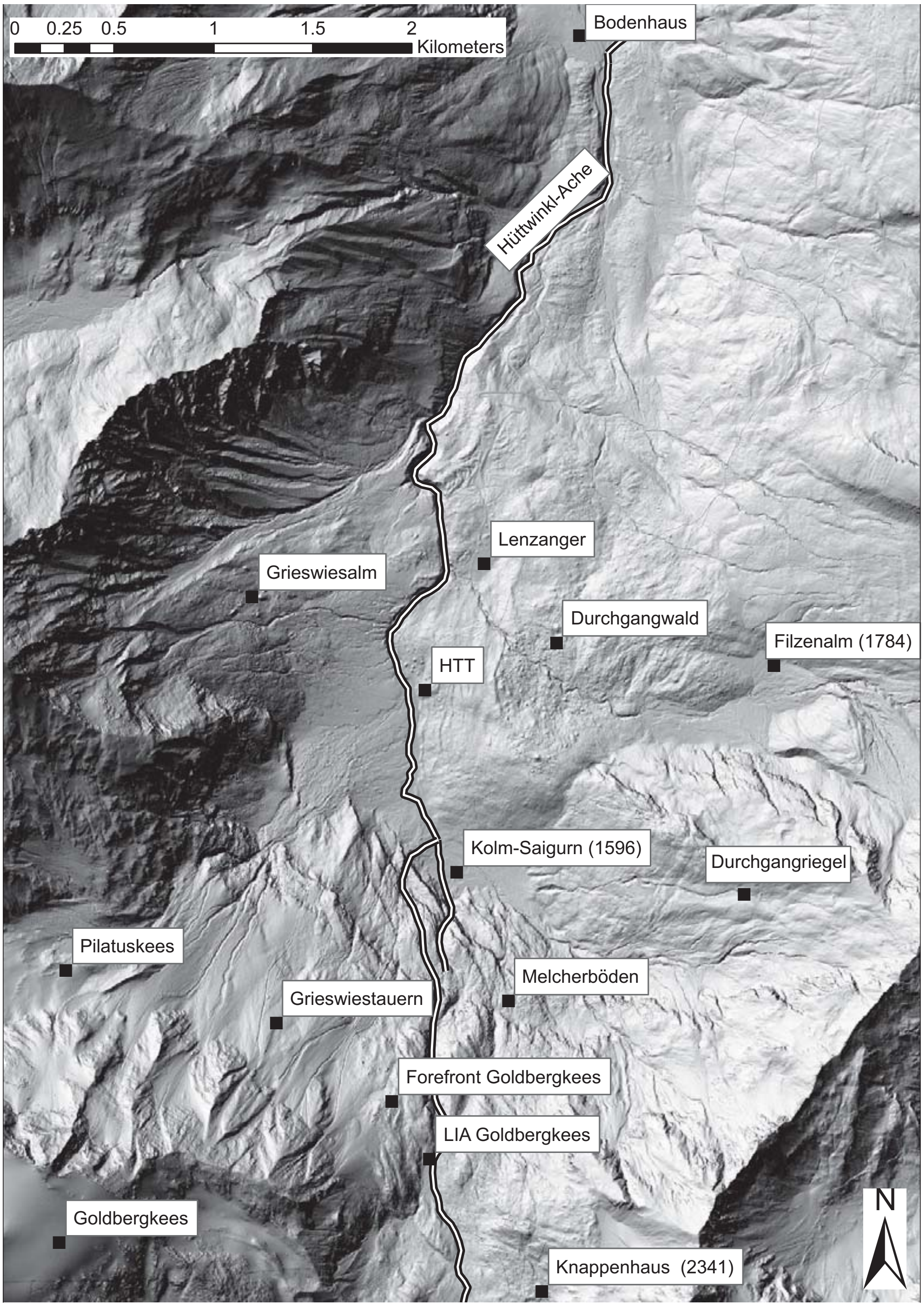

Figure 2.2.: Hillshade image generated from a 1 m resolution DEM (Digital Elevation Model). Important topographic features referred to in this work are marked on the map. Numbers given indicate elevation meter asl. Unless stated otherwise, all hillshade models are generated from the DEM generously provided to the GBA by the Government of the province of Salzburg.

temperate glaciers (Hiebl et al., 2011).

2.2. Lateglacial Stratigraphy and Terminology [Bichler]

The Lateglacial, also known as the Last Termination or Termination I is, concerning the stratigraphic record, one of the best studied sequence of the Quaternary. It spans from the Last Glacial Maximum (LGM), at approximately 20 ka BP, to the Holocene interglacial, starting approximately at 11.6 ka BP (Walker et al., 2001). There are multiple archives for proxy-climate data like marine and terrestrial sediment sequences and ice-cores. These records have been studied intensively over the last decades. By the use of dating methods with high degree of accuracy and precision by means, for example, ice-layer chronologies, varve sequences, radiocarbon, tree-ring records or pollen-analyses, palaeo-environmental information with high resolution have been gained. The North Atlantic region is one of the key areas for Lateglacial palaeo-environmental reconstructions. Especially data from ice-cores from the Greenland Ice Core Project (GRIP) and Greenland Ice Sheet Project (GISP and GISP2) play an important role as temperature proxy (Walker et al., 2001; Blockley et al., 2012).

Unsolved problems lie within the correlation of all this archives. For most correlations the ice-layer chronology and its corresponding temperature proxy of the Greenland ice-core projects are taken as a reference (Blockley et al., 2012). The change between warm- (interstadial) and cold-phases (stadial) as seen in the ice-layer chronology are not of the same age in different archives from different regions. Even in nearby archives with high accuracy and precision in northern central Europe (e.g. lake sediments) ages are varying and not all stages of the ice-cores are preserved (Litt et al., 2001).

The Alps and their foreland are even more complicated. Although the climate of the Alps is also most influenced by North-Atlantic climate, the mountain range offers a variety of possibilities for local differences. An example is shown by Starnberger et al. (2011). The authors give an insight on the difference of the onset and the termination of the LGM in global archives (marine, terrestrial and ice) and in the foreland of the Alps.

The Alpine Lateglacial starts with the withdrawal of the glaciers from the tongue basins in the foreland (Chaline and Jerz, 1984). This event is regarded to represent the beginning of Termination I or the Last Termination following the LGM. The Alpine Lateglacial is generally subdivided into stadials, a concept first established by Penck and Brückner (1909). The term stadial is used to describe a stepwise deglaciation from the maximum position of the Würm in the foreland into the Alpine valleys and finally into the cirques interrupted by halts or re-advances, defined by end moraines (Ivy-Ochs et al., 2006; Reitner, 2007).corr This palaeogeographic development has been regarded as a chronological succession beginning with the Bühl followed by the Steinach, the Gschnitz, the Daun, and the Egesen as defined in the former Inn glacier area (Mayr and Heuberger, 1968; van Husen, 1997). This concept has been refined until today, and now comprises the phase of ice-decay (Reitner, 2007), the Gschnitz, the Clavadel/Sender, the Daun, the Egesen, and the Kartell (Kerschner, 2009). As there were no absolute dating possibilities in the past, a scheme based on field and map characteristics has been established to stratigraphically correlate moraine-systems in the different regions of the Alps. Nowadays a refined scheme based on the fundamental classification of lateglacial stadials by Penck and Brückner (1909) and on the work of Heuberger (1966) is used. The scheme covers, amongst others, the positions of the moraines to each other, the morphology of the moraines, and the ELA (see section 6.2) of the system compared to the ELA of the LIA (Little Ice Age) or to the ELA of the neighbor-valleys (Kerschner, 2009).

Until the late 20th century, only radiocarbon ages supported by pollen analyses were a tool to get absolute minimum-ages for moraine-systems (Kerschner, 2009). With the introduction of exposure dating methods moraines and other landforms (e.g. landslides, polished bedrock) can be dated directly (see subsection 3.2.1). Therefore Lateglacial stratigraphy and its correlation with North-Atlantic climate has improved over the last years. Most of this dating and correlation work has been realized in the Central, Western and western parts of the Eastern Alps. Our study area is situated in a high altitude region in the central Eastern Alps, where little dating work has been done and where known moraine-systems are only classified because of their geomorphological characteristics (see Figure 2.3).

Table 2.1 gives an overview of the up to date Alpine Lateglacial stratigraphy. Please note, that all ages received from exposure dating have several uncertainties as discussed in subsection 3.2.1.

As there can be great confusion about the terminology of lateglacial stadials and interstadials, because of the usage of different concepts by different sciences (e.g. Climatology versus Geology), we will use following terms in this thesis:

- Last Glacial Maximum (LGM)
- Phase of ice-decay

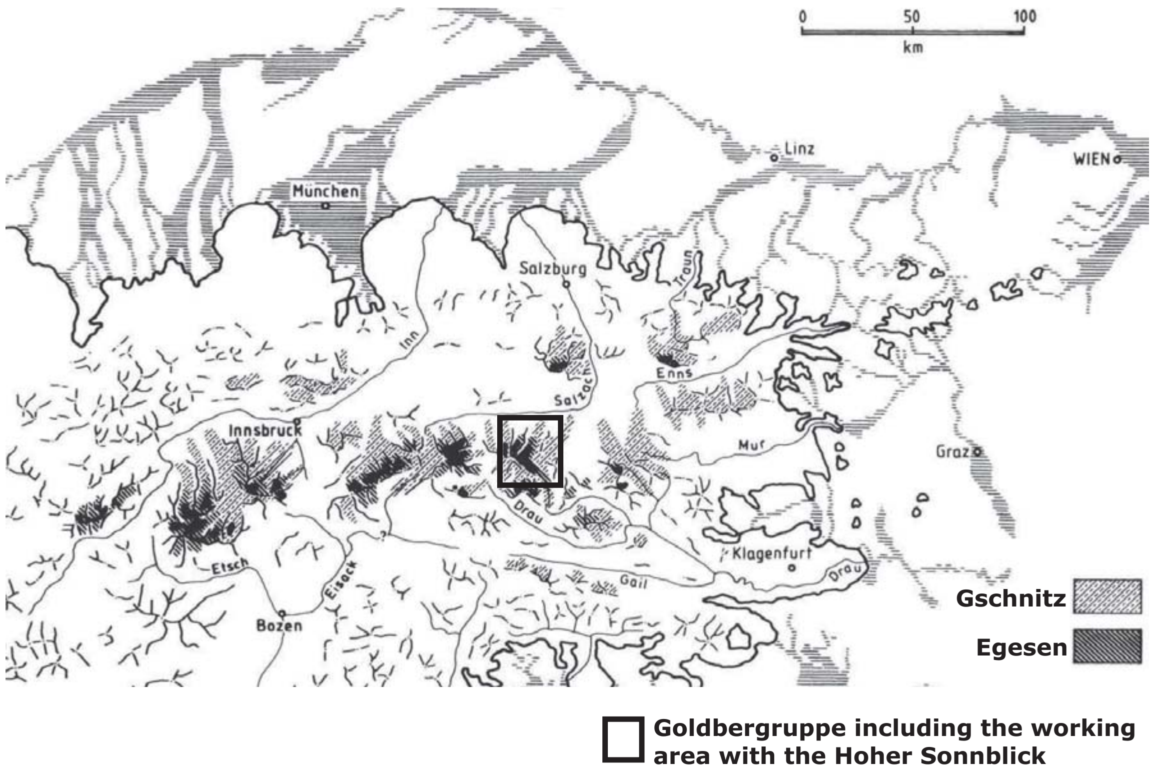

Figure 2.3.: Map after van Husen (2000) showing the field distribution of Gschnitz stadial and Egesen stadial in the Eastern Alps. Note that the map is only based on geomorphological characteristics. The black square highlights the Goldberggruppe in which the working area (north of the Hoher Sonnblick) is situated.

- Gschnitz stadial
- Bølling-Allerød interstadial
- Egesen stadial, which is equal to Younger Dryas and comprises the Kartell stadial (late Egesen).
- Preboreal
- Boreal
- LIA, when referring to the timespan between approximately 1350 AD to 1850 AD.
- LIA-1850, when referring to the terminal moraines of the LIA around 1850 AD, and the corresponding glacier extent.

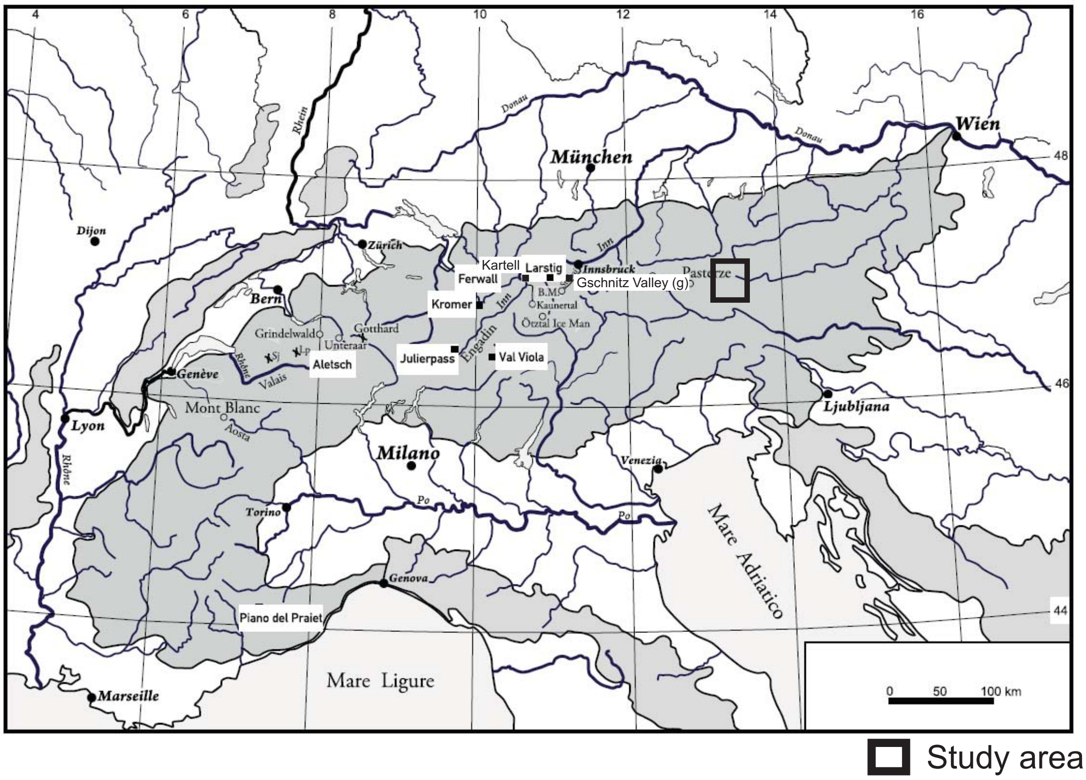

Figure 2.4.: Map modified after Ivy-Ochs et al. (2009a). The sites named in the map are corresponding to the sites in Table 2.1. (g) marks the only age of the Gschnitz stadial, the other ages are Egesen or younger. The black square highlights the Goldberggruppe where the working area is situated north of the Hoher Sonnblick. Areas above 700 m a.s.l. shown as grey shaded pattern.

Table 2.1 shows how the lateglacial stratigraphy of the Alps is defined. The results of this table are based on sites which are located in the Western, Central and western Eastern Alps. Part 1 summarizes how stadials are determined by geomorphological characteristics and how they appear in their type-locality. Part 2 summarizes (1) the correlation of the stadials with GRIP ice core stratigraphy (Blockley et al., 2012). (2) The timing of the change between stadial and interstadial in the GRIP. (3) The time-stratigraphic position of each site where ^{10}Be dating has been realized. (4) Calculating their respective ELA depressions.

age ka b2k	Stadial	Moraine and glacier characteristics	Regional situation
8	Kromer ??		
	Kartell	Well-defined, blocky, multiple moraine ridges, small rock glaciers	Cirque and valley glaciers, clearly larger than LIA, but smaller than innermost Egesen phase
11.6			
	Egesen	**Sharp-crested, often block-rich, multiple moraine ridges well documented in wide areas of the Alps. Three-phased readvance of valley glaciers and cirque glaciers Development of extensive rock glacier systems during later parts of the stadial**	**Cirque and valley glaciers, very few dendritic glaciers**
	Bølling - Allerød Interstadial		
	Daun	Well-defined but smoothed moraines, relatively few boulders, solifluction overprint during YD (Egesen); moraines usually missing in more oceanic areas of the Alps (overrun by Egesen?). Smaller than Clavadel/Senders	Glaciers slightly larger than local Egesen glaciers
	Clavadel/ Sender	Well defined, often sediment-rich moraines	Cirque and valley glaciers, some dendritic glaciers still intact
16	**Gschnitz**	**Steep-walled, somewhat blocky, large single moraines, no solifluction overprint below 1400 m Widespread readvance of large valley glaciers on a timescale of several centuries**	**Many valley glaciers, some large dendritic glaciers still intact**
	Lateglacial ice decay	General downwasting and recession of piedmont glaciers in the foreland with some oscillations of the glacier margins.Main ly ice marginal deposits; moraines indicatingglacier advance in smaller catchments.Glacial advancesalso due to ice-mechanic al causes. Comprises the classical ‘Bühl’ and ‘Steinach’ stadials	Downwasting dendritic glaciers, increasing number of local glaciers
~20 Begin of termination of LGM (LGM until ~19ka)			

Part 1 of Table 2.1

age ka b2k	Stadial	GRIP (INTIMATE)	GRIP (Correlation Age b2k)	Time-stratigraphic position ^{10}Be ages (ka): site	ELA Depression versus LIA ELA
8	Kromer ??	8.2 ka event ??		Mixed cold phase? 8.4 ± 0.7: Kromer valley	
	Kartell	Preboreal oscillation		Preboreal oscillation? 10.8 ± 1.0: Kartell cirque	-120m at type locality
11.6			11.55 ka Begin of Holocene		
	Egesen	**Greenland-Stadial GS-1**		**Younger Dryas** **12.3 ± 1.5: Julier Pass, outer** **11.3 ± 0.9: Julier Pass, inner** **12.2 ± 1.0: Schönferwall** **11.2 ± 1.1: Aletsch** **11.2 ± 0.9: Val Viola**	**-450 to -180 m for maximum advance depending on location**
12.7			12.65 ka Begin of Younger Dryas		
	Bølling - Allerød Interstadial	Greenland-Interstadial GI-1a to GI-1e		Bølling - Allerød Interstadial	
14.7			14.7 ka Begin of Bølling		
	Daun			Before Bølling	~-400 to -250m depending on location
	Clavadel/ Sender			Before Bølling	~-400 to -500m depending on location
16	**Gschnitz**	**Greenland-Stadial GS-2a**		**Before Bølling** **>15.4 ± 1.4: Gschnitz valley**	**~-650 to -700 m**
	Phase of early Lateglacial ice decay	Greenland-Stadial GS-2b		Before Bølling, older than 15 400 ± 470 ^{14}C a BP (18 020–19 010 cal. a BP)	Largely undefined between -LGM and -800 m
~20 Begin of termination of LGM (LGM until ~19ka)					

Part 2 of Table 2.1

Table 2.1 ***(previous pages)*:** Lateglacial stratigraphy of the Alps, modified after Ivy-Ochs et al. (2008) with input from Blockley et al. (2012). For all references see Ivy-Ochs et al. (2006, 2008).

2.3. Previous Research [Bichler]

A first geological overview of the area was given by Hottinger (1935), witha special focus on bedrock geology and tectonics. Exner (1956) produced a more detailed map which was used as a base for all future work. During the 1970s, 1980s and 1990s several geological and geomorphological mappings with different approaches were realized in the Hüttwinkl valley (Matura, 1966; Malecki, 1972; Alber, 1976; von Poschinger, 1986; Fellner, 1993). Especially the work of Alber (1976) served as a source for information about local bedrock geology.

Glacial and climate research was extensively undertaken by various authors (Lichtenecker, 1935, and references therein) during the late 19th and early 20th century. With its detailed mapping of the local moraine systems, the work of Lichtenecker (1935) in the area around the former Knappenhaus (miner's house) close to the Goldbergkees was a valuable source of geomorphological information. His mapping of former Goldbergkees extents, based on the work of Penck (1897), included the ridges of the LIA-1850 and a larger extent during the LIA, which he assumed to belong chronologically to the 17th century (LIA-1620 today). Furthermore he noticed a remarkable ridge-system of left lateral moraines in the forefront of the latter, which he logically assumed to be older than the LIA-1620 moraines. Consequently, he constructed a ridge-system and connected it to findings at the Radhaus (former mining building). In addition he estimated a right lateral ridge, ending up with an extent approximately 100m in front of the LIA-1620. Today the ages of the extents of the LIA are well known due to intensive investigations using ^{14}C dating and palynology, for example from Bortenschlager and Patzelt (1969) and Patzelt (1973) in the areas of climate and glacier variations in the nearby Alpine range of the *Venedigergruppe*.

Besides the Goldbergkees, geomorphological researches were focusing on the valley floor and its characteristic landscape features. Hottinger (1935) was the first to describe the morphological and geological features of the Durchgangwald as a product of a tremendous landslide down from the Grieswies-Schwarzkogel. Unfortunately, these observations were not accepted by Kieslinger (1938), who explained it as a landslide originating from the eastern slopes of the Hüttwinkl valley. He also described the landslide to consist mostly of dark phyllite and calcareous-mica-schist and connected the landslide mass to the Durchgangriegel (section 4.15) with its extension gashes. Exner (1956) agreed with Kieslinger (1938) and likewise assumed that the landslide detached from the east. He even interpreted the moraines east of the Filzenalm as overlaying the landslide masses, subsequently interpreting it as interstadial. von Poschinger (1986), after Hottinger (1935), was one of the first to compare the diverse lithologies of the landslide mass with the potential source bedrock on both flanks of the Hüttwinkl valley. As the Durchgangwald mass lacks Zentralgneis, a lithology vastly common on the eastern flanks of the valley, he concluded the only possible source to lie on the western flanks of the valley, in agreement with Hottinger (1935). von Poschinger (1986) also documented the basal till, covering the landslide mass along the creek. He concluded a lateglacial, minor glacial advance representing the Gschnitz or Daun stadial, with an assumed terminal moraine at the Bodenhaus tavern (see: section 4.7).

The Hüttwinkl Transfer Tunnel (German: *Hüttwinkl-Überleitungsstollen*, further referred to as HTT) is approximately 6 km long and transfers the water of the Hüttwinklache in the Rauris valley to the Gastein valley in the east. Construction of the tunnel started in the 1970s. The western part of this tunnel lies within the Durchgangwald landslide mass (Figure 2.5, section 4.2), which size and composition was difficult to estimate during the planning stages of the project (Brandecker, 1981). The western portal of the HTT is well visible and accessible when following the road to Kolm-Saigurn and is also easily identifiable on close up views of the hillshade model (Figure 3.1).

Geophysical investigations from Weber (1971) assumed slipped layers of schist, covered by landslide deposits in the area of the Durchgangwald. Seismic interpretations predicted to reach solid rock after 100 m. Instead, when the western part of the HTT was built, solid rock was reached only at 537 m, after cutting through the landslide deposits. Brandecker (1981) lists two main reasons for this discrepancy:

- The seismic method failed to interpret the volume of the landslide mass correctly, because huge carbonate schist, phyllite and gneiss blocks are intertwined which give unrealistic high seismic velocity, similar to solid rock.
- The border between the landslide mass and the bedrock surface is very shallow, adding to the difficulty of predicting the point where the HTT would cut through the bedrock.

Investigating the stability of the landslide mass was a key factor in all the stages of

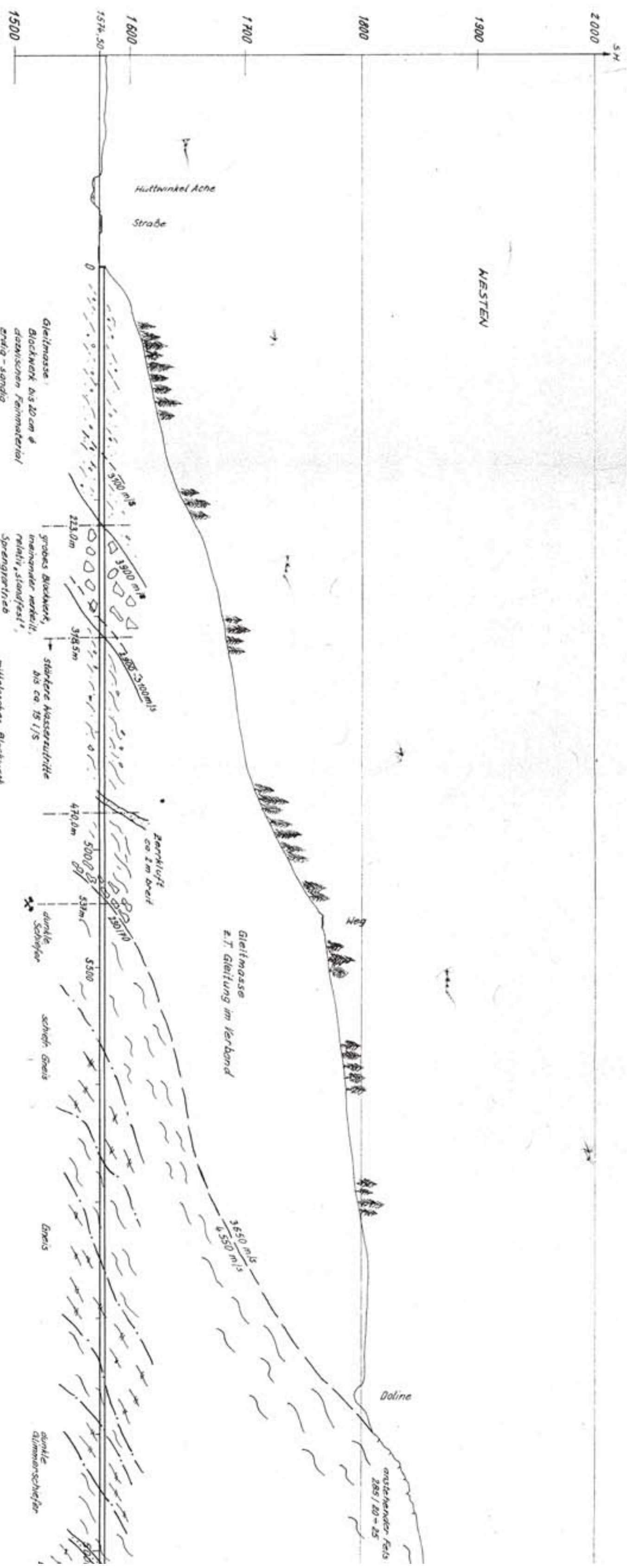

Figure 2.5.: Geologic profile of the western part of the Hüttwinkl Transfer Tunnel (Rainer, 1979), reproduced with permission from the Salzburg AG. Note that this drawing does not interpret the border between landslide mass and bedrock as shallow, even though Brandecker (1981) reports so.

the HTT project for estimating building costs. This required some knowledge of current and former transport direction. Three general hypotheses exist:

- Transport and origin of the main mass from the West from the eastern flanks of the Grieswies-Schwarzkogel, towards the Durchgangriegel and Filzenalm (Hottinger, 1935; von Poschinger, 1986; Brandecker, 1981).
- A creeping mass movement from the east, towards the valley floor and the Grieswiesalm (Kieslinger, 1938; Exner, 1956).
- A combination of the above, with a creeping mass movement from the east, covered by landslide masses from the west (Weber, 1971; Steinhauser et al., 1984).

Detailed aspects of these hypotheses are discussed in section 4.2. The tunnel and the records from the construction (Rainer, 1979; Brandecker, 1981) can help to support arguments for the different theses. The profile of the Figure 2.5 shows blocks up to 20 cm interlaced by earthy and sandy material for the first 213 m. The next 95.5 m are documented as rough, wedged blocks. Between 470 m and 537 m contains medium-sized blocks with massive water discharges up to 15 l s^{-1}. At 465 m, a 2 m wide gap in debris allowed water to discharge with more than 1000 m^3 fine material from the landslide mass. Rainer (1979) suspects an extension gash to be the reason for the massive discharge, but does not exclude the possibility of a loose soft sediment filling.

Unfortunately a detailed geologic recording of the tunnel was deemed unnecessary, especially with regards to lithological information. This would allow further interpretation regarding the internal composition, structure, and origin of the Durchgangwald landslide mass. Of great interest is also the transition zone between the bedrock and the debris. During construction, the tunnel walls were immediately fortified as the advance was progressing, a measure necessary to keep the blocks and sand from collapsing the tunnel (Rainer, 1979; Brandecker, 1981). The tunnel walls are therefore sealed off today, preventing further investigations.

Overall, the debris thickness, and in most cases the absence of internal lithological and structural zoning, do not support the theory of a creeping mass movement from the east, but instead support the theory of an one-time uniform mass movement from the west. Recorded lithological zoning along the tunnel section can be interpreted as different lithologies with distinct rock mechanical properties, showing distinct degrees of fragmentation as a result of the landslide (see: section 4.2), but lacking detailed geologic information, this remains speculation. The Durchgangwald mass is stable today and does not pose a threat to the valley and the tunnel, as concluded by von Poschinger (1986).

2.4. Morphological and Geological Setting [Bichler]

2.4.1. The Tauern Window

The Tauern Window exposes lower-plate, i.e. European, Penninic- and Sub-penninic sequences and their basement units that were covered by the Austroalpine units (Schmid et al., 2004). With its size of 160 × 30 km, it is the biggest of the intra-Alpine tectonic windows. The limits to the west and east are the Brenner and Katschberg normal faults (or shear zones), to the north the Salzachtal-Ennstal fault zone and to the southeast the Mölltal fault zone (Lerchbaumer et al., 2010).

The Tauern Window consists of 3 main parts. The eastern, central and western Tauern Window. The Sonnblick-massif belongs to the eastern part, and lies in close proximity to the transition zone to the central part.

The lithology of the Tauern Window can be divided into (see Figure 2.6):

- **Penninic nappe-system (including the Glockner nappe)**
  The Glockner nappe consist of permo-mesozoic meta-sediments, which have only been overprinted during alpine orogeny. The sequence is mainly built up by phyllite, calcareous-phyllite and calcareous-mica-schist. Less abundant are basic to ultra-basic rocks and carbonates .

- **Sub-penninic nappe-system (including the Venediger nappe)**
  The Venediger nappe consists of Paleozoic and Mesozoic crystalline-complexes and meta-sediment-formations (Schuster et al., 2006). The Zentralgneise belong to this nappe as well.

2.4.2. Kolm-Saigurn

2.4.2.1. Bedrock Geology

Several prominent geologist (see section 2.3) provided geological maps and additional information about the complex geological setting in the head of Hüttwinkl valley. We hereby try to simplify this complicated geology and take a closer look on the aspects which are important for our mapping focused on geomorphology and Quaternary geology. The western flanks below the Ritterkopf consists mainly of a sequence belonging to the Glockner nappe. The basis is built up by mica schist, sometimes garnet bearing, probably belonging to the Venediger nappe, followed by a thick sequence of dark phyllite, biotite schist and calcareous mica schist which are clearly Glockner nappe. The top

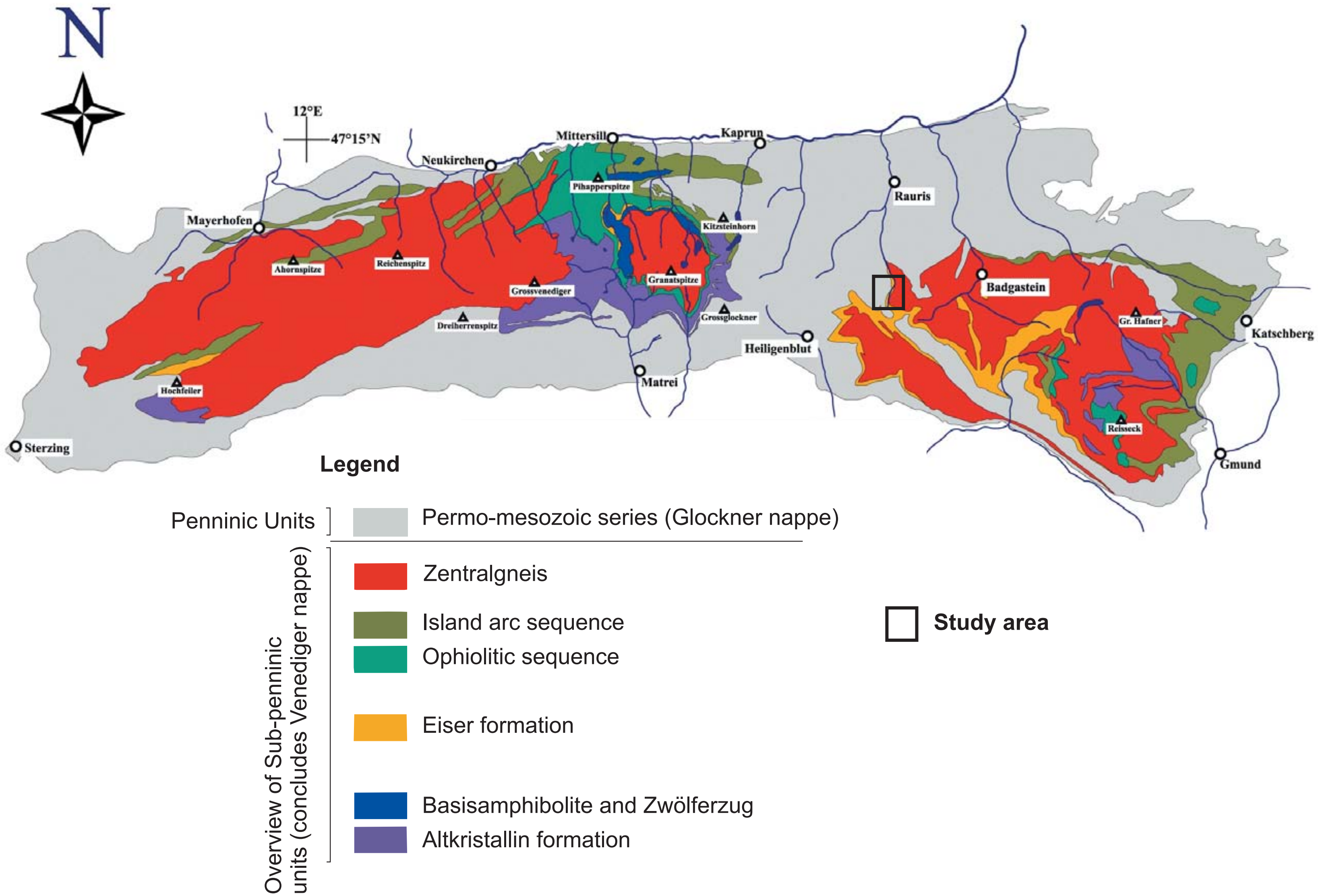

Figure 2.6.: Simplified map of the Tauern Window modified after Kebede et al. (2005).

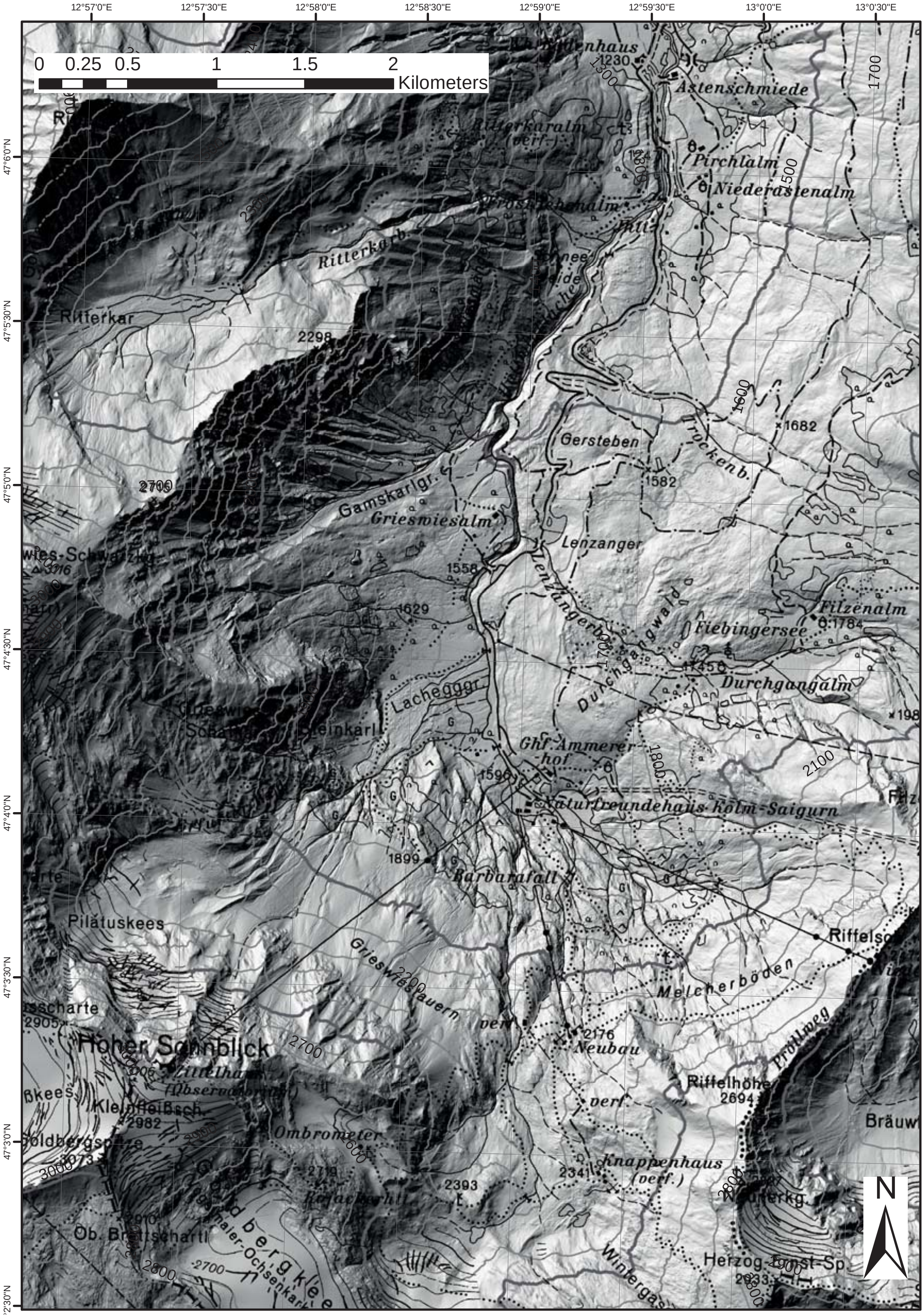

Figure 2.7.: Topographic information draped on a hillshade model of Kolm-Saigurn and the surrounding study-area.

is composed of thin layers of Quartzite and Prasinite (Alber, 1976). We used this lithology information from the western flanks for our understanding of the origin and the characteristics of the prominent Durchgangwald landslide. Our mapping of scarce bedrock outcrops is consistent with the overall geological frame provided by the work of Alber (1976).

The northernmost prominent outcrops of Sub-penninic units (Venediger nappe) occur south of Kolm-Saigurn, where garnet mica schist is forming a morphological step between the valley-floor and the Barbara-Falls. Further more south, complicated and folded mixed-layer of the Venediger nappe units (mainly biotite schist) crops out. The Hoher Sonnblick itself and its surroundings are the only massive outcrops of Zentralgneis (German for *central-gneiss*), besides a thin belt on the eastern flanks spanning from the Niederrastenalm to the Durchgangriegel. (Exner, 1956).

The Zentralgneise are metamorphic overprinted Variscian granitoids, which intruded into the Tauern Window nappes during the Carboniferous to Permian. In the eastern Tauern Window the Zentralgneise are exposed in the Sonnblick-massif and Hochalm-Ankogel-massif. They are typical ortho-gneiss with the main components quartz, potassium feldspar and plagioclase (Holub and Maschallinger, 1989). Mostly they are easily to recognize as the potassium feldspar forms augen (see Figure 2.8), hence the term *augen-gneiss* (German: *Augengneis*).

As the local glaciers (Goldbergkees and Pilatuskees) of the study area are located on the border between Penninic to Sub-penninic nappe, the existence of rounded Zentralgneis components in glacial sediments downstream is most indicative for a transport during lateglacial advances.

2.4.2.2. Morphology

The north-trending Hüttwinkl valley, a typical central Eastern Alpine valley, is significantly asymmetric. The western flanks have steep slopes with approximately 35°, whereas the eastern flanks are flat with a slope of approximately 20° and remarkable morphological steps. This asymmetric shape could be explained by large creeping masses on the eastern flanks and in addition by western trending dipping of the dominant lithology (Schieferhülle of the Glockner nappe) in the southern parts of the valley (von Poschinger, 1986; Fellner, 1993; Hellerschmidt-Alber, 1998). The border in the south and west of the valley-head are built up by summits reaching an altitude of around 3000m asl, with the Hocharn being the highest (3254m asl) amongst them. The eastern ridge to the neighbor valley of Gastein is lower with summits reaching altitudes of approximately

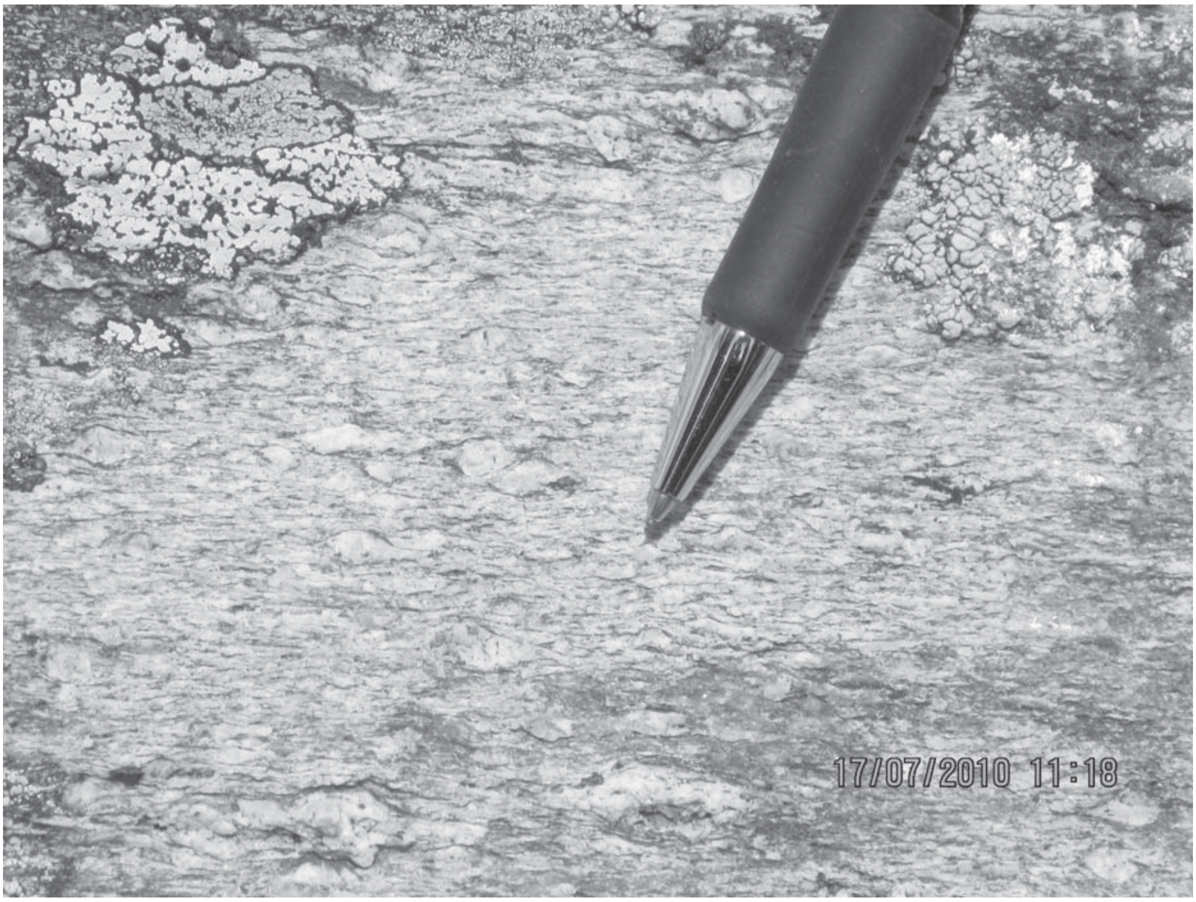

Figure 2.8.: Typical appearance of Zentralgneis in the field. The potassium feldspar forms augen, often reaching a size of several cm.

2500m asl. In the Hüttwinkl valley, as in neighboring comparable valleys, the altitude of the cirques decreases in northward direction from the central alpine main ridge in the south to the west-east trending Salzach valley (Hottinger, 1935). The valley head features two glaciated areas (Goldbergkees and Pilatuskees), large landslide deposits and several glacial deposits (also see section 2.1 and section 2.3).

2.5. Aims and Goals [Reindl]

Starting with the goal of mapping and investigating the Quaternary geology of the Hüttwinkl valley-head with updated and modern methods, an area which was last investigated nearly 30 years ago, two main areas of interest become the focus of this work. These are the area of the Durchgangwald, and the LIA-1850 forefront of the Goldbergkees at the Grieswiestauern.

For the Durchgangwald, being a key area of this study, several goals are of importance:

- Finding enough evidence to document the extent of the Durchgangwald landslide, and support any of the existing hypotheses about the origin.
- Possibly coming up with numerical ages, using the ^{10}Be and ^{14}C methods.
- Documenting the glacial advance outlined in the existing hypotheses.
- Associating this glacial advance with a lateglacial stadial, again using the ^{10}Be and ^{14}C methods.

For the LIA-1850 forefront of the Goldbergkees at the Grieswiestauern, the following goals were defined:

- Unraveling the temporal and spatial relation of the deposits in the LIA-1850 forefront.
- Possibly coming up with numerical ages for the different phases of a glacial cycle using the ^{10}Be and ^{14}C methods.
- Looking for possible correlation of the glacial deposits here with the glacial deposits of the Durchgangwald down-valley.

Finally, if the relation and reconstruction of these key features of landscape forming events show a satisfying outcome, additional goals were defined concerning the glacier dynamics of the former glacier system(s):

- Calculation of ELAs, and associating their respective ELA depressions (relative to the LIA-1850 ELA) with palaeoclimatic interpretations.
- Detailed reconstruction of the mechanics and dynamics of the former glacier system(s).

Combining these crucial points, the main goal of producing an extensive Alpine Lateglacial landscape chronology, further east than any previously dated sites in the Alps (Figure 2.4), can be reached.

3. Methods [Reindl/Bichler]

During our work we used a number of methods to investigate the relative chronology (see section 3.1) and to obtain numerical ages for important geomorphological features (see section 3.2).

3.1. Mapping [Bichler]

3.1.1. Geological and Geomorphological Mapping

The foundation of our work was laid in 2011 and 2012 with a detailed geological and geomorphological mapping of the area between the Gasthof Bodenhaus in the north (toll station), and the well established locations of the LIA-1850 moraines in the south at the forefront of the current Goldbergkees. The mapping scale was 1:10000, and the mapping area was divided into two areas, with Martin Reindl focusing on the northern area, and Mathias Bichler on the southern area. The northern perimeter is defined as the valley floor around Kolm-Saigurn (1598m asl) in the south, the scarp area on the valley flank in the west up to the Grieswies-Schwarzkogel (3115m asl) with the further valley flank running north to the Gasthof Bodenhaus (1230m asl), therefore generally following the Hüttwinklache. In the east, the mapping perimeter in the east was defined by the already generally known borders of the Durchgangwald landslide, with the easternmost point at the Filzenalm (1784m asl). The southern perimeter contained the area around the Neubau hut (2175m asl), with the southern of the Melcherböden and the Grieswiestauern with the north face of the Sonnblick. In the west, the limits were marked by the Little Ice Age moraines of the Pilatuskees, with the border to the north just starting where the cliffs behind Kolm-Saigurn start to rise from the valley head floor. While the northern area therefore has more of a N-S extension, the southern area has a general E-W extension. Overall, the mapping area encloses approximately 10 km^2. As our work aimed to unravel lateglacial processes, bedrock was only mapped where necessary, for example where the glacier produced polished bedrock surfaces in the area of the Grieswiestauern. However, lithological information about the bedrock outcrops east face of the Grieswies-Schwarzkogel is based on Alber (1976).

The resulting map is attached in Appendix C of this work. Symbology generally follows the mapping conventions as outlined by the Geological Survey of Austria, while colors where chosen in a way to reflect lateglacial deposits in better detail and chronology, such as internal zoning of landslides, and association of glacial sediments with lateglacial stadials.

3.1.2. Digital Elevation Model

High quality, 1 m resolution Digital Elevation Models (DEM), generously provided by the government of the province of Salzburg to the GBA for the purpose of geological mapping, offer the opportunity to study surface structures from the distance, therefore greatly enhancing the knowledge about the morphology of an area before going into the field. The combination with a hill-shade image and different light angles computed with GIS, also allows identification of many features otherwise completely or partly hidden in dense forests. This vital information allowed us shifting the focus in the field to key areas. In some cases, complete identification and research of landforms was only possible via hillshade-generated DEM.

Figure 3.1 gives an example close up to the hillshade model north of Kolm-Saigurn, displaying numerous distinctive landforms.

In this area some surfaces with characteristic properties stick out from the hillshade image. The rough surface in NE of Kolm-Saigurn [Figure 3.1(c)] is bordered sharply by a soft shaped surface with N-S extending line features [Figure 3.1(b)]. West of the prominent incision of the Hüttwinklache [Figure 3.1(d)], another soft, seemingly flat surface hints possible alluvial fans and debris flows towards the valley floor [Figure 3.1(a)]. Even man-made features, like the western portal of the Hüttwinkl Transfer Tunnel, can be identified on the example hillshade model [Figure 3.1(f)].

3.1.3. Geographic Information System - GIS

Integration of data gained during mapping campaigns is a key factor for successfully answering geologic and gemorphological questions. Sample sites and features were mapped and recorded using standard Global Positioning System (GPS) handheld devices. Digitizing hand drawn field maps and incorporating GPS data was made possible by the extensive use of the ArcGIS suite by ESRI. Cross-sections, profile construction, modeling

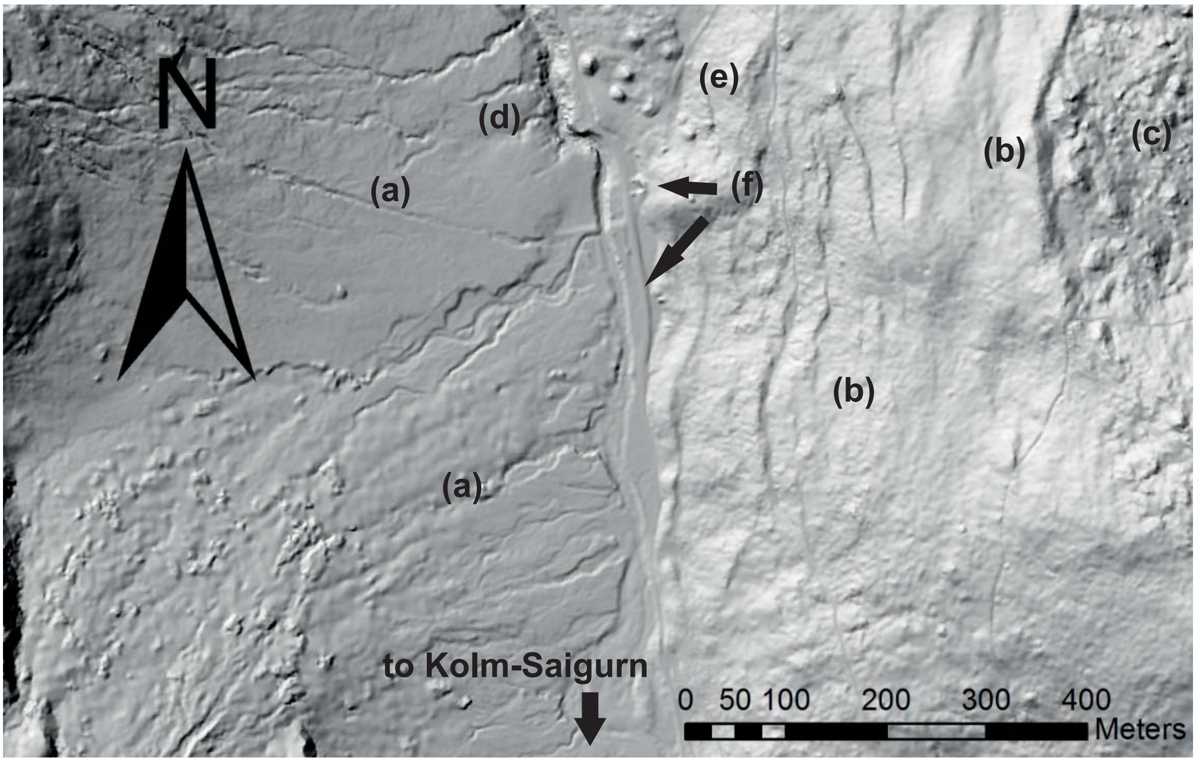

Figure 3.1.: Example close-up hillshade model from the area north of Kolm-Saigurn. Several prominent landforms and features can be identified: (a) Alluvial fans and debris flows with creeks from the W and SW indicating the flow direction (b) several parallel ridges running from S to N, with a prominent ridge separating the smooth from the rough surface in (c). The Hüttwinklache incising into the valley floor, starting to form a shallow canyon (d). Distinctive round hills (e) Man-made features like the toll road leading to Kolm-Saigurn and the western portal (f) of the Hüttwinkl Transfer Tunnel (see section 2.3).

of lateglacial surfaces, landslide volume calculations and overview sketches were mainly produced using ArcMap, while 3-dimensional models were generated using ArcGlobe and ArcScene, sometimes modified and improved using CorelDraw. Centering around the ArcGIS suite and a high-resolution Digital Elevation Model (subsection 3.1.2), glaciers models were augmented by the use of spreadsheets and data processing via Wolfram Mathematica.

3.1.4. Lithofacies Description

Where applicable, the sediments at the outcrops were classified using lithofacies codes (Table 3.1). Generally, this followed the methods and codes as outlined in Keller (1996).

This standardization allows easier comparison of the sediment record and single sites, and facilitates further use for questions regarding hydrogeology.

Table 3.1.: Major and minor classification for lithofacies codes used in this study, modified after Keller (1996).

Major classification	
Facies Code	Lithofacies
SC	grain supported scree
Gc	grain supported gravel
Gm	matrix supported gravel
Dc	grain supported diamictite
Dm	matrix supported diamictite
SSC	scree with sand matrix
GS	gravel-sand
S	sand
P	peat
F	fines (clay and silt)
Minor classification	
Grain Size (Gravel/Scree)	
g	gravel (2–60 mm)
c	cobbles (60–200 mm)
b	boulders (> 200mm)
Texture	
m	matrix-supported
c	clast-supported
Structure/Layering	
l	laminated (<1 cm)
b	bedded (>1 cm)
m	massive
g	graded

3.2. Dating Methods [Reindl]

3.2.1. Surface Exposure Dating

During the last decades surface exposure dating using cosmogenic nuclides has become a nearly standard tool in helping to solve a various range of questions regarding the timing and rate of processes that form the surface of the earth. The first accelerator measurements for ^{10}Be were reported by Raisbeck et al. (1978), and early measurements of cosmogenic ^{10}Be in rock were reported in the early 1980s by Klein et al. (1982). This includes glacial and landslide chronologies which are most relevant to this study (Ivy-Ochs et al., 2007; Ivy Ochs and Kober, 2008; Schindelwig et al., 2012).

While the focus of applications of cosmogenic nuclide dating has long been put on moraines and polished bedrock connected to cold stadials (Ivy-Ochs et al., 2008; Kerschner and Ivy-Ochs, 2007; Kerschner, 2009), dating landslides has also become a common application for cosmogenic nuclides during the last years (Ivy-Ochs et al., 1998; Kubik et al., 1998; Hormes et al., 2008; Ivy Ochs and Kober, 2008; Ivy-Ochs et al., 2009b; Akçar et al., 2012). In some areas, glacial advances can even be constrained by landslides (Sanhueza-Pino et al., 2011), allowing to construct detailed chronologies.

As cosmogenic nuclides are built-up continuously in minerals exposed to cosmic radiation, the age of their exposed surface can be determined by measuring their concentration. Common cosmogenic nuclides include ^{10}Be, ^{26}Al, and ^{36}Cl. Owning to the fact of our cooperation with the ETH Zürich, the ^{10}Be method was available to us. The ^{10}Be method relies on the fact that most ^{10}Be is constantly generated from Oxygen and Silicon in the rock's minerals from exposure to cosmic rays (Cerling and Craig, 1994; Gosse and Phillips, 2001, and references therein).

Quartz, SiO_2, is very abundant in the lithologies of the Hohe Tauern alpine range, either in the form of Zentralgneis and even more in quartzite. Where quartz contents are low, as in biotite-gneiss and garnet-schist, sampling an area with quartz veins often resulted in a satisfactory amount of rock sample material for further processing and dating. In two cases, glacially polished bedrock allowed us to extract sample material directly from thick quartz veins. Prerequisites for successful dating are suitable samples sites, for example boulders, which are in clear relationship to the landform subject to investigation. Furthermore, boulders, be it from landforms like moraine ridges or landslides, should be as big as possible but generally posses a minimum volume of $1\,m^3$ and be in a stable position, because bigger boulders are less prone to toppling during erosional processes. Sampling areas on specific boulders should be as flat and as far as possible from the edges, to exclude edge-effects. The sampling area should have a dip of less than 45°. Care should be taken to avoid areas where possible spallation of surface material occurred. Sampling material should only be obtained from the topmost 4 cm. Depending on the quartz content of the underlying rock lithology, an amount of 200 g might suffice, but more is desirable. During our sampling sessions, the amount of material obtained by chisel and hammer ranged from approximately 500-1000g, while samples sites where a gasoline-driven stone saw could be employed delivered up to 2 kg of material, with the side-effect of much faster extraction. Care should be taken to note specific characteristics of each sample site in the field, because snow or sediment cover, and shielding from trees might require correction for lower production rates in the age calculation (Dunne et al., 1999; Plug et al., 2007; Dunai, 2010).

Based on mapping work, three main areas (two landslides and the intermediate glacial advance and retreat, see chapter 4) were identified and suitable boulders where chosen. All samples were taken during the summer of 2011, and were prepared as described in detail in Ivy-Ochs et al. (2006). Samples were taken either traditionally by chisel and hammer, or in combination with a portable, gasoline powered stone saw with diamond blades. The latter method allowed better sampling of flat surfaces, far from the edges, otherwise inaccessible by chisel. The goal was to extract 1–2 kg of raw material from the first 4 cm from the boulders and bedrock surfaces. Location, elevation, surface orientation, volume, lithology, coverage and possible tree shielding were documented for each sample (Table 3.2). Subsequently, the samples were taken to the University of Vienna for further processing. The samples were crushed, grinded and sieved multiple times, to grain sizes ranging from 0.2 mm to 0.8 mm. The grains were then further processed in the hydrofluroic acid laboratory, where approximately 125 g from each sample was washed and cleaned from chunks of organic material, mostly lichen, growing on the rocks surface. All water used in sample preparation was purified and all chemicals during leaching were grade *pro Analysi*. Chemicals used in later steps were grade *suprapure*. Further organic contamination and carbonates where removed from the samples by hydrochloric acid and overnight placement on a rotational shaker table ensuring that all of the grains were in suspension all of the time. The sample was then again cleaned with purified water before other minerals were removed by hydrofluoric acid treatment. Treatment by hydrofluoric acid involved overnight leeching in 40 ml of HF and 400 ml purified water on the rotation shaker table. This step was repeated four times, until mica and other minerals could not be identified anymore by the naked eye in between the quartz grains. All samples were at least once treated in an ultrasonic bath, to break up mineral aggregates. Some mica-rich samples (DUR2, DUR8, DUR9, DUR10, and SON10) required additional treatment in the form of heavy liquid separation under the supervision of Dr. Florian Kober from the ETH Zürich Geological Institute, where sample fractions exceeding 2.69 g cm^{-3} and lower than 2.62 g cm^{-3} were removed. This overall procedure ensured only quartz grains were processed during the subsequent dissolution steps.

Table 3.2.: ^{10}Be samples overview. Coordinates are in lat/long, datum WGS 1984. Sample lithology: ZG = Zentralgneis, Qu = Quartzite, BtG = Biotite-gneiss, GS = Garnet-schist, QV = Bedrock quartz vein. Coverage indicates the measured soil and plant coverage at the time of sampling.

Name	Latitude	Longitude	Elevation [m]	Surface Orientation	Dip	Volume [m^3]	Lithology	Coverage [cm]
DUR1	47.07643	12.98334	1638	008	10	180	ZG	4
DUR2	47.07577	12.98339	1643	350	05	24	ZG	0
DUR3	47.07436	12.9829	1623	210	02	16	ZG	6
DUR4	47.07374	12.98274	1631	000	00	6.12	ZG	3
DUR5	47.0861	12.98396	1520	072	25	9	Qu	2
DUR6	47.08656	12.98385	1516	090	32	100	Qu	0
DUR7	47.0859	12.98428	1522	038	08	60	Qu	1
DUR8	47.07454	12.99171	1730	350	10	2250	BtG	0
DUR9	47.07793	13.00304	1779	127	30	224	GS	0
DUR10	47.07431	12.99065	1732	076	003	576	GS	9
SON1	47.05642	12.98044	2231	306	18	5.4	ZG	0
SON2	47.05642	12.98045	2228	299	12	1.5	ZG	0
SON3	47.05687	12.97922	2213	93	22	14.8	ZG	0
SON4	47.05706	12.97931	2212	116	25	6.9	ZG	0
SON5	47.05756	12.98149	2183	67	5	60	ZG	0
SON6	47.05755	12.98145	2184	180	10	-	QV	0
SON7	47.05595	12.98239	2214	238	0	9.2	ZG	0
SON8	47.05725	12.98193	2190	148	5	-	QV	0
SON9	47.05720	12.98200	2192	88	2	13.5	ZG	0
SON10	47.05566	12.98197	2209	206	10	14.4	ZG	0

Chemical dissolution and extraction of ^{10}Be was undertaken at the ETH Laboratory of Ion Beam Physics, under the supervision of PD Dr. Susan Ivy-Ochs, following the protocol described in Ivy-Ochs (1996). Samples were dissoluted in teflon beakers on heater tables, by adding a mixture of HNO_3 and HF repeatedly. After dissolution the samples were fumed with concentrated HNO_3, aqua regia and HCl. Be was consequently isolated using multiple ion exchange columns and precipitation steps. The resulting solution was then further prepared by lab technicians for measurement at the Accelerator Mass Spectroscopy (AMS) facilities of the ETH Zürich.

Topographic shielding was calculated from a 1 m DEM (see subsection 3.1.2), and a combination of integrated GIS tools and a Mathematica program written for this purpose (see Appendix A.2, based on public available DEM data from, http://dds.cr.usgs.gov/srtm/version2_1/SRTM3/). The resulting azimuth and elevation pairs were then calculated to a topographic shielding factor at http://hess.ess.washington.edu/math/general/skyline_input.php.

Surface exposure ages were calculated using the ^{10}Be -^{26}Al exposure age calculator at http://hess.ess.washington.edu/math/al_be_v22/Age_input_NENA_calib.html using a sea level, high latitude ^{10}Be production rate of 3.88±0.19 atoms per gram SiO_2 per year, with a muon contribution of 2.2% (Stone, 2000). Scaling to geographic sample latitude and altitude follows Stone (2000). Ages are corrected for erosion from rock surface weathering with a rate of 1 mm/ka (Ivy-Ochs et al., 2004). All ten samples of the Durchgangwald (*DUR* prefix) where corrected by 2% for attenuation of cosmic ray flux in temperate forest (Plug et al., 2007). Two bedrock samples (SON6 and SON8) were corrected for a snow coverage of 50 cm for half a year with an attenuation length of 160 g cm^{-3} and a snow density of 0.3 g cm^{-3} following Dunai (2010). The corrections for individual errors where calculated with fault propagation for each affected sample. All age errors stated on individual exposure ages reflect analytical uncertainties only at the 1σ level. External uncertainties, such as production rates, were not regarded. Uncertainties of calculated mean ages from multiple samples reflect the single biggest uncertainty of these individual sample ages and their individual uncertainties.

3.2.2. Radiocarbon Dating

Since the advent of radiocarbon dating in the 1940s (Arnold and Libby, 1949), many applications have been found to solve questions of geomorphological and Quaternary research (Deplazes et al., 2007). Its ease of use and reliable results are a key factor in producing a detailed overall picture for this work.

We used the radiocarbon method to get minimal ages on specific landforms such as landslides, moraines and glacially polished bedrock. As landslides often block valley creeks and rivers, the water, unable to freely flow further downvalley, produces dammed reservoirs (section 4.3, section 4.4). As the current in such a reservoir is much less than in a flowing creek, small particles, normally in suspension can sink to reservoir floor and produce lake sediments. These sandy or even silty sediments often contain vast amounts of organic materials, which then can be used with the radiocarbon method to produce an age which reflects a minimal age for the underlying landform.

Overall, seven samples were taken during the course of our work (see Table 3.3). Four samples were extracted using Dachnowsky-type probes generously borrowed from Prof. Dr. Dirk van Husen and the Geological Survey of Austria, two samples were taken using generator-driven pile core sampling while one sample was even dug by hand. Because of limited resources, no full cores were taken, instead we aimed to directly sample the lowermost sediment layers. Nevertheless, especially the longer cores (MDUR1 and MDUR3) may have recorded a more extensive late glacial history.

Table 3.3.: ^{14}C samples overview. PCS = Pile Core Sampling, DP = Dachnowsky probe, MD = manual digging

Sample	Depth	Core Start	Core End	Location	Extraction Method	Material
MDUR1	4 m	1 m	4 m	Lenzanger	PCS	wood
MDUR2	1.5 m	0.9 m	1.5 m	Kolm-Saigurn	DP	roots
MDUR3	5.08 m	1 m	5.08 m	Filzenalm	PCS	macrofossils
MDUR4	1.8 m	0.9 m	1.8 m	Grieswiesalm	DP	roots/macrofossils
MSON1	2.1 m	0 m	2.1 m	Melcherböden	DP	macrofossils
MSON2	2.1 m	1.8 m	2.1 m	Melcherböden	DP	macrofossils
MSON3	0.34 m	0 m	0.34 m	Grieswiestauern	MD	macrofossils

The resulting cores were then sent to Dr. Ruth Drescher-Schneider for preparation of well defined subsamples (e.g. macrofossils) and the ^{14}C content of the base layer was measured at the ETH Zürich. The resulting dates are discussed in chapter 5. Uncalibrated radiocarbon ages are given as ^{14}C year BP. Radiocarbon dates have been calibrated using OxCal 4.1 at the 2σ level, with the IntCal09 data set (Bronk Ramsey, 2009; Reimer et al., 2011). Calibrated ages are given as years cal BP for better comparison to ^{10}Be dates.

3.2.3. Errors and Limitations

It must best stressed, that the limitations and drawbacks of these methods (Gosse and Phillips, 2001; Ivy Ochs and Kober, 2008; Dunai, 2010) have to be always kept in mind. Sensible choices when applying and combining them into a synthetic date need to be made, to come as close a possible to the real age of the landform in question.

With ^{10}Be dates, always keep in mind that the errors given only present analytical errors in the 1σ range, stating the probability of this observation is only 68%. Likewise, ^{14}C soil and bog base-layer sample dates only represent the minimal age of accompanying landforms, because soil and bog formation only started an uncertain time lapse after the sample became ice-free. Dates presented here from the radiocarbon method have analytical errors stated in the 2σ range (95% probability), with *years cal BP*. Further complications with the radiocarbon method stemmed from the difficulties of finding enough organic matter in the deeper cores, and disturbance and contamination with younger organic matter, such as roots, in the shallow cores, possible by ground avalanches. Surprisingly, only the shallow cores of the Grieswiestauern and Melcherböden gave acceptable results, as the lower cores likely suffered from the aforementioned problems. Carefully combining these methods can therefore tremendously help coming up with the best possible dates.

4. Field Evidence [Reindl/Bichler]

The foundation of any good chronology is a detailed record of the observations and findings in the field. Where applicable, each topographic area is described with regard to their morphology, sedimentary record, lithology, and key points with an interpretation offered at the end of each section. Topographic locations presented throughout this chapter (Figure 2.2) refer to locations as documented in the geologic map in Appendix C and the official map (`http://www.amap.at`) from the Austrian *Bundesamt für Eich- und Vermessungswesen*.

4.1. Hüttwinklache [Reindl]

The Hüttwinklache is crossing the study area from south to north, originating at the current glacier terminus of the Goldbergkees, and also crossing many of the areas later described in this chapter (Figure 4.1).

At the forefront of the LIA moraine, the creek produces a deep incision in the steep terrain down to the area of Kolm-Saigurn, an area famous for its waterfalls, and, in winter, icefalls (section 4.9, Figure 4.15). In the area of Kolm-Saigurn (section 4.4) the creek flows less turbulent and is the source of typical creek sediments as sandbanks and gravel deposits. The creek here flows right at the border between the Durchgangwald in the east (section 4.2), and multiple talus fans from the direction of the Pilatuskees and the scarp of the Grieswies-Schwarzkogel (section 4.5). These alluvial fans and debris flows push the creek towards the Durchgangwald, while they fill up the valley floor. A shallow profile along the creek highlights this process (see Figure 4.2).

The profile starts at the top with 10 cm grain supported, subrounded to subangular gravel (Gc), partly imbricated. Lithology is mostly made up from Zentralgneis, with traces of biotite-mica-schist and quartzite. This topmost layer is followed by massive sand (Sm) and fine sand and silt layers (Fm/Sm), both 5 cm thick. Going deeper in the profile, an approximately 3 cm thick layer of gravel lies atop a thin layer of dark peat (P), notably dividing the profile in an upper and lower part. Below this peat, massive

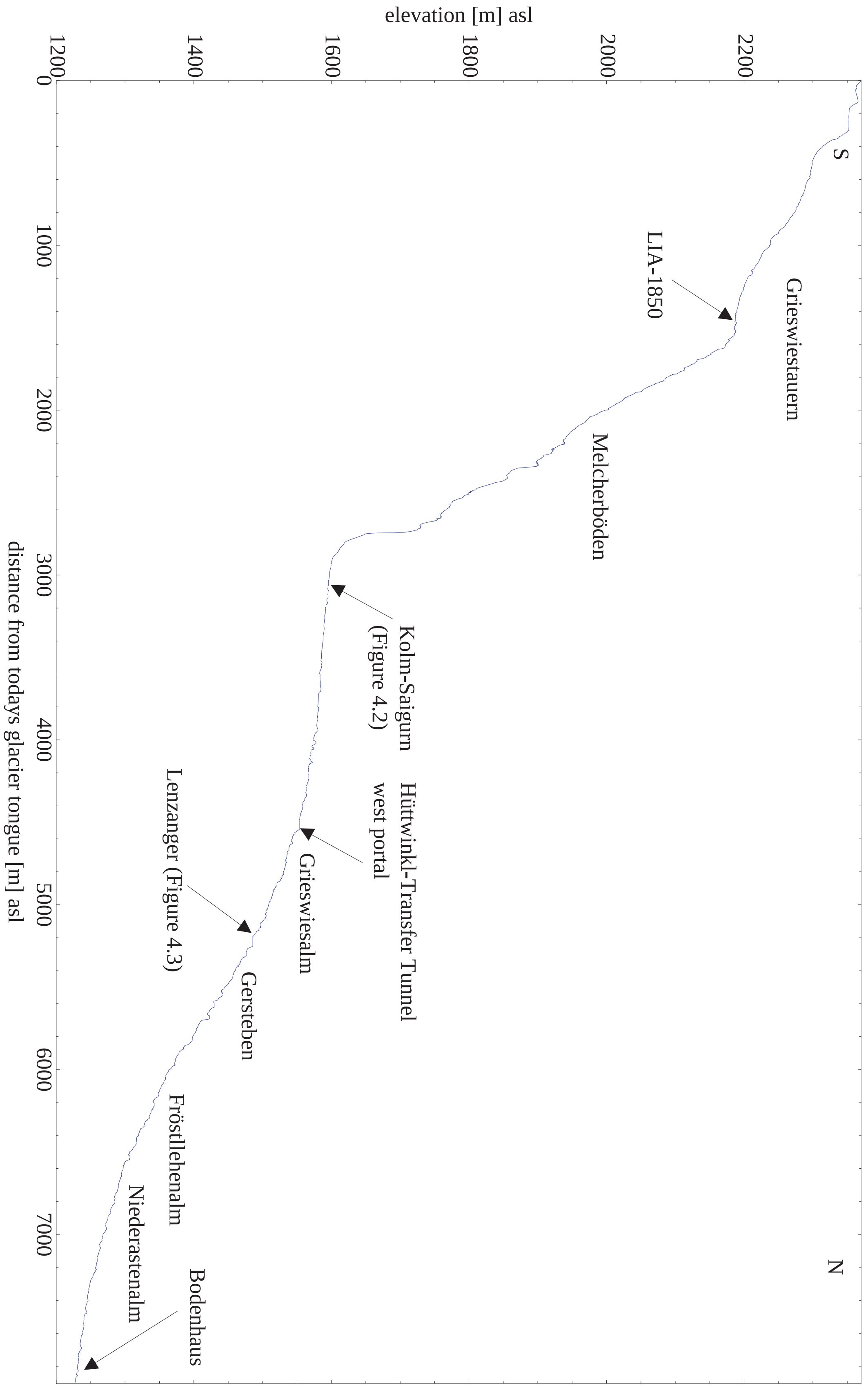

Figure 4.1.: Profile along the path of the Hüttwinklache, starting at the present glacier outflow in the south and ending at the Bodenhaus in the north.

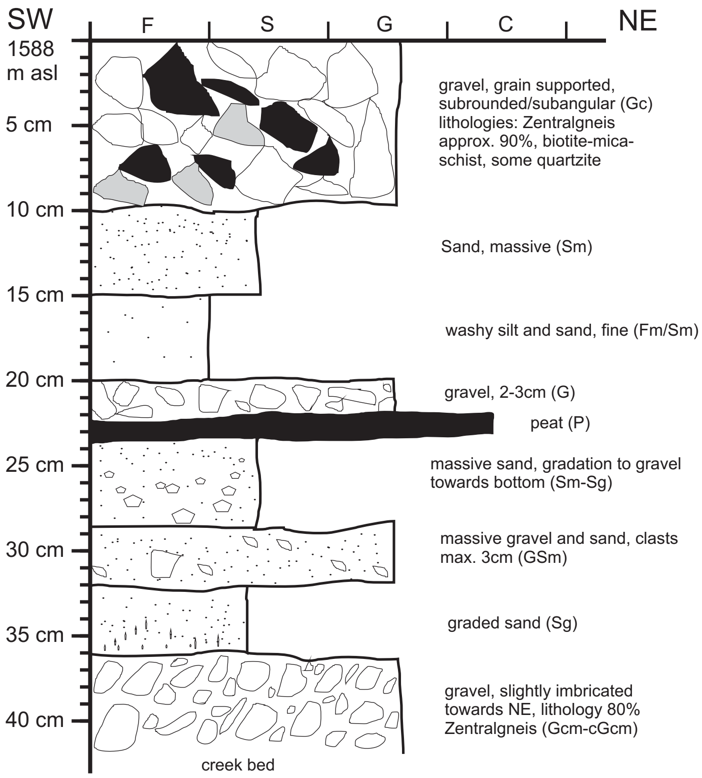

Figure 4.2.: Profile of the Hüttwinklache, as located north of Kolm-Saigurn. The profile is located at an approximately 0.5 m deep incision and sheds some light on the very recent sedimentary history in this area.

sand with a gradation to gravel sets in with a thickness of approximately 5 cm (Sm-Sg), further followed by a 5 cm thick layer of massive gravel and sand deposits with clasts (GSm) up to 3 cm in diameter. The final two visible layers of the profile consist of a 5 cm thick layer of graded sand (Sg), topping a layer of slightly imbricated layer of gravel. The imbrication in this lowermost layer trends towards the NE. Lithology of the gravel is mostly made up from Zentralgneis (Gcm-cGcm).

The sedimentary evidence in this profile starts with fluvial sedimentation in a high energy enviroment with the typical spectrum of partly imbricated gravel. Sand may represent infill of the channel. Shallow water conditions, which even led to the onset of peat build up, followed again by more energetic conditions. The imbrication confirms the theory of mass transport from the west, as additionally visible from the hillshade model and the Zentralgneis clasts which can only originate from the Sonnblick/Hocharn area (see section 2.4). This peat was then buried again with multiple layers of sand and gravel until the onset of the current surface and soil. Overall, the profile here shows the complicated interaction between the sediments from the Hüttwinklache from the south and the talus fans from the SW producing overbanking and channel-fill situations.

Much of the water is removed from the creek via the Hüttwinkl Transfer Tunnel since its opening in 1981, but during the Holocene the creek was able to start to incise again, beginning at the western portal of the Hüttwinkl Transfer Tunnel.

On its way through the valley, the creek produces a canyon, dividing the area of the Grieswiesalm on the orographic left side from the Lenzanger on the right side. Steep, up to 30 m deep slopes mark the ridges of this canyon. On the orographic right flank of the canyon a 20 m high profile marks a key point in understanding the late glacial chronology of events (Figure 4.3)

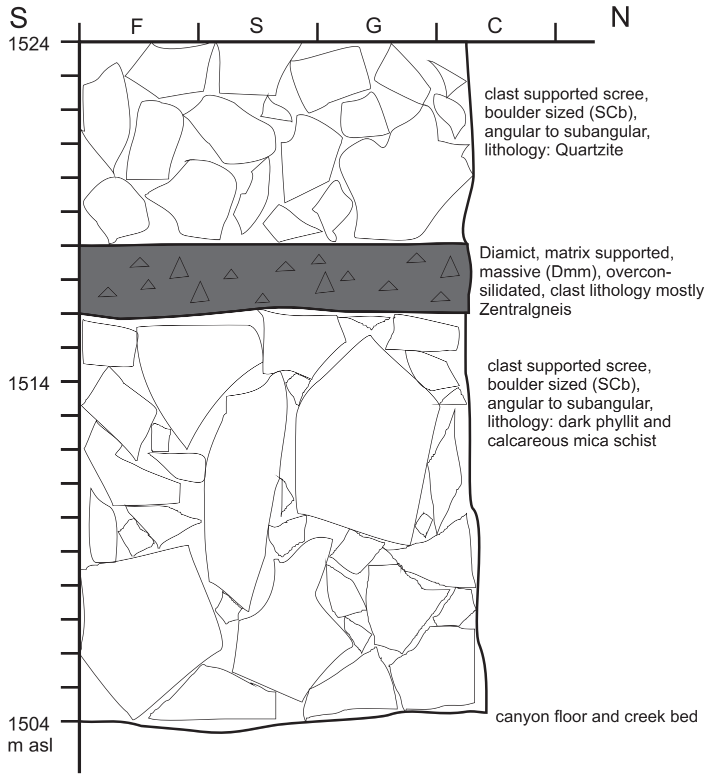

Figure 4.3.: Profile of the Hüttwinklache, as located west of the Lenzanger. The profile covers the vertical area between the terrain edge on top and the creek at the bottom.

The canyon floor and creek bed here is filled with meter-sized mica-schist blocks. Garnet is rare in these blocks, but can be found sporadically. These conditions can be traced up to 12 m above the creek bed. Diamict, matrix supported, well consolidated, and massive (Dmm), covers the next 2 m of the profile. Zentralgneis makes up most of the components, with other lithologies like garnet-mica-schist rarely occuring. The diamict is then covered by 6 m of meter sized quartzite boulders, up to the erosional edge of the creek canyon.

Looking at the overall profile, we interpret the lowermost blocks as landslide boulders from the Durchgangwald landslide (see section 4.2), covered by a layer of basal till from a glacial advance, which in turn was again covered by a quartzite landslide (section 4.5, section 4.6) after the recession of the glacier.

Deposits made up by quartzite boulders disappear at the onset of the distinctive terrain step, north of Gersteben (see section 4.7). Instead, thin basal till, similar to deposits more upstream cover the blocks on the creek's orographic left flank. Basal till can mostly only be identified by the existence of subangular, striated Zentralgneis clasts, because neither the sand matrix is strictly good consolidated, nor can deposition of Zentralgneis from the Hüttwinklache itself be excluded. This becomes apparent when investigating the bed load, which includes all lithologies found upstream. Most common are the well rounded Zentralgneis and calcareous-mica-schist blocks, but garnet-mica-schist and biotite-schist can also be found, up to several cubic meters in volume.

Further downstream, towards the Bodenhaus (see section 4.7), the creek loses momentum as the valley flattens out. Up to the Niederastenalm, the creek is always bound to the orographic left flanks of the Hüttwinkl valley where no alluvial fans and debris flows from the west filled up the valley floor and the creek was able to incise into the lateglacial deposits. Now as the terrain flattens out, it is able to flow more freely in the center of the valley. Angular to subangular biotite-schist boulders mark the flanks, while the bed load seems unchanged from the upstream sections. South of the Bodenhaus, several parallel erosion edges can be identified along the creek path. At the Bodenhaus, the creek cuts through a distinctive border. South, the terrain is dominated by large, angular blocks of garnet-mica-schist and biotite-schist, while to the north the flats of the Bodenhaus (section 4.7) abruptly change the morphological appearance of the valley. This border marks the northern extent of the Durchgangwald landslide (see section 4.2).

4.2. Durchgangwald [Reindl]

4.2.1. Description

Delimitation of the Durchgangwald area can be difficult. Due to its size overlaps with other topographic areas exist. The local name *Durchgangwald* only refers to the forest dominated area between the triangle Kolm-Saigurn, Filzenalm and Lenzanger. The natural borders in the west are the Hüttwinklache and the area of the Grieswiesalm, the basin of Kolm-Saigurn delimits the Durchgangwald-landslide to the south together with the ridges of the Durchgangriegel. The Filzenalm marks the most easterly point. North of Gersteben and Lenzanger a distinctive terrain step prominently separates the Durchgangwald from the more northerly areas of the Niederastenalm and Pirchlalm. This step is surmounted by the toll road by the means of four serpentines, easily identifiable on topographic maps.

Even though the landslide solely consists of loosened rock on the surface, we were able to map the extent of three distinct lithologies. The western sector is dominated by three areas containing unsorted, angular, sometimes house-sized calcareous-mica-schist blocks (see map in Appendix C). Some outcrops show that the calcareous-mica-schist makes up the subsurface lithology of the till covered slopes east from the Hüttwinklache. The calcareous-mica-schist can be traced below the till to the creek, where outcrops show big, up to several meters in diameter, angular boulders. A small occurrence exists east of Gersteben, and a slightly bigger area can be mapped north of the Trockenbach and the serpentines. The central area consist mainly of a uniform belt where big boulders are rare. Towards the Filzenalm and the southeastern border garnet-schist becomes more common, forming a belt from the Trockenbach to the basal till deposits north of the Ammererhof. This area is characterized by chaotically deposited boulders on the surface. All the material was deposited chaotic. In general, the boulders are angular, delimited by more or less sharp foliation and cleft areas. Sand and silty material is distributed non-uniform between the blocks, and sometimes it is even completely missing, allowing for extensive voids between the blocks. Sometimes the sand and silt seems to form a matrix around the blocks, making it difficult to distinguish the landslide from glacial deposits. In this case, the presence of Zentralgneis and better rounded components is an indicator for glacial deposits. Water filled depressions are present all over the Durchgangwald, attributing to the alternative local name *Rauriser Urwald* (primeval forest). Weathering of the mica-schist-rich blocks results in the formation of fine grained, partly clayey, material. These clay minerals allow for a perfect sealing of the soil, as also documented by von Poschinger (1986). Even during long dry periods the water does not evaporate or ooze away, giving a habitat to a rich fauna of midges and insects.

As outlined before by (section 2.3), the western part of the Durchgangwald is covered by till (Dmm). Components are mainly calcareous-mica-schist and Zentralgneis, with an approximate 1:1 ratio in the south in the area of Kolm-Saigurn and a tendency of a higher schist proportion towards the north. East of the Ammererhof, sand and silt deposits alternate with till. North of the Ammererhof, a series of parallel ridges can be identified (Figure 4.4), with the highest ridge marking the border to the undisturbed landslide deposits. Starting at the valley bottom, up to nine parallel moraine ridges can be identified. Moraine ridges 1–7 are generally equally spaced by approximately 50 m (also see: section 6.1), while number 8 is set of by approximately 100 m from the first batch. The right lateral maximum moraine ridge, number 9, has the biggest offset from the first group. Several Zentralgneis boulders mark the course of the ridges up to the area of the western portal of the HTT (section 2.3).

Apart from this glacial landscape described above, several huge blocks of of calcareous-mica-schist have been deposited on the Zentralgneis bearing till northwest of the western portal of the HTT. The internal layering is not consistent between these blocks. They show a high degree of weathering, sometimes to the point where the only form self contained hills with a thick soil cover. This thick soil cover makes them almost unrecognizable as blocks from the outside. The weathered mica-schist from these blocks seals the soil from infiltrating water into the till sediments and underlying blocks. This is similar to the areas in the east of the Durchgangwald, as described above. Therefore, rain and surface water is unable to escape the sealed depressions adjacent to the distinctive till covered ridges, forming small ponds and shallow bogs. Where the hills seem to be made up by multiple blocks, components display an angular, clast supported, monomict character (SCc, sometimes SSC). While this phenomenon is limited to the northwestern area of the HTT portal, delimitation can be difficult in areas where calcareous-mica-schist is visible below the till, which is especially true uphill from the valley floor and the Hüttwinklache.

4.2.2. Interpretation

The lowermost and oldest deposits in the Durchgangwald stem from a single, tremendous landslide, covering the valley floor and reaching up to the opposite valley side to the Filzenalm (section 4.3). As mapping shows, the northern sector of the landslide mass broke off from the main mass and dynamically flowed downvalley forming a sturzstrom to the area what today is the Bodenhaus (section 4.7), thus forming the Gersteben step. This means that the basin of Kolm-Saigurn at 1600 m asl was free of glaciers during this event and allows us to set the lateglacial timeframe for this event. The lithology of the boulders in the Durchgangwald landslide reflects the lithology of the bedrock in the Grieswiesalm (section 4.5) on the western flanks of the Hüttwinkl valley. Zentralgneis and greenschist, as found on the eastern flanks, are not present inside the landslide mass, therefore further suggesting the origin of the Durchgangwald landslide from the

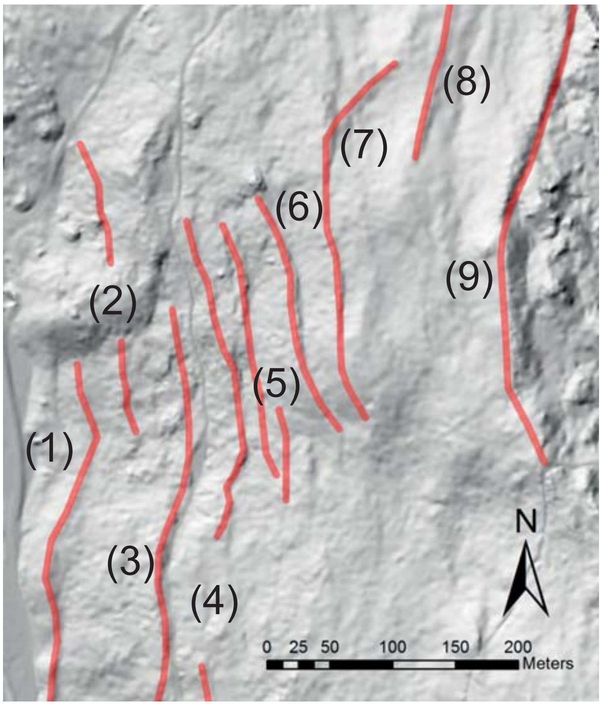

Figure 4.4.: Hillshade model overview of the Durchgangwald moraine ridges, marked by numbers 1–9.

prominent scarp of the Grieswies-Schwarzkogel.

Basal till deposits and ridges on the Durchgangwald not only document the maximum extent of the glacier following the landslide event, but also document the advance and retreat thereof. The till and sand successions of Kolm-Saigurn (section 4.4) very well display the glacial advance in the basin, when ice quickly started to fill up the valley head, flowing down from the Goldbergkees and blocking creeks from continuing into the basin. A maximum ice thickness of approximately 180 m was reached in the basin, while the glacier tongue transported Zentralgneis from the higher areas of the Sonnblick and Hocharn areas, together with calcareous-mica-schist from the Durchgangwald landslide toward the Lenzanger and the Gersteben step. This maximum extent is very well preserved on the right lateral side, but much less at the glacier terminus. The left lateral pendant was later reworked and is not visible anymore (section 4.5).

Following a supposedly quick, intense glacial advance to the maximum extent, several phases of stabilization of the ice margin during recession can be identified in the field (Figure 4.4), east of the western portal of the Hüttwinkl-Transfer-Tunnel (section 2.3). Internal grouping of the ridges is difficult, because they are evenly spaced, and only the right lateral moraine has a different offset, but the evidence still suggests a slowly decaying glacier with multiple stable, sometimes re-advancing phases, typical for an Egesen-type glacier (Kerschner, 2009).

The strongly weathered calcerous-mica-schist boulders northwest of the HTT portal can be interpreted as outliers from the Quartzite landslide (section 4.5), where blocks came down on the thin till coverage, but a separate later event or deposition by the decaying glacier cannot be excluded.

4.3. Filzenalm [Reindl]

4.3.1. Description

The Filzenalm, together with the Durchgangalm, is located to the east and southeast of the Durchgangwald landslide (section 4.2) and mark the eastern limits of the study area. An unpaved dirt track leads here from Kolm-Saigurn (section 4.4) and the Ammererhof, allowing us to study the various deposits towards the Filzenalm. When entering the area Durchgangalm, we leave the rough forest of the Durchgangwald and enter an open area of alpine meadows. The Filzenalm and the Durchgangalm are separated by a creek, giving some insight of the very recent sedimentary history of the area. A typical cross section at the creek flanks [located at Figure 4.5 (b)] starts with a 20 cm soil coverage at the top, followed by 10 cm of flaky, subangular or subrounded components, classified as GS. Lithologies include biotite-schist and Zentralgneis, up to 10 cm in diameter. Continuing to the creek bed, we can identify 40 cm changing layers of gravel, sand, fine sand, and silt. The subangular gravel is mostly clast supported. The lowermost visible parts again display fine, sandy sediments. Further upstream from the Durchgangalm, in a similar cross-section, an imbrication to the west can be identified.

The direct surroundings of the Filzenalm show a similar picture. An exception is a wedge of wetlands [Figure 4.5 (c)]between two tongues of the rough, blocky, terrain of the Durchgangwald landslide [Figure 4.5 (a)]. The approximate size of this area is 10 000 m^2 and still contains open water areas towards the center and most western parts. A drilling resulted in a maximum depth of 5.08 m where weathered layers of biotite-rich schist was met. Deposits were strictly confined to water rich sandy and silty sediments, poor in organic material. No peat was found during the drilling, except for a thin top layer of organic material.

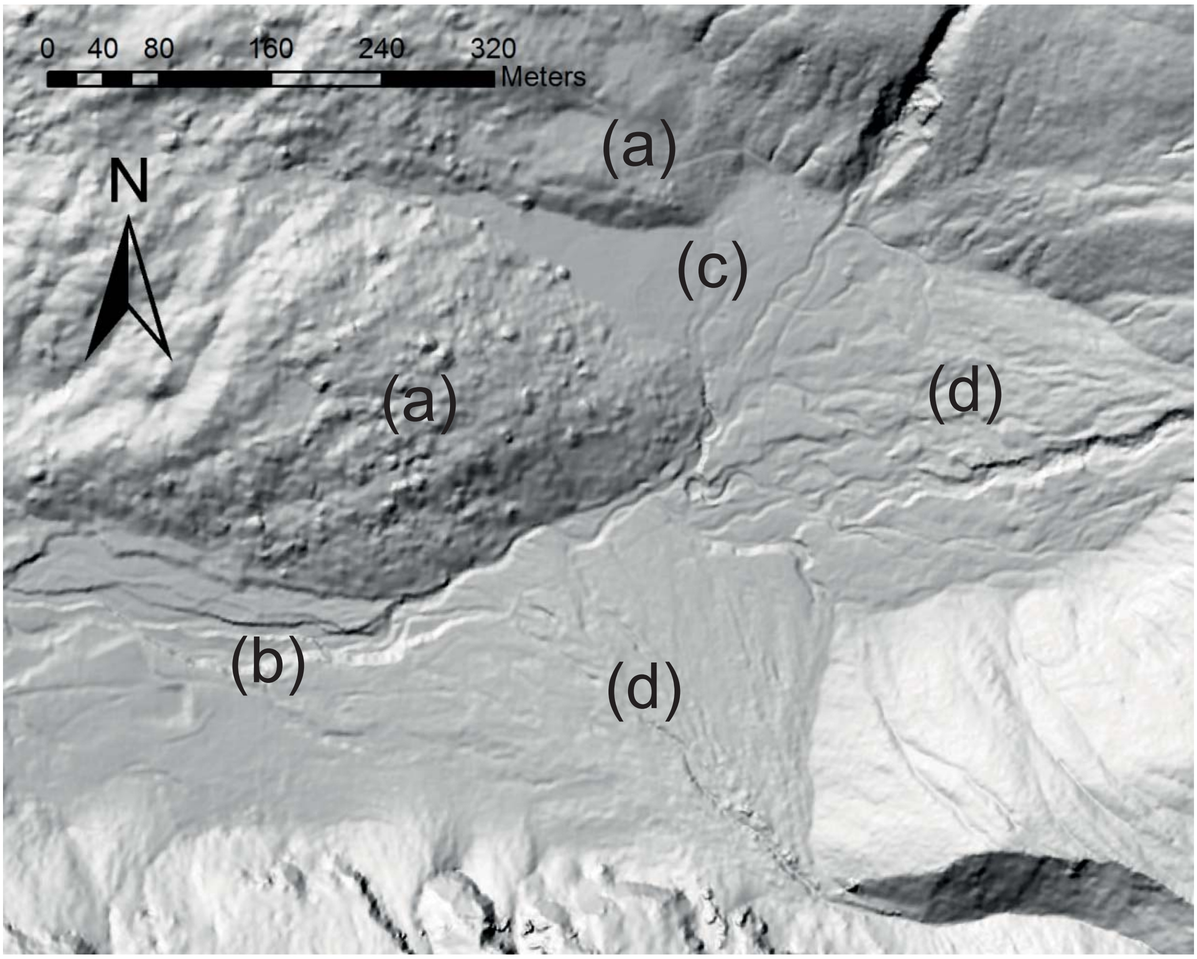

Figure 4.5.: Hillshade model overview of the Filzenalm and Durchgangalm areas, with the tongues of the Durchgangwald landslide (a), the E-W flowing creek with several cross-sections (b), the Filzenalm wetlands (c), and talus fans from the W and SW (d).

4.3.2. Interpretation

The sedimentary facies of the outcrops along the creek incision indicates a small braided river system in recent times, with a flow direction from E to W, as also present today. Several alluvial fans and debris flows from the S and SE influenced this area, as visible in Figure 4.5. The Filzenalm alluvial fan shows a transport from the east, overlapping the deposits of the Durchgangwald landslide. Sediments of the Filzenalm wetlands therefore can only be younger then the Durchgangwald landslide and could be used for ^{14}C dating. The Filzenalm wetlands indicate a blocking of the creek from the E when the landslide came to rest, thus forming a lake at its eastern border, as documented by the sandy and silty sediments of the drilling. Lack of both peat and extensive organic sediments indicate a constant filling with sand and silt from the east which is today almost complete as the wedge reaches the point of full siltation. Assuming that this process started right after the landslide and deposition occured constantly, the Filzenalm sediments contain evidence for the Holocene history of the area and even parts of the Lateglacial development. Further investigation of the Filzenalm wetland and additional core drilling could help to understand the lateglacial and Holocene history further.

4.4. Kolm-Saigurn [Bichler]

4.4.1. Description

The basin of Kolm-Saigurn marks the terminal point of the valley head of the Hüttwinkl valley. Before and during the LIA, Kolm-Saigurn was the central point of mining activity in the area, with transportation from and to the surrounding mountain peaks and flanks (chapter 2).

To the south and west, the terrain quickly rises to the glacier polished bedrock of the Melcherböden (section 4.14) and the plateaus and talus fans of the Grieswiestauern (section 4.9). To the east, the ruptured ridge of the Durchgangriegel (section 4.15) runs below the Durchgangwald landslide mass and its glacial deposits.

Sediments in the flat basin consist mostly of fluvial and alluvial sand and gravel from the creeks meeting here, as outlined by the Hüttwinklache cross section located in the western part of the area (section 4.1) which also documents the input of alluvial fans and debris flows from the west and south west. It is likely that the Durchgangwald landslide formed a natural dam, and blocked the historic Hüttwinklache from continuing to flow downvalley and therefore formed a lake with sand and silt deposits in the basin of Kolm-Saigurn (von Poschinger, 1986).

Sand and silt deposits (Sm) can be found uphill behind the Ammererhof, where they are interlaced with a diamict (Dmm) containing Zentralgneis clasts. At the triple-point, where the Durchgangwald landslide, the creeping mass from the Durchgangriegel (von Poschinger, 1986) and the mountain pasture of Kolm-Saigurn meet, thin layers of clay and silt are preserved (see Figure 4.6). Slightly more to the south two massive terraces developed. They are built up by mighty gravel, sand and silt layers (approximately 10 m high) and topped by a thin layer of basal till (Dmm). The components of gravel-stone size, consisting mostly of dark phyllite and mica-schist, are subrounded to rounded and sometimes show imbrication to the W. The terraces overlap the Durchgangriegel creeping-mass coming from the east (see Figure 4.7.

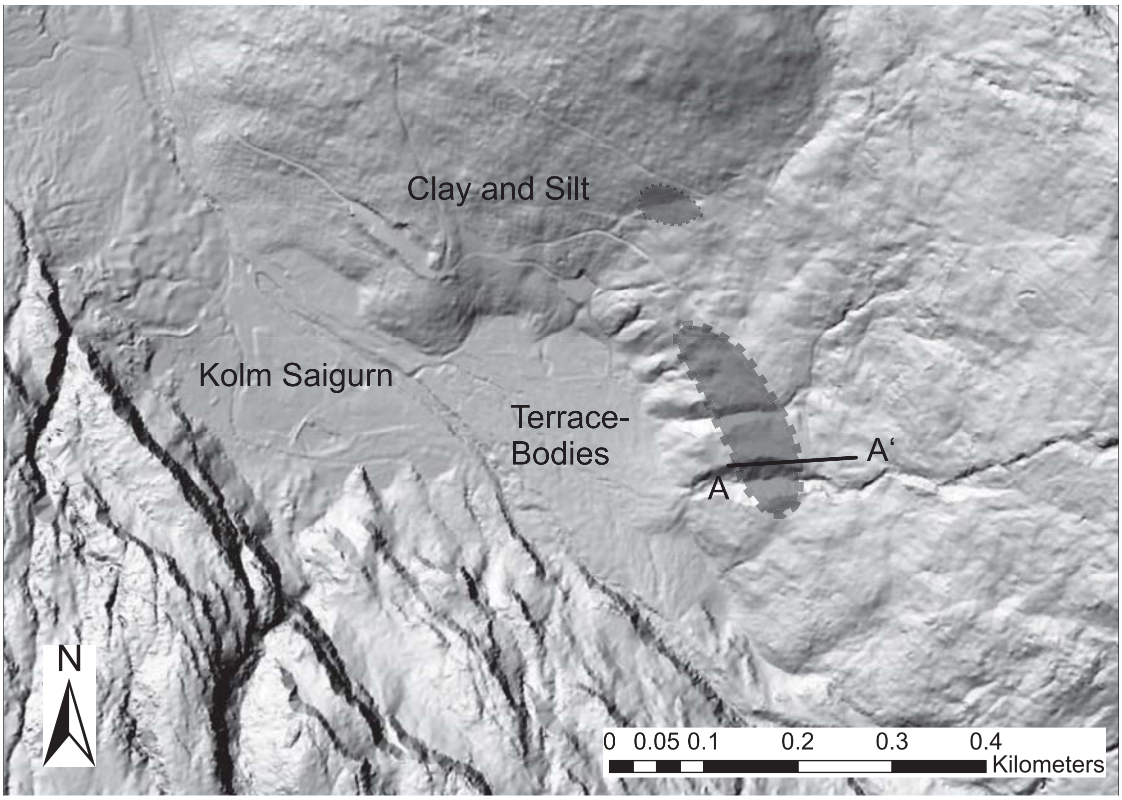

Figure 4.6.: Hillshade model overview of the area east of Kolm-Saigurn. Our evidence for ice-margin sediments as described in subsection 4.4.1 are marked. The cross-section line shown refer to the detailed cross-section in Figure 4.7.

4.4.2. Interpretation

Especially the clay and silt layers as well as the terrace bodies are of great interest. We interpret these sediments as the only evidence of the advancing glacier, where the growing ice blocked creeks from delivering their suspension load into the valley, therefore forming ice margin lakes and deltas during stable phases of the advance. Finally as a result of ongoing increase of ice thickness, the glacier advanced over the ice marginal sediments and deposited a till (Dmm) on top. The process then started all over again until the maximum ice thickness was reached. The clay layers show at least a partial time of lacustrine conditions at the ice-margin. As the terrace bodies overlap the creeping-mass from the Durchgangriegel, they seem to have stabilized the latter.

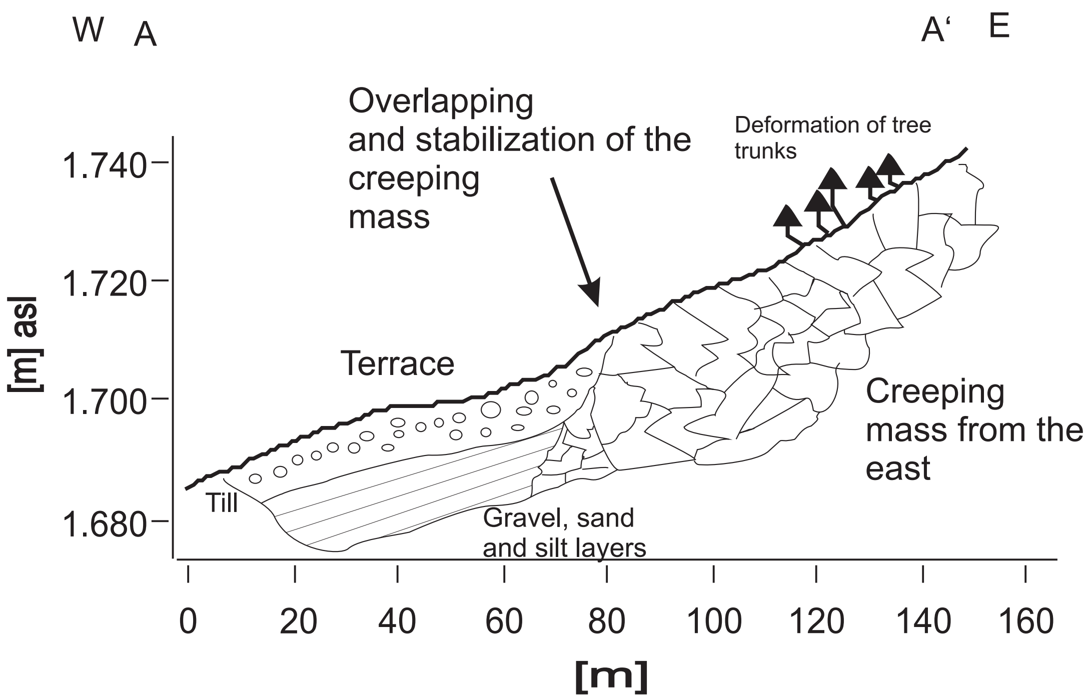

Figure 4.7.: Simplified profile of the overlapping situation marked in Figure 4.6.

4.5. Grieswiesalm [Reindl]

4.5.1. Description

The Grieswiesalm area encompasses the orographic left side of the Hüttwinklache (section 4.1), northwest of Kolm-Saigurn and reaches up to the summit of the Grieswies-Schwarzkogel (3116m asl). The southern valley floor here is mostly free of trees, in contrast to the Durchgangwald which builds up the orographic right valley floor and flank (section 4.2). Instead, extensive, slightly inclined meadows with alpine dairies dominate the scene, interlaced with meter-sized boulders of varying lithology and angularity. Zentralgneis can be found uniformly distributed in the sediment record of the area, and is not bound to any distinctive morphological landforms in the area. Close to the Hüttwinklache, several small outcrops document the very recent history of this area (section 4.1).

The steep flanks west of the Grieswiesalm (Figure 4.8) form a half-circle opening towards the east, exposing the varying bedrock lithology. Bedrock mapping by Alber

(1976) shows a succession from the top of calcareous-mica-schist, sometimes quartzitic with interlaced bands of quartzite in the northern section of the half-circle, followed by dark, phyllitic biotite schist, and, lowermost, garnet-mica-schist visible on the north and south ends of the half-circle. The summit area of the Grieswies-Schwarzkogel itself is made up from biotite-rich dark phyllite.

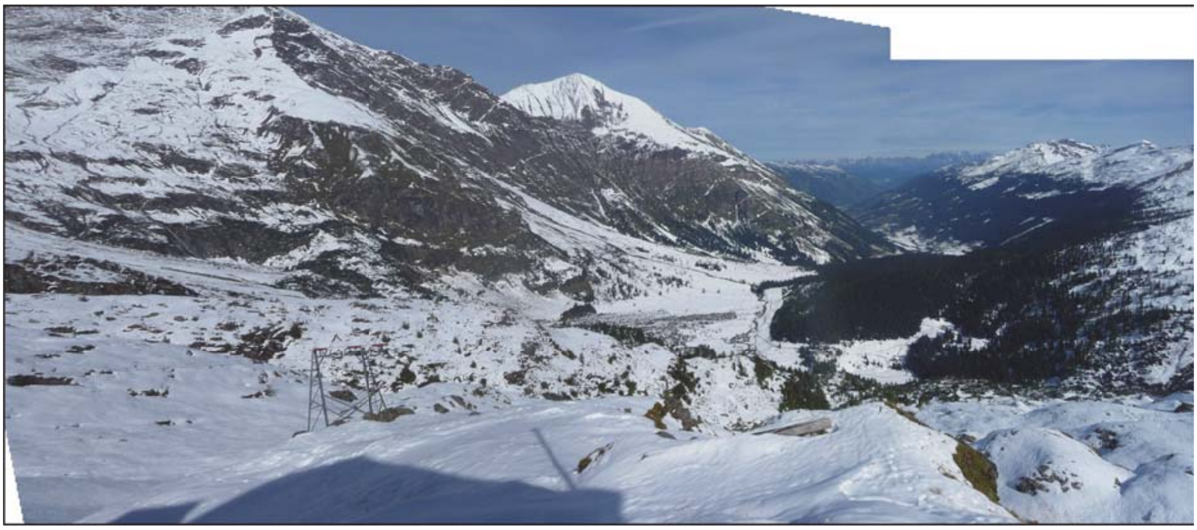

Figure 4.8.: North looking composite panorama image of the Grieswiesalm (center), the Durchgangwald (right) and the Grieswies-Schwarzkogel south face (left). The east facing flanks of the Grieswies-Schwarzkogel, forming a distinctive half-circle, are dominated by steep bedrock, lacking any snow cover.

Around the Grieswiesalm alpine dairy morphology is similar to the southern area. Sedimentary evidence of several outcrops in the vicinity of the dairy shows a succession of different layers of silty, massive, sometimes fine sand (Sm) and gravel (GSm), topped by a soil cover of approximately 3 cm. Other outcrops display successions of clay and gravel (Fm to Gm), bound to the shallow angled areas, similar to the southern Grieswiesalm sectors. Often extremely weathered calcareous-mica-schist blocks can be found embedded in these fine sand sediments, sometimes forming hills several meters in size. The close proximity to the hills northwest of the western portal of the HTT (section 2.3, section 4.2), suggests a common history of these phenomenons. Layering of these blocks is internally consistent, but varies between separate blocks in the area.

Towards the Hüttwinklache, quartzite blocks embedded into fine sand become more abundant, seemingly forming islands peeking out from the flat areas surrounding them in the direct vicinity of the Grieswiesalm. A shallow peat bog lies on the biggest quartzite island, just west of the Hüttwinklache. Probing resulted in a baselayer of extremely weathered, biotite-rich dark phyllite at a depth of 1.8 m.

4.5.2. Interpretation

Sedimentary evidence shows the Grieswiesalm is dominated by multiple alluvial fans and debris flows from the southwest, towards the direction of the Pilatuskees and from the west, the steep eastern flanks of the Grieswies-Schwarzkogel. As no outcrops of Zentralgneis are documented there, these alluvial fans and debris flows often resedimented former till and possibly even eroded the left lateral moraine ridges of the Kolm-Saigurn glacier system (section 5.2, section 4.2).

The half circle east of the Grieswies-Schwarzkogel can be interpreted as the scarp of the Durchgangwald-landslide (section 4.2). Lithology strongly suggest an origin from this area, as the succession matches the deposits of the Durchgangwald landslide, assuming a uniform slipping of the whole eastern flank of the Grieswies-Schwarzkogel towards the east. This mechanism explains the garnet-rich phyllite blocks of the Durchgangwald, west of the Filzenalm. Overall, the Durchgangwald boulder lithology succession reflects the bedrock lithology succession in this area.

The quartzite and calcareous-mica-schist blocks can be attributed to one or several smaller events where bedrock slid down the flanks when the valley was ice-free during the Holocene. Especially the calcareous-mica-schist blocks where eroded and weathered during the time, forming distinctive hills, while the Quartzite blocks of the Grieswiesalm form the western areas of the landslide deposits of the Lenzanger. The sum of visible quartzite area blocks not covered by alluvial fans and debris flows on the orographic left side is approximately 60 000 m^2. An unknown area is today covered by alluvial fans and debris flows, but can be estimated to attribute another 40 000 m^2 of quartzite blocks surface area.

4.6. Lenzanger and Gersteben [Reindl]

4.6.1. Description

The Lenzanger area marks the orographic east pendant to the Grieswiesalm (section 4.5) on the orographic left side of the Hüttwinklache [section 4.1, Figure 4.9 (e)]. Today, the Lenzanger area is a parking space [Figure 4.9 (c)] for tourists visiting the head of the Hüttwinkl valley. The parking space is founded on silt and sand sediments (Sm), a drilling on the northern border of the parking area, resulted in 4 m of these sediments on a baselayer of weathered calcareous-mica-schist. The Durchgangwald area encompasses this area on the south and east [Figure 4.9 (a)]. Zentralgneis bearing diamict (Dmm) can be found when leaving the flats of the parking space [Figure 4.9 (b)]. Uncovered calcareous-mica-schist boulders can be found outside the diamict covered areas on the east [Figure 4.9 (a)], and again appear on the outcrops of the Hüttwinklache, separating the Lenzanger from the Grieswiesalm, therefore running below the Lenzanger sediments. In several of these outcrops fine, white, precipitated lime can be found, stemming from the dissolution and weathering of calcareous-mica-schist blocks. Quartzite blocks up to 10 m in diameter are prominent between the parking space and the Hüttwinklache. Sometimes calcareous quartzite boulder deposits also extend further north towards the terrain step of the Gersteben and serpentines of the toll road, until the onset of Zentralgneis-bearing diamict again marks the northern end of the angular block deposits. The overall surface area of the quartzite-blocks covered area can be estimated to be around 0.3 km^2.

4.6.2. Interpretation

Three major events and their deposits can be identified in the Lenzanger area, making it one of the key areas for this study. The Durchgangwald landslide deposits can be found in the outcrops of the Hüttwinklache as lowermost layers. East of the Lenzanger, the landslide is covered by till from the advance of the Kolm-Saigurn glacier system (chapter 6). Till coverage is thin at the border and grows to the amount of 2 m in the outcrops of the Hüttwinklache. After the ice melted, a minor landslide, mostly consisting of calcareous quartzite and calcareous-mica-schist from the Grieswiesalm scarp covered the till and blocked parts of the Hüttwinklache and the creek from the Filzenalm, therefore forming the Lenzanger Lake, which remnants are today used as the Lenzanger parking space. The only uphill source of the quartzite can be found on the northern sectors of the Grieswiesalm scarp. In contrast to the Grieswiesalm, the quartzite blocks here mark the top-most Holocene sediments and are not embedded or covered by resedimented deposits and talus fans. Estimating the overall volume of the quartzite landslide is difficult, and it can only be ascertained to be of much smaller size than the Durchgangwald landslide. Remnants of the former lake can be found on the northern outskirts of the parking space, where a minor open water area exists between quartzite boulders. Today, the Hüttwinklache, and partly, the creek from the Filzenalm cut through these sediments.

As the Lenzanger parking space is located in a distinctive pocket alongside the path of the former ice, it can be suspected that this area marked the terminal point of at least

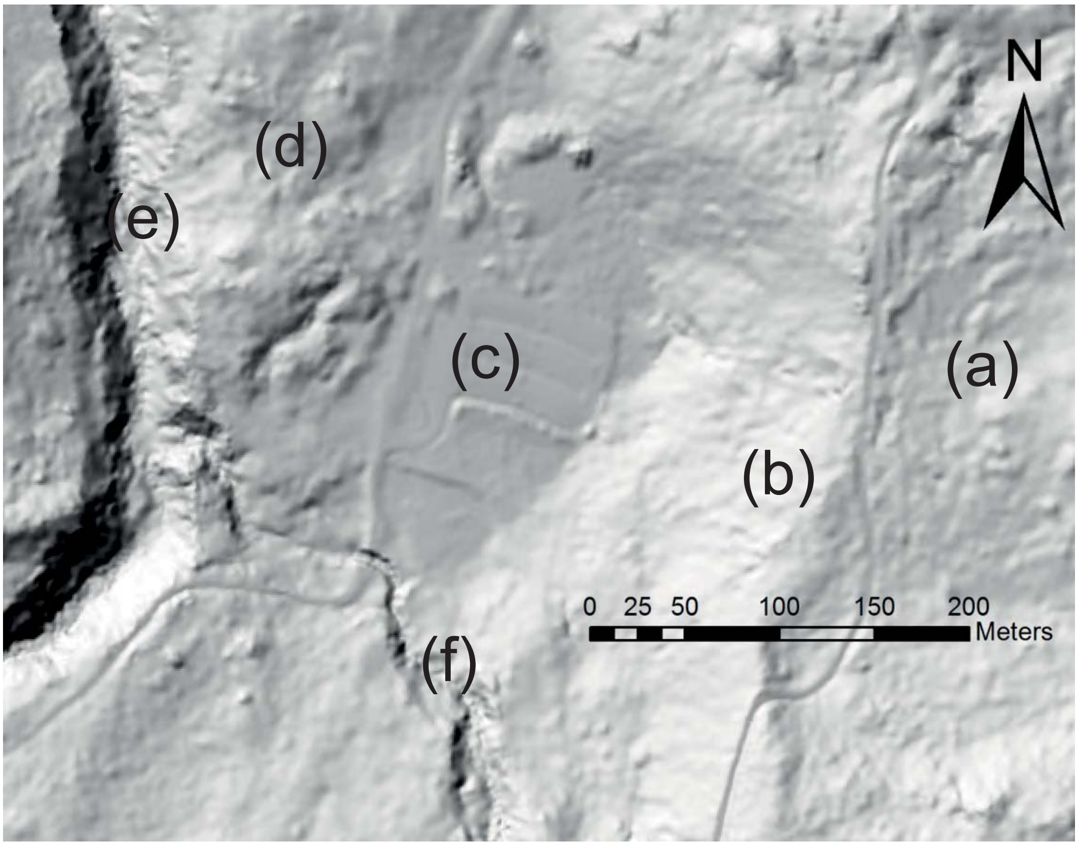

Figure 4.9.: Close-up hillshade image of the Lenzanger area. The flat parking space with separate lanes is well visible (c), as is the Hüttwinklache (e) and the creek from the Filzenalm (f). (a) marks the area of the Durchgangwald, separated from the Lenzanger area by (b) glacial deposits building up a relatively smooth surface with an apparent right lateral ridge. (d) marks the rough terrain of quartzite boulders adjacent to the Grieswiesalm.

the decaying Kolm-Saigurn glacier, now covered by lake sediments and the quartzite landslide. Extrapolating the moraine ridges of the Durchgangwald at Kolm-Saigurn, this seems plausible but cannot be proved as no evidence for terminal moraines could be identified in the field. Still, the unique setting of three major events and their sedimentary record allows us to reconstruct a chronology where each event is temporally constrained by neighboring events. This is especially true for the timing and extent of the glacial advance and retreat which is limited both by the Durchgangwald landslide and the Quartzite landslide.

4.7. Bodenhaus [Reindl]

4.7.1. Description

The Bodenhaus delimits the northern border of our study area. The term *Bodenhaus* actually refers to the inn, situated on the valley floor at the booth of the toll road leading S to Kolm-Saigurn. It separates the wide, flat grass terrain in the north from the rough, uneven and elevated forest areas in the south [Figure 4.10(a)]. The southern limit of the border can be found at the Trockenbach, a creek bearing meter-sized Zentralgneis boulders from the east, originating from LGM deposits uphill. The Hüttwinklache [Figure 4.10(d)] divides the area up to the Niederastenalm in two areas: the alpine dairy of the Fröstllehenalm in the west [Figure 4.10(e)], and the former mining areas and smitheries of the Astenschmiede (the German word for smithery is *Schmiede*), the Pirchlalm and the Niederastenalm [Figure 4.10(b) and (c)]. The Astenschmiede, being a former smithery area displays extensive man made slag deposits. Contrary to the distinctive terrain drop on the opposite of the valley, north of the Fröstllehenalm [Figure 4.10(e)], the terrain here decreases less abruptly.

Two distinctive, almost perfectly round, crater-shaped depression are also located in this area. The bigger one has a diameter of approximately 20 m, and is also very well visible on the hillshade image. The second is located slightly northwest of the first, being much smaller with an approximate diameter of 5 m. Both are currently filled with water and plants and remained inaccessible for baselayer sampling with the methods available to us.

Deposits to the left and to the right of the creek are made up from dark, biotite-rich phyllite angular to subangular boulders, typically up to several meters in diameter, the exception being a lens of garnet-mica-schist between the Astenschmiede and the Pirchlalm, only marginally reaching over to opposite valley floor. The degree of weathering and decomposition of the blocks is comparable to boulders found in the Durchgangwald (section 4.2). The garnet-mica-schist lens displays some remarkable meter-sized boulders on its northern border, just south of the Astenschmiede. These boulders are made up by prasinite containing well visible quartz and chlorite grains, with very weak foliation. Similar bedrock lithology can be found north of the Grieswies-Schwarzkogel summit and, much more prominent, on the flanks of the Ritterkopf (3006m asl), west of the Ritterkaralm [Figure 4.10(f)]. The rough boulder areas are often covered by sand, silt, and gravel successions, bound to the outflows from several creeks at the Fröstllehenalm and along the eastern rim where the terrain starts ascending towards the eastern flanks of the Hüttwinkl valley. Especially the sediments on the eastern rim, up to the sharp terrain drop north of Gersteben often contain subangular calcareous quartzite blocks. Roundness of these blocks and the fact that they are by far not comparable in size to the quartzite blocks of the Lenzanger suggest fluvial transport from the numerous adjacent creeks. Further deposits along the pathway of the toll road display a rough, biotite-schist boulder-dominated picture. The exception being another garnet-mica-schist area, half-way towards the serpentines of the toll road, and a few serpentinite blocks alongside the road just north of dry bed of the Trockenbach. The picture changes here with most of the boulders being made up by calcareous-mica-schist, similar to the deposits of the Durchgangwald area. South of the confluence of the Trockenbach and the Hüttwinklache, rare occurrences of rounded Zentralgneis can be found on the otherwise calcareous-mica-schist rich deposits. A typical sediment record here is polymict, with fine components of serpentinite, quartz and scratched, striated, subrounded Zentralgneis, forming a seemingly shallow ridge.

Generally, the morphology of the Bodenhaus area contrasts with the Durchgangwald. While the wave-like ridges of the Durchgangwald have a N-S orientation, the shallow ridges of the Bodenhaus area, especially on the orographic left area, display a general W-E elongation. The morphological difference between the western valley flank at the Bodenhaus [Figure 4.10(f)], with its convex, east facing, shapes and the wave-like structures in the valley floor [Figure 4.10(e)] is also remarkable.

4.7.2. Interpretation

The characteristics regarding lithological composition suggest a close tie between the Durchgangwald landslide in the south and the Bodenhaus in the north. The short but steep terrain change just south of the Bodenhaus inn marks the front of extensive landslide deposits, similar in weathering and decomposition as sediments found in the Durchgangwald landslide. Like the Durchgangwald landslide, garnet-mica-schist deposits are bound to the eastern half of the valley, but instead of forming a belt they are concentrated in a few lenses. Only the calcareous-mica-schist deposits can be traced throughout the Durchgangwald and Bodenhaus area. The scattered prasinite boulders of the Astenschmiede likely originate from the northern sector of the Grieswies-Schwarzkogel, but the Ritterkar as a source is also possible. The same is true for the serpentinite blocks north of the Gersteben step. Contrary to von Poschinger (1986), who regarded this specific part of the Durchgangwald landslide north of the Gersteben step as solely originating from the west, we connect these sediments directly to the main landslide mass

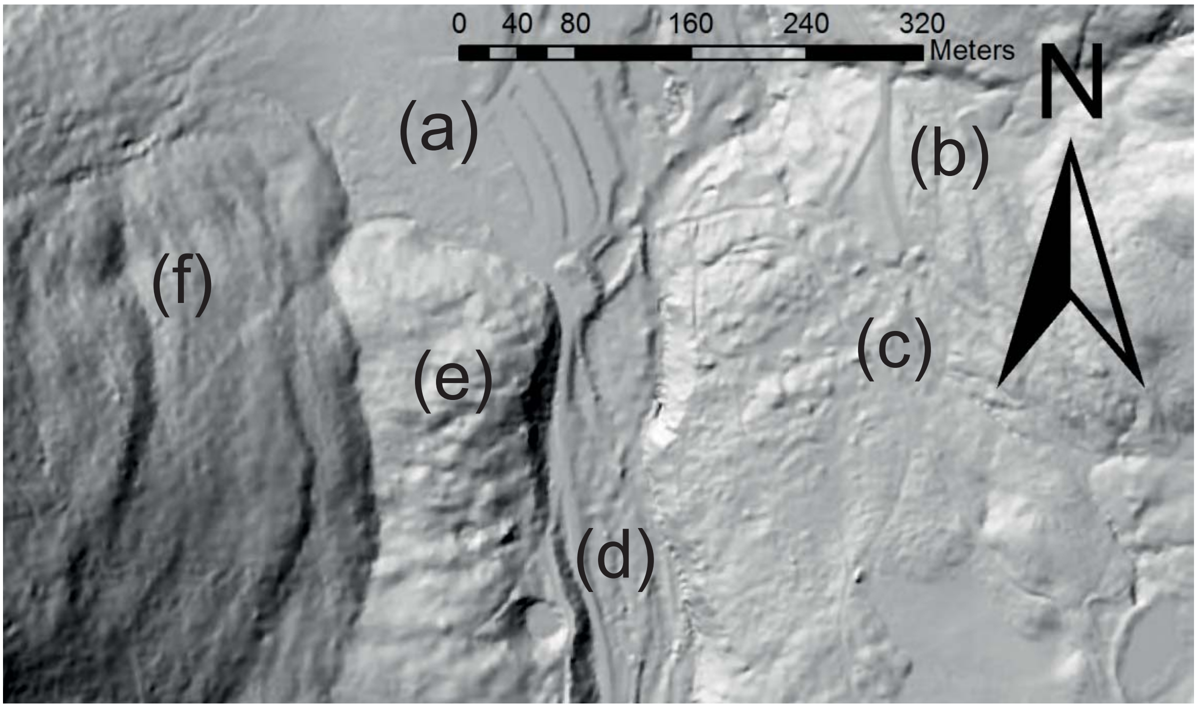

Figure 4.10.: Close-up hillshade image of the Bodenhaus area marking the flat area of the Bodenhaus inn and the toll booth area with adjacent parking space (a), the Astenschmiede (b) and Pirchlalm (c) with distinctive big boulders visible. (d) marks the bed of the Hüttwinklache with multiple erosional flanks and (e) the rough are north of the Fröstllehenalm. The convex bulges of the creeping soil and bedrock movements of the Ritterkaralm is marked by (f)

to the south of the Gersteben step. According to our reconstruction, when the landslide came down from the eastern flank of Grieswies-Schwarzkogel, it first filled up the valley floor up to the Filzenalm, but as the northern parts of the landslide mass were only free to flow north, they broke off from the main mass, thus streaming to the area what is today the Bodenhaus. The wave-like morphology seen today is the result of this process, indicating a fluidisation typical for rock avalanches forming a sturzstrom (Heim, 1932) due to dynamical fragmentation (McSaveney and Davies, 2006). The event left behind the distinctive terrain step between the Trockenbach and Gersteben, which is today overcome by the winding path of the Kolm-Saigurn toll road and its serpentines. Later, creeks from the east and west transported sediments from the valley flanks on the landslide deposits, forming extensive alluvial fans and debris flows, as they are today visible at the Fröstllehenalm and the areas around the Pirchlalm and Niederastenalm. From the Ritterkar, creeping bedrock and soil is slowly overlapping the western parts of the landslide mass [Figure 4.10 (f)], visible by the convex surface features.

Glacial sediments deposited on landslide material are not present north of the Fröstllehenalm, therefore excluding a glacial advance down to the Bodenhaus inn, as stated by von Poschinger (1986). The polymict ridge of the Hüttwinklache and the Trockenbach confluence area can be interpreted as the remnants of the small terminal moraine of the glacial deposits as described in section 4.2, deposited by a thin glacier tongue, flowing down the Gersteben step. Flooding from the Trockenbach and the Hüttwinklache subsequently degraded and resedimented this area, only leaving behind marginal traces of the former terminal moraine. Only thin basal till sediments south of the Trockenbach and the quickly decaying till coverage further suggest an at least temporary dry calving of ice from the Gersteben step, with ice blocks tumbling down, together with subglacial, intraglacial and supraglacial transported sediment. Glacial coverage north of the Gersteben step can only be estimated to have lasted for a very limited time before decaying and retreating to the higher elevated areas of the southern valley head.

The origin of the distinctive crater-like hole north of the Fröstllehenalm remains unclear. A possible explanation is the dissolution of material, embedded in the garnet-mica-schist landslide mass. This could encompass dead-ice-like inclusions, or calcareous blocks. But due to the high fine sediment content in the sturzstrom deposits, a sinkhole-like origin due to suffosion by groundwater seems most likely (Poscher and Patzelt, 2000). Similar phenomena have been document during the construction of the HTT (section 2.3).

4.8. Knappenhaus [Bichler]

4.8.1. Description

The Knappenhaus is nowadays a ruinous building, which was used by the workers of the former gold mine. As the mining activity ranges back into the medieval several documents describing or illustrating the former glacier extent of the Goldbergkees are preserved. It is situated on the orographic right side of the former LIA Goldbergkees glacier at an altitude of 2350m asl. Two parallel grain supported large ridges with subangular to angular components (mostly Zentralgneis) with a maximum size of 35 m^3 (bSCc) oriented S-N are developed just in front of the Knappenhaus. Behind the Knappenhaus well glacially polished bedrock is present. Approximately 50m higher the bedrock seems to get rougher and more angular.

4.8.2. Interpretation

Based on the mapping of Lichtenecker (1935) and historical records the inner moraine of the two parallel ridges is a right lateral moraine from the LIA (1850 AD) of the Goldbergkees. Though the age of the second ridge (closer to the Knappenhaus) is a matter of discussion. We did not take samples for exposure dating, as we focused our work on the clear forefront of the Goldbergkees. Therefore one can discuss if this ridge represents the prominent known 1620 stadial or if it is related to the so called 8.2 ka event. We think the latter can be ruled out, as we did not find or date any indication for the 8.2 ka event, where we investigated the succession from the Egesen to the LIA (see section 4.10 and chapter 5). The connection of these two ridges with their continuation at the lower part (see section 4.10) is difficult, because at the steep topography between them no ridges are preserved. As mentioned in section 4.10 no evidence for an older moraine, mapped by Lichtenecker (1935), has been found. The border between the polished and non-polished bedrock behind the Knappenhaus could be interpreted as a trim-line, showing the ice-thickness of a former glacier.

4.9. Grieswiestauern [Bichler]

4.9.1. Description

The steep slopes in front of the Sonnblick north face are called Grieswiestauern. In the north face a small area is still glaciated and rockfalls occurs nearly every day. Due to its exposure and steepness, the north face provides continuously material for the alluvial-fans and debris-flows at the Grieswiestauern. In the central part of the Grieswiestauern at an altitude of 1980m asl, a large sedimentary body (260m in length, 70m in width and 60m in height) built up by loose sediments with a sandy-silty matrix with subangular-subrounded components (Dmm) can be recognized. The body is topped by the alluvial fans and debris flows coming from the Sonnblick north face and by several huge subangular-angular blocks (Zentralgneis). Four to five erosional channels are formed, giving the impression of the body in the field and in the hillshade image to be of a hand- or foot-like structure.

4.9.2. Interpretation

The large body is clearly built up by glacial sediments and thus we think it represents an ice-marginal deposit. As we know the ice thickness from the Kolm-Saigurn glacier system from mapping and modelling (see section 6.3) and the ice thickness from the LGM (much higher than the ice-margin body), the timing of the forming of the ice margin lies in between LGM and the Kolm-Saigurn extent.

4.10. Goldbergkees [Bichler]

4.10.1. Description

The Goldbergkees is glaciated at present and very well studied by the ZAMG over the last 125 years (e.g. Schöner (2009)). At the summit the glacier is exposed towards the SE. In a long loop the Goldbergkees changes its direction until it reaches a N exposure. The highest point of the glacier is the summit of the Hoher Sonnblick (3106m asl). Today's extent is approximately 1200m linear distance further in the south than the LIA (1850 AD) extent. The latter is more or less exactly known from historical records. The LIA moraine of the Goldbergkees is well defined by grain supported large angular blocks (bSCc) building up parallel to sub-parallel ridges. The terminal moraine is a single ridge on a flat surface and reaches an altitude of 2190 m asl. The left lateral moraine is, likely because of the steep terrain, not preserved, whereas the orographic right side is dominated by multiple lateral moraines (see Figure 4.13).

4.10.2. Interpretation

Our mapping results confirm the LIA-1850 reconstruction of Lichtenecker (1935). For the terminal-moraine and the inner moraines on the orographic right side we totally agree with Lichtenecker (1935), that this is the maximum extent of the LIA-1850. It is not clear for us, if the most outlying ridge is part of the LIA-1850 system or if it is the continuation of the 1620 moraine from the Knappenhaus (see section 4.8). We did not find any evidence for the older moraine (larger extent) which Lichtenecker (1935) mapped starting form the Knappenhaus and ending near the Radhaus. In this thesis we use the end-moraine of the LIA as a reference point for our calculations and for our model of the past glacier.

4.11. Forefront Goldbergkees [Bichler]

4.11.1. Description

In the front of the LIA end-moraine from the Goldbergkees a little plateau rises to an elevation of approximately 2220 m asl. This plateau is about 300 m in length and 120 m in width and lowers gently to an altitude of approximately 2170 m asl towards the north. Behind this plateau the surface drops off interrupted by two flat steps to Kolm-Saigurn. Due to its flat surface several large (up to 20 m^3) subrounded to rounded Zentralgneis boulders are preserved. Some of the glacially polished bedrock is still covered with till. On a few parts the bedrock forms little depressions and allowed the accumulation of till sediments (see Figure 4.11). The polished bedrock is interlaminated by several up to 30 cm thick quartz veins. Due to the slower weathering rate of quartz, the veins stick out several cm from the surrounding bedrock.

West of the little plateau a succession of three lateral ridges is evolved. The ridges start at an altitude of approximately 2230 m and reach an altitude of approximately 2200 m. The area around the ridges is covered with till (Dmm). The innermost ridge in the east has steep slopes and a high of approximately 8 m to 10 m with a relatively sharp crest. The ridge is built up by a sandy to gravelly matrix-supported diamict (Dmm), containing a mixture of subangular to subrounded particles (Zentralgneis) and angular to subangular bedrock particles (mica-schist). Few larger (up to 5 m^3) subrounded to rounded Zentralgneis boulders are incorporated in the till matrix. Two of these boulders seem to be in a stable position on the crest of the ridge. Whereas several other boulders look like gravitationally toppled out of the ridge. The orientation of the ridge is towards the NNE and it is remarkable that the other ridges of the system are a little oblique to it. At the north end the surface steepens and the ridge seems to split up into several smaller ridges. Characterizing the outer ridges in the field is more complicated. Although the matrix composition is well comparable, the surface and morphology of the outer ridges look quiet different. This is due to a Zentralgneis rockfall, topping the area with large (up to 100 m^3 and more) angular boulders. Two parallel ridges, oriented towards N, are clearly developed (see Figure 4.12). It is noticeable, that the middle ridge in the system has rockfall deposits on the western slope, but not on the eastern slope (see Figure 4.14). In front of the end-moraine of the LIA from the Goldbergkees and between the plateau and the western bedrock slope a little depression caught up an accumulation of subrounded to rounded Zentralgneis boulders (up to 20 m^3) (see Figure 4.13).

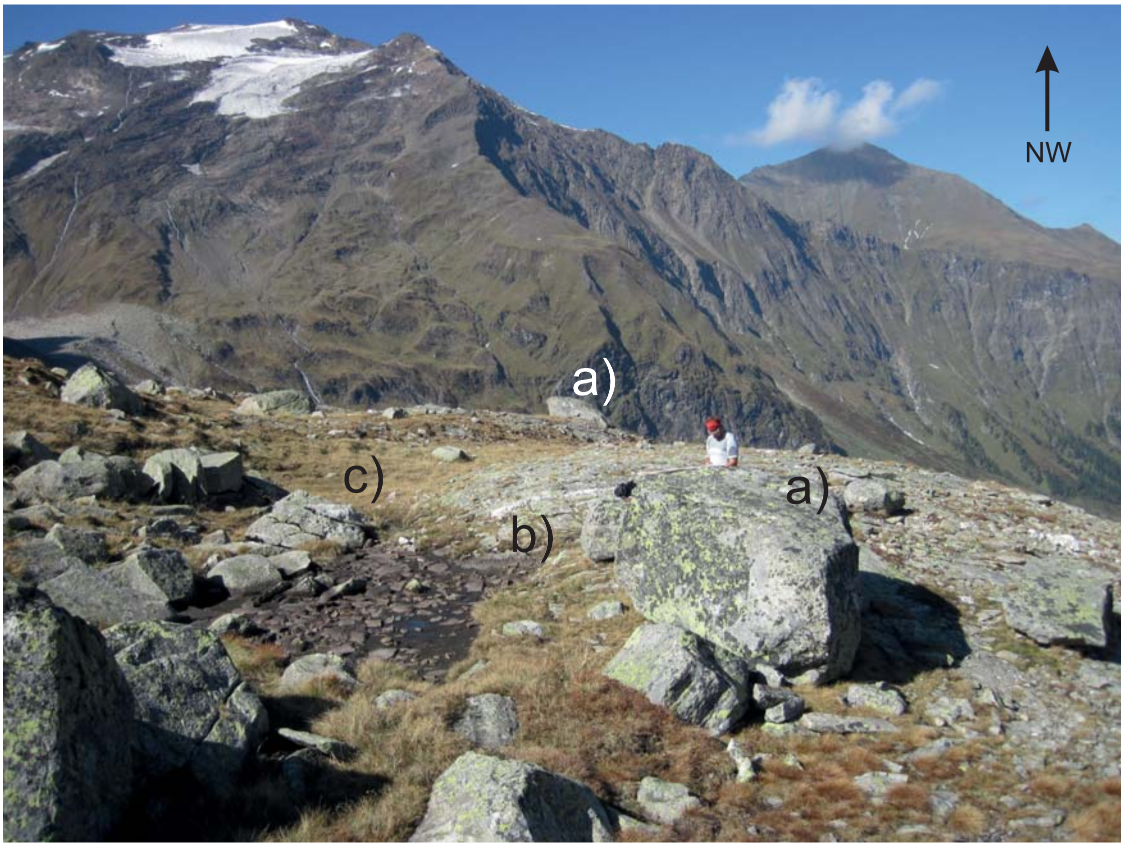

Figure 4.11.: Field picture of the plateau just in front of the LIA-1850 of the Goldbergkees. The summit in the back is the Hocharn. a) marks sampled boulder for ^{10}Be dating b) marks a quartz vein in bedrock sampled for ^{10}Be dating c) marks a little depression where sediment has been dug out for ^{14}C dating

4.11.2. Interpretation

The lithology of the boulders indicates a bedrock source in the south. In addition the apparent rounding or the subrounded shape proves a sub- or englacial transportation. These boulders represent a retreat phase of a former glacier larger than the LIA extent. Samples from four of these boulders and from two quartz veins in bedrock sites just next to two of the boulders have been taken for exposure dating (see map). Furthermore a sample in a little water depression site filled with sediments (mostly reworked till) have been dug out for getting radiocarbon ages of the base layer. The innermost ridge of the ridge system is an ideally shaped lateral moraine of a stable phase of a past glacier. The composition of the sediments (till) and the rounded components prove the glacial genesis. Due to the flat topography, the relatively fine grained moraine body is preserved. Two

Figure 4.12.: Field picture of the ridge-system west of the plateau. Viewing direction is SW. The ridge in the front is the well developed innermost ridge. In the back two more ridges topped by large angular boulders can be seen.

samples have been taken for ^{10}Be exposure dating from Zentralgneis boulders from the crest of the moraine. We think the outer ridges are also formed by a glacier. The fine grained ridge sediments are showing a glacial character. One can not ignore, that the topping of the outer ridges and its surrounding area is dominated by very large angular boulders, which do not fit the sub- or intra glacial transportation theory. But we observed two different kinds of the large boulders. One part seems to be more weathered than the other (indicated by high-standing weathered out quartz veins). Therefore it seems to be plausible to split up the genesis of the blocky topping into two events. The first event is the formation of the ridges accompanied by supra-glacially transported rockfall material (older and thus more weathered). The second event is a younger rockfall just from the steep slopes of the Sonnblick north face behind the ridge system. All the moraines are regarded to belong chronologically to one glacial system with multiple

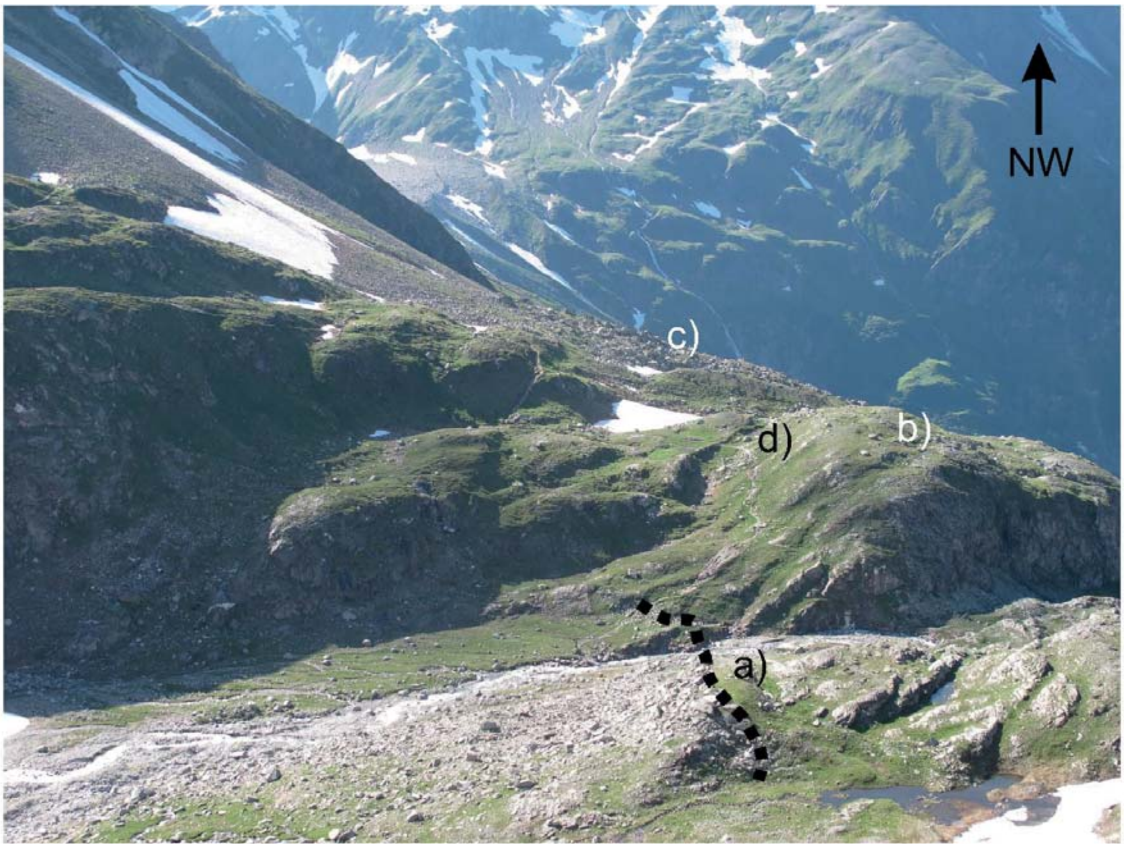

Figure 4.13.: Field picture of the LIA-1850 of the Goldbergkees and its forefront. a) is the maximum extent of the LIA marked by a bSCc moraine. b) is the plateau with several subrounded to rounded Zentralgneis boulders. c) is the moraine system which marks the maximum extent of a former glacier and its retreat. Please note that the outer ridges are influenced by adjacent rockfall. d) is the depression where Zentralgneis boulders accumulated.

phases of a stationary ice-margin. Relatively seen these moraines must be older or at least as old as the glacially related phenomenons on the plateau. The outermost moraine is the maximum extent of an advancing glacier and the other moraines are recessional moraines of a stable phase or the product of a re-advance during a retreating phase. A re-advance may be seen at the middle ridge, where a possible re-advancing glacier bulldozed some of the large angular boulders of the supra-glacial rockfall. This would explain the middle moraine with its accumulation of boulders on the western slope. We took samples from two Zentralgneis boulders from the outermost moraine for exposure dating. If the accumulation of boulders just in front of the LIA-1850 terminal-moraine stands as an event for its own, it must be chronologically in between the ages of the

Plateau and the LIA. In our opinion this represents a tongue of a retreating glacier older than the LIA maybe belonging to the 'Plateau' or to the 'moraine system' or to both.

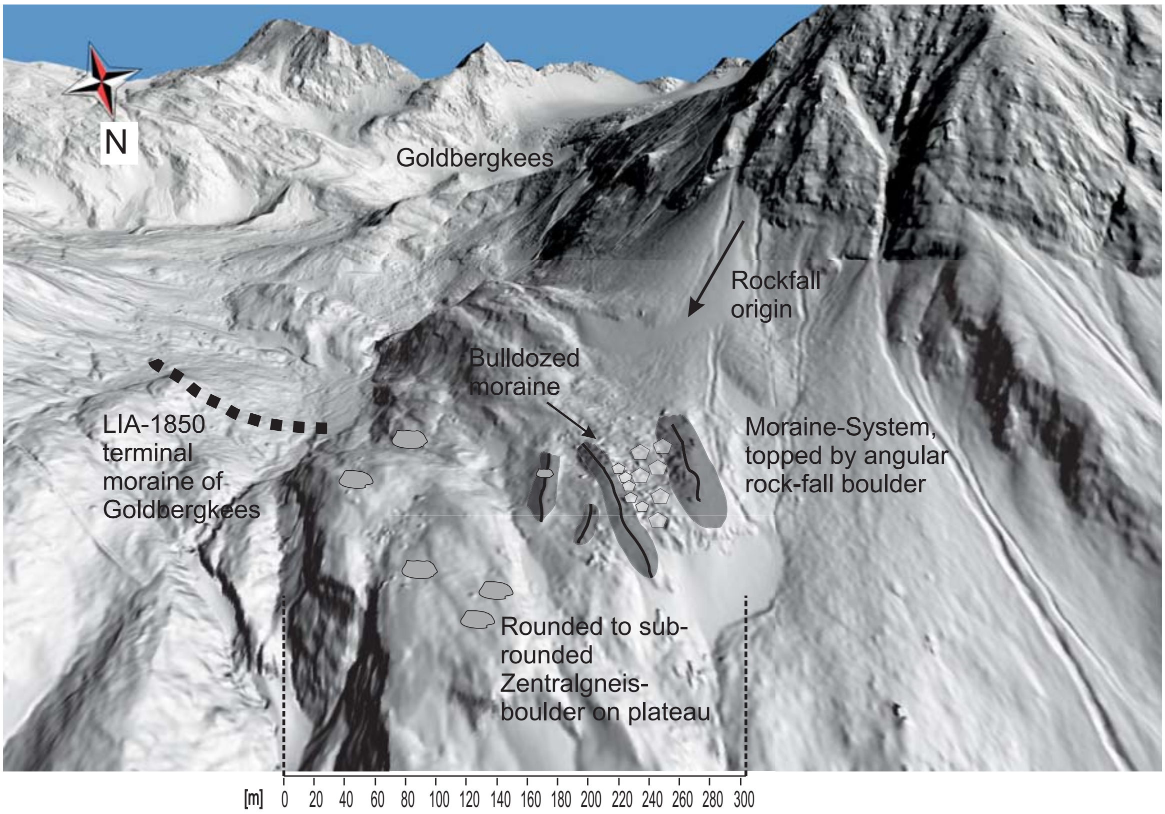

Figure 4.14.: Simplified sketch on hillshade model draped on DEM of the situation at the forefront of the LIA-1850 from the Goldbergkees as described in subsection 4.11.1. View to the south.

4.12. Pilatuskees [Bichler]

4.12.1. Description

The Pilatuskees is glaciated at the present, but its ice volume is much less than the ice volume of the Goldbergkees. The ice is concentrating in a cirque at approximately 2200 to 2400m asl and on the higher parts of the steep slopes which surround the cirque. The exposure of the possible glaciated area is towards E to SE. The highest point of the glacier is the summit of the Hocharn (3254m asl). A massive (15–20m high) matrix-supported (Dmm) right lateral moraine of the LIA (known by historical records) is preserved. Some younger multiple ridges can be clearly identified as well. These are built up by cobble to block size subangular to subrounded components (bSCc). Where the supposed LIA-1850 terminal moraine should be (around 2200m asl), the slope gets steep and 4-5 large (10–15m high) longitudinal ridges, built up by Dmm, are present. This ridges reach down to an altitude of approximately 2000m asl.

4.12.2. Interpretation

The LIA-1850 maximum is well defined on the glaciers right lateral side by the massive moraine ridge. On the orographic left side, the outermost of the multiple smaller ridges marks the LIA-maximum. The origin of the large longitudinal ridges is discussable. We think the most plausible explanation is fluvial erosion, cutting into a mass of Dmm, deposited during the LIA over the edge of the step. The maximum extent of the LIA-1850 can therefore be found at the lowermost parts of these longitudinal ridges (around 2000 m asl). Although this determination is special in case of topographic features we use this LIA-1850 end-stadium for our calculations and models in this thesis (chapter 6). This assumption remarkably lowers the LIA-1850 maximum extent by approximately 100 m, compared to the Goldbergkees. Regarding the modeling of the former Kolm-Saigurn glacier system this lowering is directly connected to ELA calculations (see section 6.2) for the Pilatuskees.

4.13. Forefront Pilatuskees [Bichler]

4.13.1. Description

In the front of the LIA-maximum of the Pilatuskees no phenomena (boulders, ridges) comparable to the Goldbergkees are preserved. Though one extraordinary large lateral moraine ridge is present. It starts at an altitude of 1750m asl and reaches down to the valley floor (1600m asl). Although the ridge is at least 20m high, its hardly recognizable in the field, due to its vegetation. Few dug outcrops at the start and the end of the ridge revealed a silty-sandy matrix with subrounded to rounded (up to 1 m^3) components, mostly made up by Zentralgneis (Dmm).

4.13.2. Interpretation

The stand alone huge moraine body is challenging to relate to the other observed moraine systems in the area. Geometrically it most likely belongs to one of the multiple parallel lateral moraines down-valley north of Kolm-Saigurn (see subsection 4.2.2). According to the moraine-system of Kolm-Saigurn and its dimension, the ridge should have developed during a relatively long lasting stable phase while the Kolm-Saigurn glacier retreated.

4.14. Melcherböden [Bichler]

4.14.1. Description

The area between the LIA of the Goldbergkees and Kolm-Saigurn is dominated by steep slopes interrupted by two flat steps. Due to the flatness of these steps, they tend to accumulate sediment and water and form therefore bogs. The largest peat bog has an area of about up to 500 m^2 and a maximum depth of 2.1m (see Figure 4.15). We drilled two sediment cores there for ^{14}C dating and palynological investigations (see subsection 3.2.1). From our first impression in the field enough organic material is incorporated in the cores, though one has to be careful by picking the right material for ^{14}C dating as the bog is surrounded by wide rooting larches.

4.14.2. Interpretation

The formation of the steps is a matter of discussion. As we did not concentrate on bedrock mapping, we can not completely explain the formation as a result of the change of the lithology or of the change of the dip of the layers. Though the previous mapping by (Alber, 1976) and our bedrock mapping work might show that a change in lithology from mica-schist to calcareous-schist is the reason for the formation of the upper step. But summing up the overall lithological impression is to complicated to clear the question somehow. From ice-thickness modeling (see section 6.3) we could interpret the lower step formed by glacial erosion. We think the bogs at the Melcherböden first formed after their last glacial cover. Thus the base layer of our drilled sediment core should yield a minimum age of the Goldbergkees glacial system, which is related to it.

4.15. Durchgangriegel [Bichler]

4.15.1. Description

The mountain crest east and above the Durchgangwald is called the Durchgangriegel. Tension gaps at the crest (german term: *Bergzerreißung*) are a proof for the movement

Figure 4.15.: Field picture of the Melcherböden looking from N to S on the way down from the Neubau-hut. The area in the middle of the picture is the bog described in subsection 4.14.1.

of the entire slope and some outcrops show how the bedrock (mostly mica-schist and calcareous-schist) is partly loosened due to gravitational movement. The Durchgangwald landslide mass overlaps the Durchgangriegel, forming a shallow depression following this sharp border. Further south where the Durchgangwald mass ends, all morphological and geological features, up-slope of the Kolm-Saigurn terraces (see section 4.4) to the crest, are part of a creeping mass. The border between releasing and accumulation of the creeping mass is well identifiable in the field and on the hillshade image and is marked by a row of wells. Several terrace-like steps are recognizable on the slope of the creeping mass. One special outcrop shows a sequence of creeping mass topped by till, and topped again by creeping mass (see Figure 4.16). In the lower parts where the slope is forested, marked deformations of tree trunks, due to the underlying creeping mass in combination with possible solifluction, are ubiquitous.

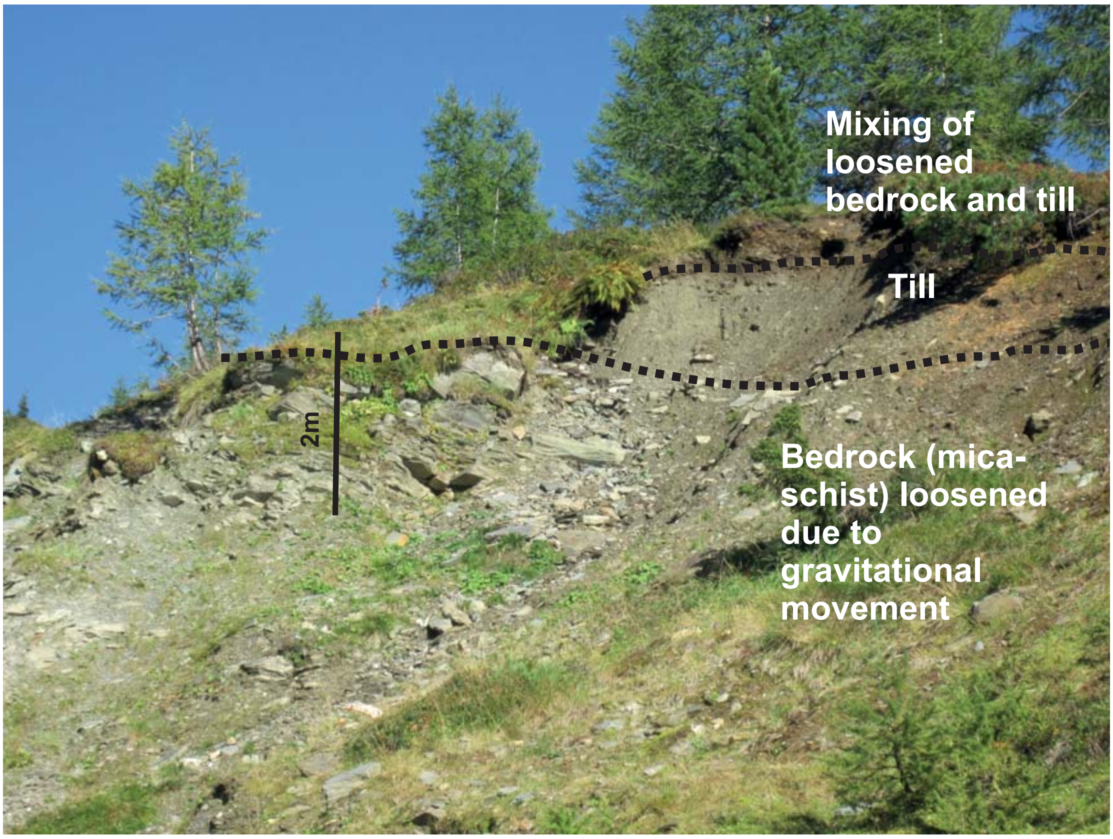

Figure 4.16.: Picture of an outcrop situated in the Durchgangriegel creeping mass. This is the only outcrop at the entire slope where till is preserved. Viewing direction is towards east.

4.15.2. Interpretation

The overlapping of the Durchgangwald landslide on the Durchgangriegel, and thus its stabilization is evident in the field. The fragmented bedrock would have promoted further gravitational movements, if the Durchgangwald landslide had not stabilized the toe by its own weight. This can be seen in the south part of the Durchgangriegel, where the whole slope is still slowly creeping towards the valley floor.

This lasting and ongoing process is pointed out by two details. First, the deformation of tree trunks in the lower part. Second, the overridden till at one outcrop, indicating how partly fragmented bedrock from above crept over glacially deposited sediments, and therefore keeping them from being solifluctated (see Figure 4.16). As the altitude of the outcrop is too high above the valley floor, the till cannot be linked to the Kolm-Saigurn glacier system and thus is a deposit of an older glacial phase of the Lateglacial or even the LGM.

Our findings further support the ideas of Hottinger (1935) and von Poschinger (1986) regarding the landslide origin from the west. The obvious flat surfaces in the upper part of the creeping mass could be explained by a rotational component within the mass movement.

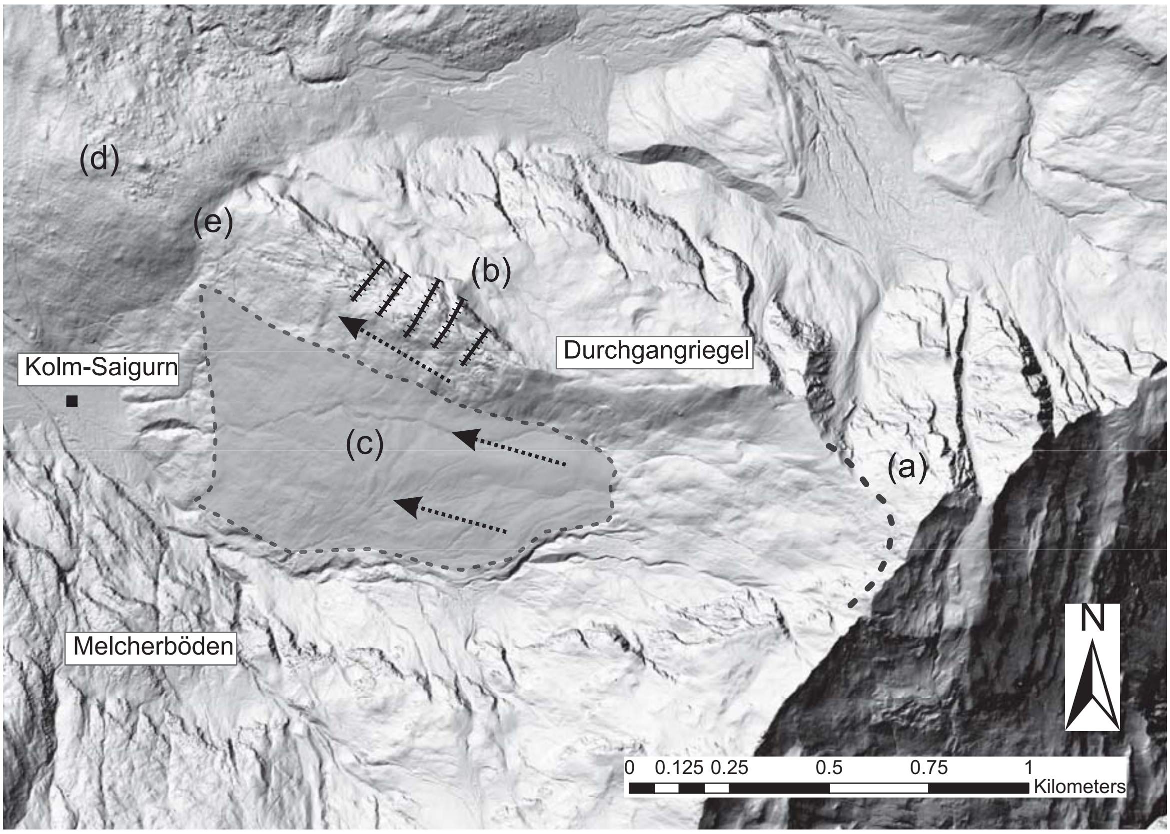

Figure 4.17.: Hillshade model of the area east of Kolm-Saigurn. a) marks the scarp of the creeping mass. b) are extension gashes of the Durchgangriegel due to its movement. c) marks the creeping mass. d) marks the south-eastern part of the Durchgangwald landslide. e) marks the overlapping situation of the Durchgangwald landslide on the Durchgangriegel and thus its stabilization.

4.16. Summary [Bichler]

This section provides a short overview regarding the most important features presented in this chapter. The most important landscape-forming events are summarized by their characteristic starting with the lowermost and therefore oldest features. Figure 4.18 shows an overview of the key areas for understanding these events.

The incision of the Hüttwinklache at the Lenzanger (section 4.1) revealed a vertical profile with a relative chronology of the most influential landscape-forming events.

4.16.1. Durchgangwald Landslide

The Durchgangwald landslide (section 4.2), originating from the scarp of the Grieswies-Schwarzkogel (section 4.5) in the W, makes up the valley floor and large parts of the eastern flanks up to the Filzenalm (section 4.3), and from Kolm-Saigurn (section 4.4) to the Bodenhaus (section 4.7). Three main lithologies building up the landslide have been identified, calcareous-mica-schist, dark-phyllite and mica-schist, showing the same succession as the outcrops of these lithologies in the scarp. Rotational glide mechanics for the main part of the Durchgangwald landslide and a following sturzstrom to the Bodenhaus area (section 4.7), forming the Gersteben step (section 4.6), are documented. The landslide damned creeks from the east and south, thus forming the wetlands at the Filzenalm (section 4.3) and lacustrine sediments at the Kolm-Saigurn basin (section 4.4).

4.16.2. Kolm-Saigurn Glacier System

The Durchgangwald landslide is topped by basal till in the western areas, smoothing the rough surface of the landslide, which is strongly contrasting with the unaffected areas in the east (section 4.2). The advance of the glacier is documented by unique deposits in the Kolm-Saigurn basin (section 4.4) and the Durchgangriegel (section 4.15). Traces of the till cover can be found until the Gersteben step north of the Lenzanger parking space (section 4.6 and section 4.7), marking the maximum extent of the glacier-system. The till cover is accompanied by a succession of nine right lateral moraines north of Kolm-Saigurn (section 4.2), documenting multiple phases of stabilization during the glacier retreat. Thus this moraine system is comparable to the morphological characteristics of Egesen-like retreat phases. The ridge at the forefront of the Pilatuskees (section 4.12 and section 4.13) likely represents the continuation of one of the inner right lateral ridges of the Durchgangwald (section 4.2). It is this overlying basal till from the glacier system, far away from any LIA glacial deposits of the Goldbergkees or the Pilatuskees, that indicates the interstadial context of the previous Durchgangwald landslide.

At the forefront of the LIA-1850 (section 4.8) of the Goldbergkees (section 4.10 and section 4.11), on the Grieswiestauern area, three left lateral ridges and a plateau with several large rounded glacially transported boulders are preserved (section 4.9). On a terrain step towards Kolm-Saigurn on the Melcherböden, several peat bogs developed after glacial retreat (section 4.14).

Topographic and geomorphological, as well as sedimentary characteristics of the glacial deposit here can be connected to the glacial deposits downvalley in Kolm-Saigurn and the Durchgangwald, again documenting the retreat phases typical for an Egesen-like glacier system.

4.16.3. The Quartzite Landslide

Around the Grieswiesalm (section 4.5) and the Lenzanger area (section 4.6), the till cover is topped by a small quartzite landslide. The landslide blocked the Hüttwinklache (section 4.1) and formed a reservoir, whose remnants can today be found at the Lenzanger parking space.

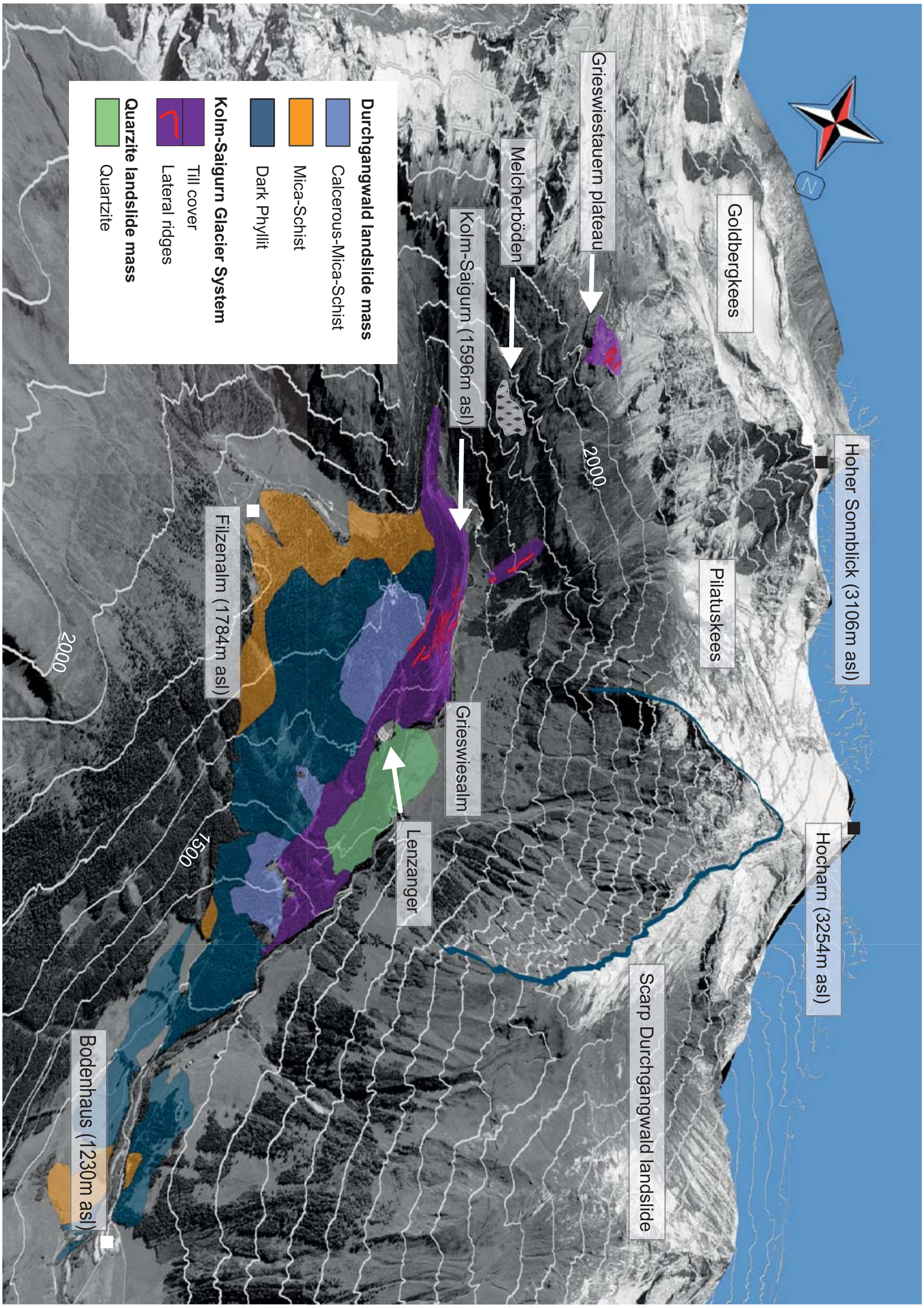

Figure 4.18.: Overview of the key areas for understanding the main landscape forming processes in the study area from the Lateglacial to Holocene. Viewing direction is WSW.

5. Dating [Reindl/Bichler]

Dating landforms is an important cornerstone when revealing the chronology of an area. As an example, assignment of landforms like moraines to stadials can be often derived from characteristic field evidence and a solid mapping of cross-cutting relationships but is quite often difficult. This is even more true for landslides, unless they are in some way accompanied by glacial advances (Sanhueza-Pino et al., 2011). Modern tools, such as dating with terrestrial in-situ cosmogenic nuclides and radiocarbon dating, provide data and arguments in establishing better local chronologies (see chapter 3). The head of Hüttwinkl valley offers the unique possibility to combine rich field evidence of diverse landforms into an already solid chronology, backed by modern tools, providing facts on specific points in time for the origin of these landforms.

Table 5.1 and Figure 5.1 present these dates, taken from two bedrock and eighteen boulder samples and processed with the ^{10}Be method. Two boulder sample sites, SON3 and SON7, were not successfully measured. Four boulder samples, DUR2 (26890±3320), DUR3 (16440±2950), SON2 (18910±2860), and SON4 (5680±740) have uncertainties in excess of 10% (1σ)of the measured Be content and were expelled from further considerations.

Figure 5.2 shows all taken samples for dating and their results. A detailed discussion of these results is provided in section 5.1, section 5.2, and section 5.3.

5.1. The Durchgangwald landslide [Reindl]

The deposits of the Durchgangwald landslide (section 4.2) represent the lowermost units in the head of the Hüttwinkl valley. Three boulders (in years BP) DUR8 (13380±1100), DUR9 (11960±730), and DUR10 (13120±920) were successfully sampled and measured. Samples were taken from areas rich in quartz veins on the garnet bearing biotite-gneiss angular boulders up to several meters in diameter. The resulting ages cluster around a mean age of 12.8±1.1 ka (Table 5.2) The age of DUR9 is somewhat younger, which might have been caused by post-depositional toppling or spalling.

Name	Elev. [m asl]	Thick-ness [cm]	Shiel-ding corr.[a]	^{10}Be 10^4 atoms/ gram[b]	Exposure Age [years BP][c]	Exposure Age, corrected [years BP][d]
DUR8	1730	4	0.98679	20.88±1.36	12980±1000	13380±1100
DUR9	1779	4	0.96723	19.00±0.67	11610±670	11960±730
DUR10	1732	4	0.98545	20.47±0.99	12720±880	13120±920
DUR1	1638	4	0.97218	16.29±0.64	11000±690	11320±720
DUR2	1643	4	0.97155	38.67±4.24	25800±3100	26890±3320
DUR3	1623	4	0.97185	23.32±3.95	15900±2800	16440±2950
DUR4	1631	4	0.97123	15.32±1.49	10400±1100	10710±1180
SON1	2231	3	0.97752	28.71±1.94	12460±1040	12590±1060
SON2	2229	3	0.97758	43.06±6.03	18620±2770	18910±2860
SON4	2212	3	0.96063	12.62±1.51	5660±730	5680±740
SON6	2184	3	0.98117	23.06±0.79	10300±610	10870±650
SON8	2190	3	0.98197	24.05±1.08	10680±710	11280±760
SON5	2183	3	0.98166	25.71±1.16	11480±770	11600±780
SON9	2192	3	0.98217	25.87±0.98	11480±710	11590±720
SON10	2209	3	0.97667	22.83±0.79	10060±600	10150±610
DUR5	1520	4	0.96505	15.26±1.24	11360±1100	11690±1120
DUR6	1516	4	0.94914	13.18±0.88	10000±830	10280±860
DUR7	1522	4	0.97156	10.65±0.70	7840±640	8050±670

[a] Shielding correction includes both the dip of the sampled surface and the shielding due to the surrounding topography following Dunne et al. (1999). We assume a rock density of 2.65 g cm^{-3}.
[b] AMS measurement errors are at the 1σ level, including the statistical (counting) error and the error due to the normalization to the standards and blanks. Sample ratios are normalized to the standard 07KNSTD (Nishiizumi et al., 2007).
[c] Age errors include analytical uncertainties only.
[d] Exposure ages for all samples have been corrected for a surface erosion (weathering) rate of 1 mm/ka. All DUR samples have been additionally corrected for 2% tree shielding following Plug et al. (2007). Samples SON6 and SON8 have been corrected for 4.684% snow coverage following Dunai (2010) instead.

Table 5.1.: Boulder and bedrock information, AMS measured ^{10}Be concentrations and calculated exposure ages for landslides, glacier boulders and bedrock in the head of the Hüttwinkl valley, Austria (47.07°N, 12.98°E). Samples are sorted to reflect their association with specific landforms and relative position from field evidence (chapter 4). From table top to bottom (stratigraphic oldest to youngest): Durchgangwald landslide, Kolm-Saigurn glacial retreat stadials, Grieswiestauern glacial retreat stadials, final Grieswiestauern glacial retreat, Quartzite landslide. For detailed boulder locations and volumes see Table 3.2. All measurements were performed at the ETH Zürich Laboratory of Ion Beam Physics.

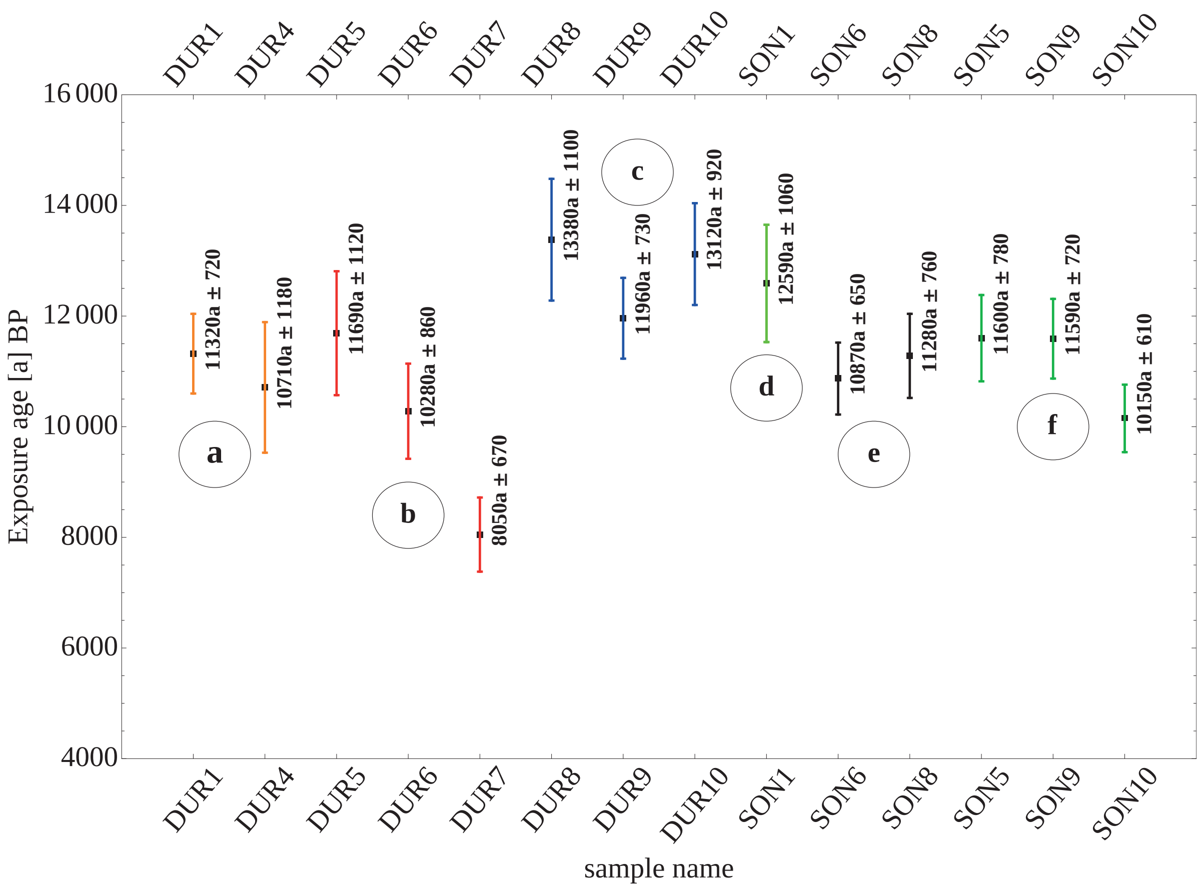

Figure 5.1.: Plot of the measured ^{10}Be results. Only results with errors below 10% are plotted. The samples are grouped into six batches: Group (a) are two samples just north of Kolm-Saigurn, from a set of parallel moraines, (b) are three samples from the quartzite landslide at Lenzanger, (c) are three samples from the Durchgangwald landslide, (d) is a boulder from the innermost ridge of a set of at least three parallel ridges at the Grieswiestauern plateau, (e) are two glacially polished bedrock surfaces at Grieswiestauern, and (f) is a set of three boulders adjacent to the previous bedrock surfaces.

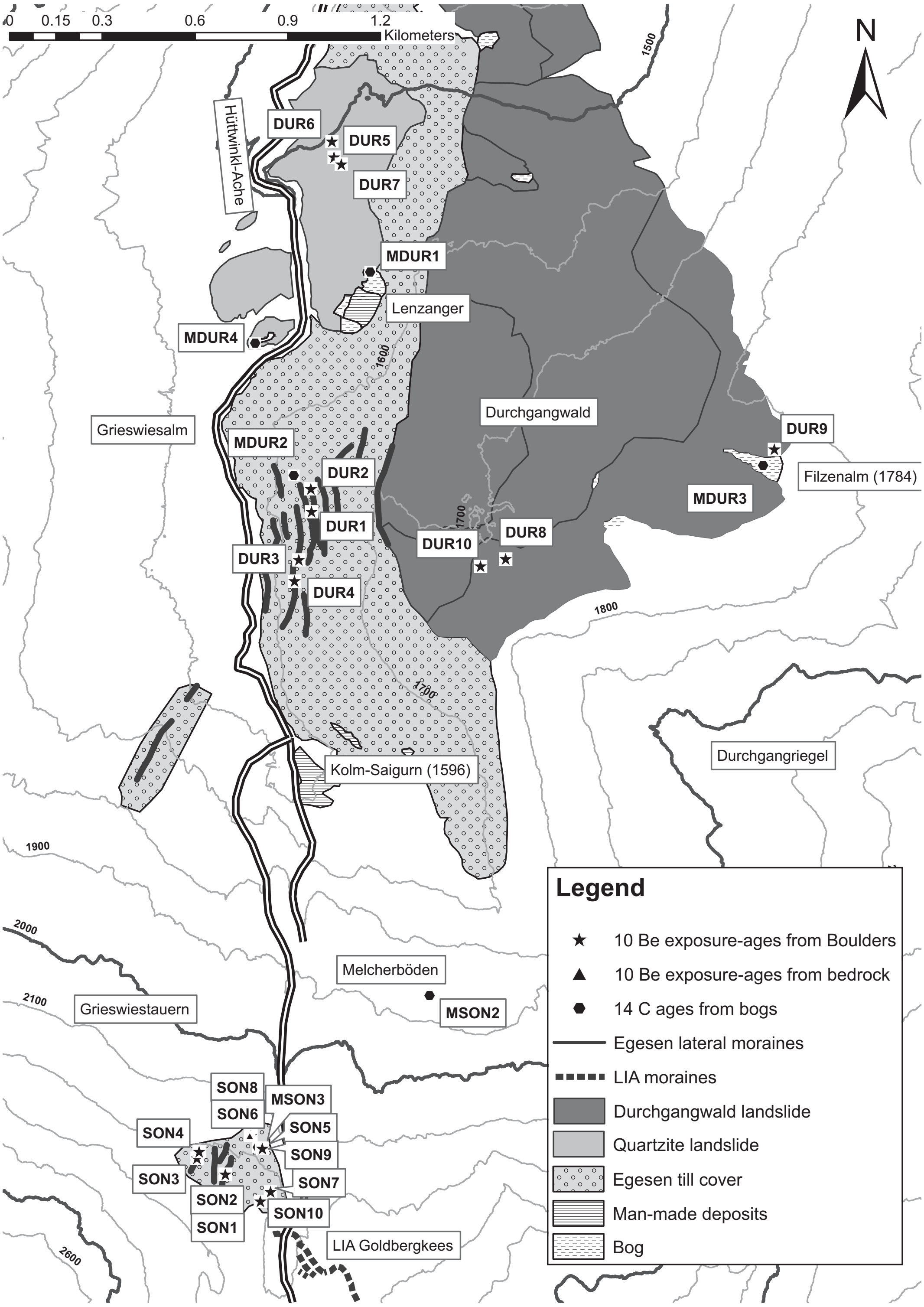

Figure 5.2.: Sketch map displaying all attempted sample sites for ^{10}Be and ^{14}C dating with information about the associated landform as documented by mapping.

The 5.08 m sediment core (MDUR3)at the Filzenalm (section 4.3) was only successfully measured at a depth of 4.6 m, for lack of suitable organic matter in the lower, silty, base layers. The result of 8446±753 years cal BP as a minimum age does not contradict the ^{10}Be dates.

Table 5.2.: Mean age of the Durchgangwald landslide, from ^{10}Be dating.

Name	Exposure Age, corrected [years BP]
DUR8	13380±1100
DUR9	11960±730
DUR10	13120±920
mean	**12820±1100**
MDUR3	8446±753 y cal BP

The age of 12.8±1.1 ka BP could place the Durchgangwald landslide at the end of the Bølling-Allerød interstadial (Yu and Eicher, 2001), ranging from 14.7ka–12.7ka BP, shortly before the onset of the Younger Dryas stadial, making it one of the rare interstadial landslides in the Eastern European Alps.

5.2. The Kolm-Saigurn Glacier System [Bichler]

5.2.1. Glacial Advance and Maximum Extent

Due to the lack of suitable bedrock or boulders, the advance or the maximum extent of the glacial advance on the Durchgangwald could not be sampled with the ^{10}Be method. Luckily, the Durchgangwald landslide, happening at 12.8±1.1 ka BP provides a maximum age of the glacial advance following the Bølling-Allerød interstadial. While theoretically the glacial advance could have also occurred during the remainder of the Holocene from this evidence, the following cold phase of the onsetting Younger Dryas (12.7 ka BP) is inferred to be the cause for this glacial advance, as further supported by samples taken from lateral moraines, representing states of retreat from the decaying glacier.

5.2.2. Glacial Retreat

Traces of the retreating glacier, and stabilization phases during this process, can be found in two areas in the head of the Hüttwinkl valley. These are at the multiple, parallel lower moraine ridges, of the Durchgangwald (section 4.2), at 1630m asl, and the Grieswiestauern plateau (section 4.11), at 2230m asl.

5.2.2.1. Kolm-Saigurn basin

Four samples were taken from the moraine ridges 3 and 4 (section 4.2) representing the right lateral moraine states of the retreating glacier after the advance on the Durchgangwald landslide. Two samples were taken on each of the moraine ridges from Zentralgneis boulders. Unfortunately, no other moraine ridge show potential boulders for ^{10}Be dating. DUR1 and DUR2 were taken from ridge number 4, while DUR3 and DUR4 were taken from ridge number 3, running parallel to number 4 with a vertical distance of 10 m. Dating of the boulders resulted in ages (in years BP) of 11320±720 for DUR1 and 10710±1180 for DUR4 (Table 5.3) Samples DUR2 and DUR3 were not considered due to errors in excess of 10%. Samples DUR1 and DUR4 give a mean age of 11.02±1.18 ka BP, placing the final retreat phase of the glacier in the basin of Kolm-Saigurn, after the end of the Younger Dryas stadial at approximately 11.5 ka BP.

Table 5.3.: Mean age of moraines of the glacial retreat process in the basin of Kolm-Saigurn, from ^{10}Be dating.

Name	Exposure Age, corrected [years BP]
DUR1	11320±720
DUR4	10710±1180
mean	**11020±1180**

5.2.2.2. Grieswiestauern and Melcherböden

Ten Zentralgneis samples for ^{10}Be processing were taken from the prominent Grieswiestauern (section 4.11)plateau, flanked by the left lateral moraine ridges of a lateglacial advance. Contrary to the Kolm-Saigurn basin, no interaction with landslides is visible, therefore the only possibility to directly date the glacial timeframe is by the means of suitable boulders on the moraine ridges, exposed, glacially polished bedrock on the plateau within the former glacier bed and via indirect means from bog and soil samples, also within the former glacier bed (see Figure 5.3).

Four samples were taken from boulders from the left lateral moraines, the first two from the innermost moraine, representing the final retreat state of the glacier in this area. Two more samples were taken on the outward parallel ridges. Three out of four samples

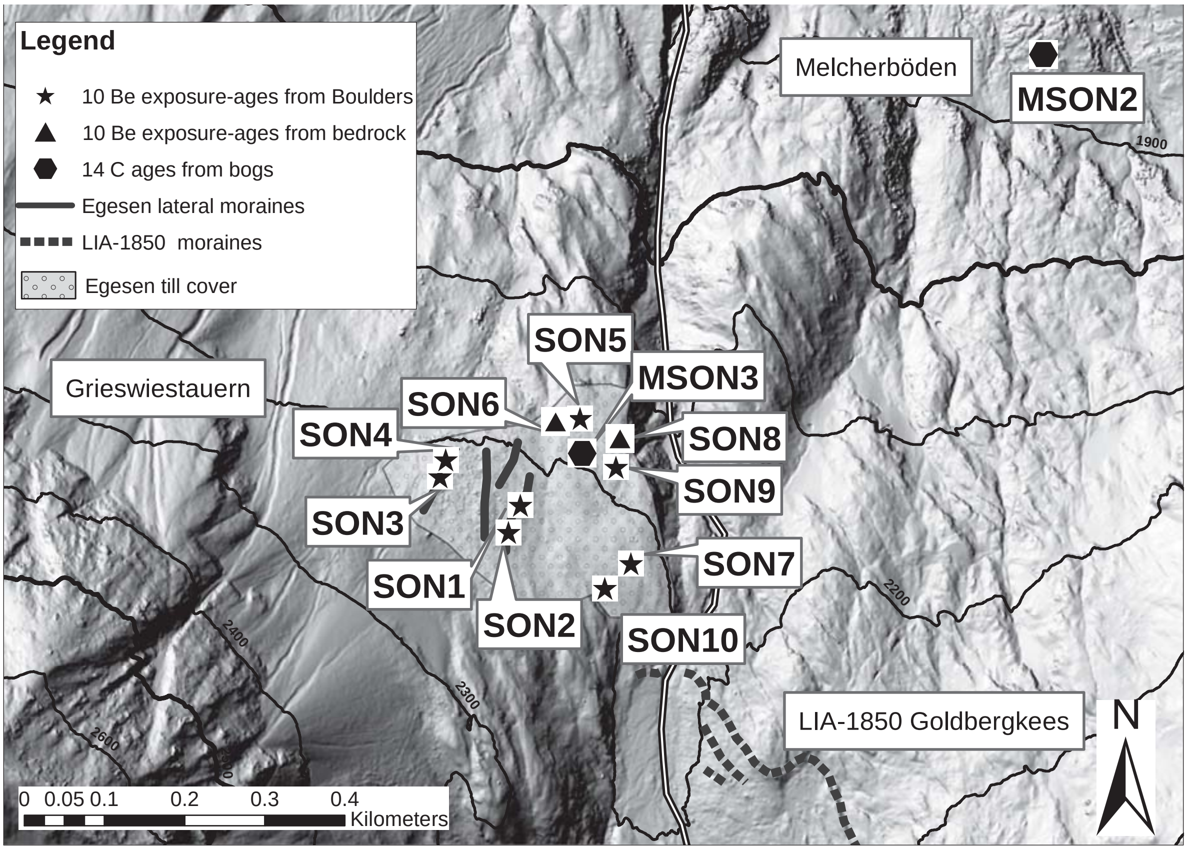

Figure 5.3.: Detailed overview on ^{10}Be and ^{14}C samples taken at the forefront of the LIA from the Goldbergkees (see section 4.11). Sample names are referring to Table 5.1.

were successfully measured, with SON3 yielding no result. Samples SON2 and SON4 had analytical errors in excess of 10% percent and were excluded from further processing their results. Revisiting these sample sites, we concluded edge effects to be an important factor for the excessive errors, as the method of sample taking with chisel and hammer did not allow selecting the optimal center flat areas of the target boulders, but instead forced us to concentrate on areas more to the edges, where sampling was possible at all. The remaining sample, SON1, shows a last stabilization phase for the innermost moraine ridge of 12590±1060 years BP, placing it in the Younger Dryas stadial. Considering the mean retreat age of the glacier in the Kolm-Saigurn basin is 11.02±1.18 ka BP, this number seems unlikely high, but is still within the stated errors, under the assumption that both features were deposited by the same event.

The plateau samples consist of the boulders (ages in years BP), SON5 (11600±780), SON9 (11590±720), and their neighboring glacially polished bedrock sites SON6

(10870±650) and SON8 (11280±760, see Table 5.4). SON10 is set back approximately 100 m, only 50 m in front of the LIA terminal moraine and displays a somewhat younger age of 10150±610, implying it may have have been subjected to post-depositional toppling or spalling. Because of their exposed nature above the timberline, boulders SON5, SON9, SON10 were only corrected for erosion, but not for snow coverage or forest shielding. Bedrock samples SON6 and SON8 where corrected for a snow coverage of 50 cm during a course of 6 months (Dunai, 2010). Overall, samples SON5, SON6, SON8, and SON9 cluster well and result in a mean age of 11340±780 years BP, representing the transition where the Egesen-time Goldbergkees was just marginally bigger than during the LIA, and already in a retreat beyond the LIA limits, as sample SON10 suggest.

Table 5.4.: Mean age of the glacial retreat at the Grieswiestauern, LIA forefront, from ^{10}Be dating, with accompanying ^{14}C soil dating. Both ^{14}C dated sites indicate the minimum age when the terrain became ice-free.

Name	Exposure Age, corrected [years BP]
SON5	11600±780
SON6	10870±650
SON8	11280±760
SON9	11590±720
mean	**11340±780**
SON10	10150±610
MSON2	11280±74 y cal BP
MSON3	8884±238 y cal BP

These results are backed by a dug soil sample (MSON3, 8884±238 years cal BP), adjacent to SON8 and SON9, and a peat sample from a peat baselayer from the step terrain heading towards the Kolm-Saigurn basin, the Melcherböden (MSON2, 11280±74 years cal BP, Table 5.4). The latter sample suggest that the basin of Kolm-Saigurn and the Melcherböden were ice-free by that time, therefore excluding any glacial ice further downstream from the Goldbergkees.

5.3. The Quartzite landslide [Reindl]

Three samples were taken from quartzite boulders overlying the glacial sediments of the Egesen advance at the Lenzanger and Grieswiesalm (section 4.5, section 4.6). The Quartzite landslide represents one of the topmost deposits in the Hüttwinkl valleyhead, barring the numerous alluvial fans and debris flows. All three samples were successfully measured, even though precautions had to be taken for the high pyrite content found in the quartzite boulders (ages in years BP). Samples DUR5 (11690±1120) and DUR6 (10280±860) give a mean age of 10990±1120, suggesting the quartzite landslide happened on ice-free terrain shortly after the Younger Dryas stadial (Table 5.5). DUR7 (8050±670) is somewhat younger indicating post-depositional spalling or toppling.

Table 5.5.: Mean age of the Quartzite landslide, from ^{10}Be dating.

Name	Exposure Age, corrected [years BP]
DUR5	11690±1120
DUR6	10280±860
mean	**10990±1120**
DUR7	8050±670

The Quartzite landslide, together with the radiocarbon sample MSON2 from the Melcherböden, poses a limit on the retreat of the glacier from the Kolm-Saigurn basin, which can be assumed was complete by approximately 11ka BP. It is likely that the Quartzite landslide barely missed the rapidly retreating glacier tongue of the Kolm-Saigurn glacier system.

Figure 5.4.: Southwest looking picture of the boulder DUR9 from the Durchgangwald landslide, dated to (11960±730 y BP). In the background the north face of the Sonnblick (3106m asl) can be seen with the summit observatory. Picture location is the distal part of the Durchgangwald landslide, in the area of the Filzenalm.

6. Glacier Dynamics [Reindl/Bichler]

Many of the landforms in the study area were affected by the dynamics of the ice flow through the valleys. The rich field evidence allows us to reconstruct many features of the former dynamics. In this chapter we take a look on the maximum extent of glaciers during the Egesen and Younger Dryas stadial, and some features of the retreating glacier systems. No review of an Egesen glacier would be of course complete without taking a look at the implications of climatic changes, and we therefore will also take a look at the climatic key figures we can interpret from the field evidence.

6.1. The Kolm-Saigurn Confluence Situation [Bichler]

In the initial phases of our project we only considered the Goldbergkees as the main ice body in the valley head in and around Kolm-Saigurn. During our work it became apparent that this assumption cannot be valid for all aspects of the glacier dynamics. The main reason lies within the existence of the Pilatuskees, originating from the summit of the Hocharn at 3254 m asl. The Pilatuskees is in some aspects similar to the Goldbergkees to its south (see Figure 6.1):

- Accumulation area is a South-East facing flank.
- Accumulation possible from summit over a well defined area down to lower lying areas.
- Valley floor turning East and eventually North.

There are of course some key differences between the two glaciers:

- The Hocharn summit is almost 150 m higher than the Sonnblick summit, adding possible accumulation area.
- The South-East flank of the Hocharn rises much steeper from the valley floor in Kolm-Saigurn.

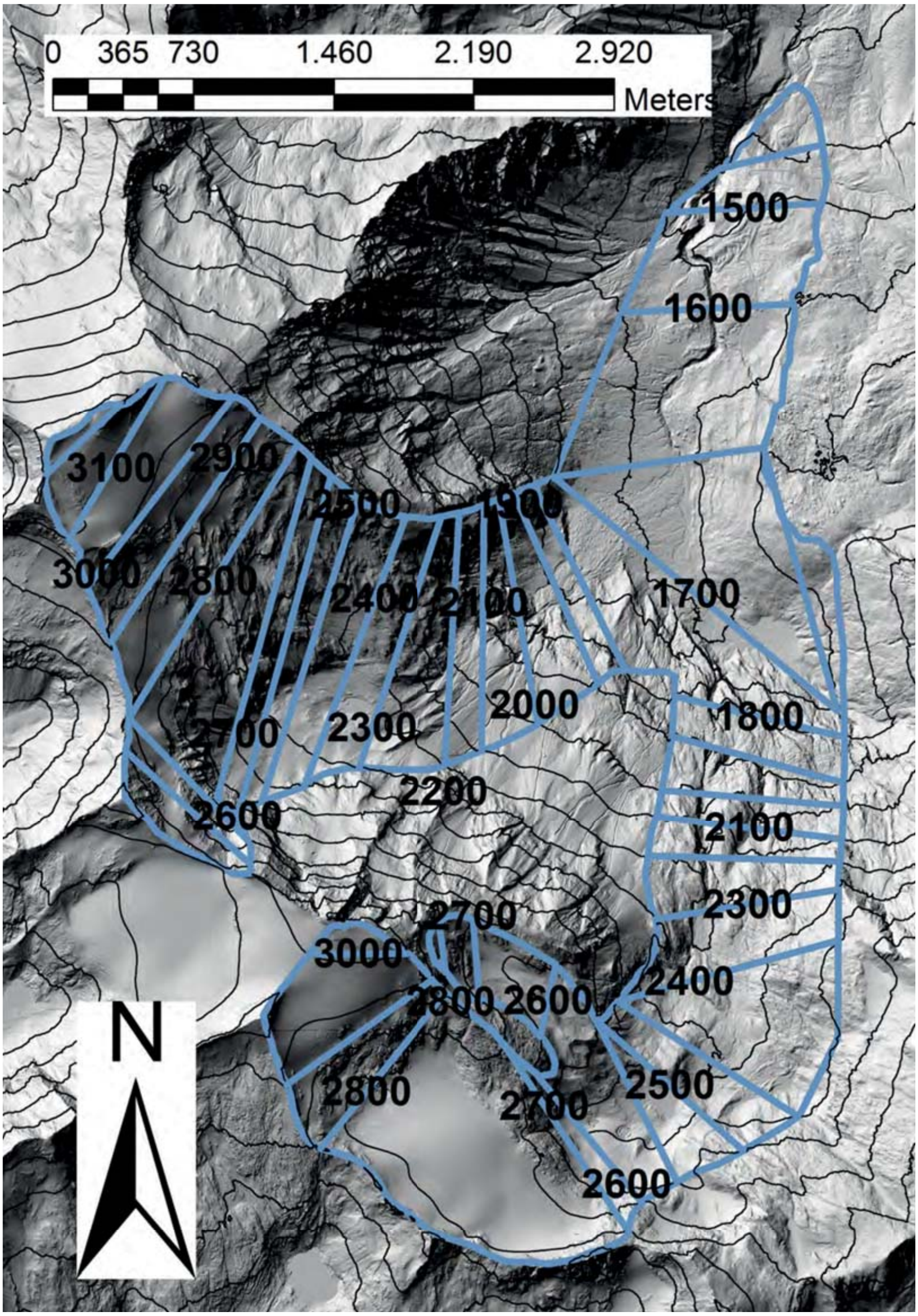

Figure 6.1.: Approximated Egesen glacier surface, based on geomorphologic evidence and interpolation between valley sides. The numbers refer to the former Egesen-age glacier contour lines. For easier reconstruction a flat ice surface is assumed.

- The basin of the Goldbergkees is better shielded by surrounding ridges and the valley floor gradient is smaller, until it drops sharply north of the Neubau hut.
- Parallel Egesen ridges are missing at the immediate forefront of the LIA-1850 extent of the Pilatuskees. This can be attributed to the much steeper terrain there, supporting erosional processes.

When considering the glacier dynamics of the former Egesen glaciers, we need to consider what role these two glaciers played. Overall, the accumulation areas of the two glaciers should be comparable in size, with the Pilatuskees having a possible key advantage with the added accumulation area from the north face of the Sonnblick.

The key for understanding the influence of the Pilatuskees lies in the valley floor of Kolm-Saigurn. While the immediate forefront of the LIA-1850 Pilatuskees does not contain traces of Egesen lateral moraines, the valley floor further down exposes a partly eroded moraine ridge (see Figure 6.2 and section 4.9). The general longitudinal direction suggests an origin from the Pilatuskees forming the right lateral moraine. Extending the ridge north, we hit the parallel recessional moraines. Looking closely at the innermost and youngest moraine ridges, the direction of the southern end is bent towards the direction of the Pilatuskees and does not strictly follow the directional flow of the Goldbergkees directly from the south. This is especially true for the Egesen moraine ridges number (1), (3), and although interrupted, number (4).

The moraines (1) and (3) show a distinctive wiggle, between the Pilatuskees-facing southern end, and the north end. Moraine ridge (4) can be interpolated to a single ridge, with a missing central section, similar to the two younger moraines. A uniform flowing glacier on a uniform topography would not have produced such a lateral moraine, but one that follows the topography with a uniform, shallow gradient towards the north. The gradient of moraine ridge (3) is shown in Figure 6.3. Interestingly, the gradient points uphill for 120 m. The moraine ridge gains 17 m in elevation over the course of this distance. After reaching an elevation of 1627 m, the ridge decreases again with approximately 3.8 m per 100 m.

Belonging to the late Younger Dryas, these moraines reflect a late state of the glaciers junction when the ice was decaying between several stadials during the late Egesen (chapter 5), also referred to as *Kartell* (Fraedrich, 1979; Sailer, 2002; Kerschner, 2009). During the late Egesen the Pilatuskees was attributing ice volume to the glacier confluence, locally elevating the ice thickness by 17 m. The moraine ridges reflect this increase in ice volume and allowed the moraines to deposit in an uphill direction. It is possible

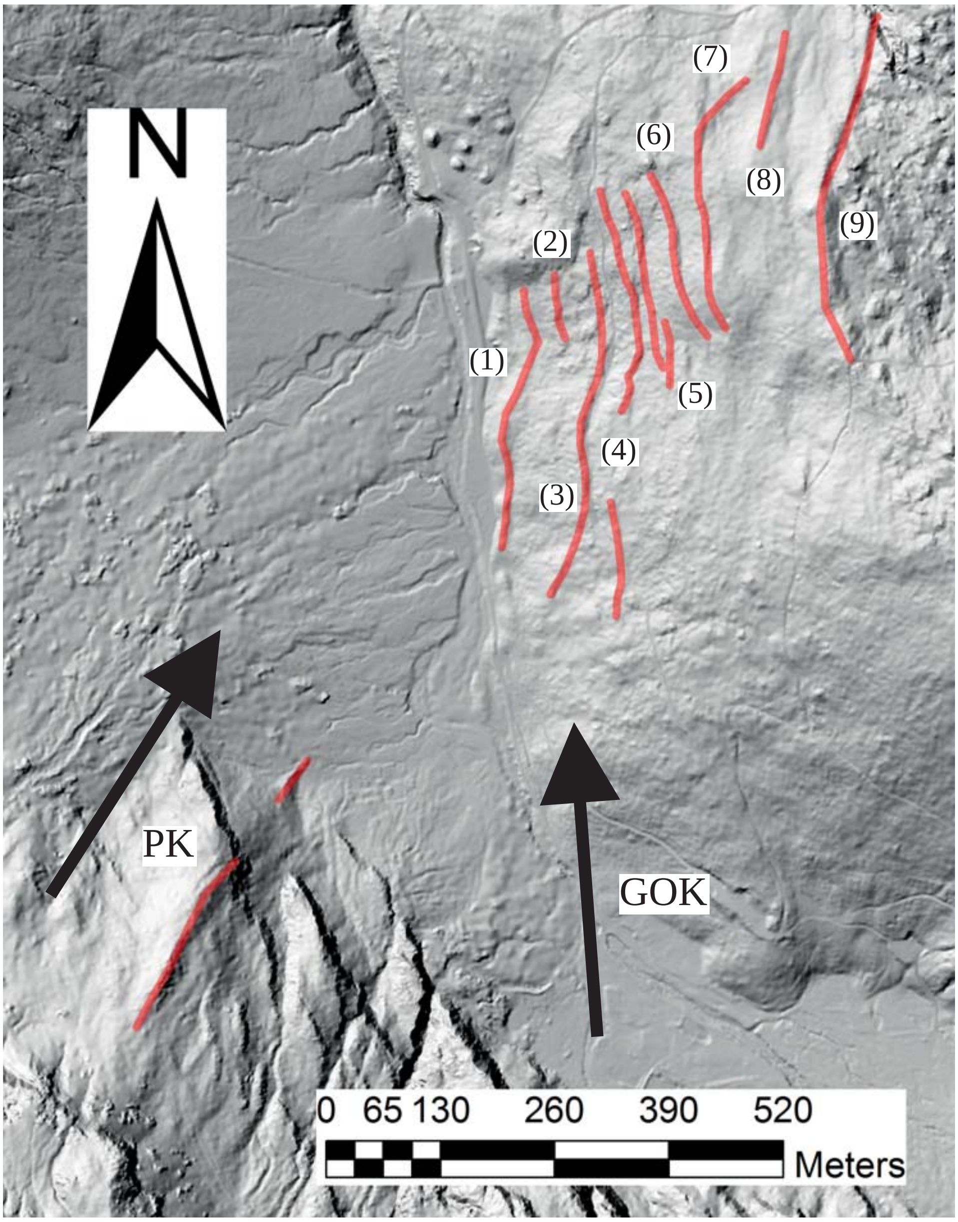

Figure 6.2.: Hillshade model of the area just north of Kolm-Saigurn. The arrows mark the flow direction of glaciers. PK = Pilatuskees (right lateral moraine and ice flow direction), GOK = Goldbergkees ice flow direction. The Egesen moraines are numbered from 1 to 9. Ridge 9 marks the Egesen maximum extent.

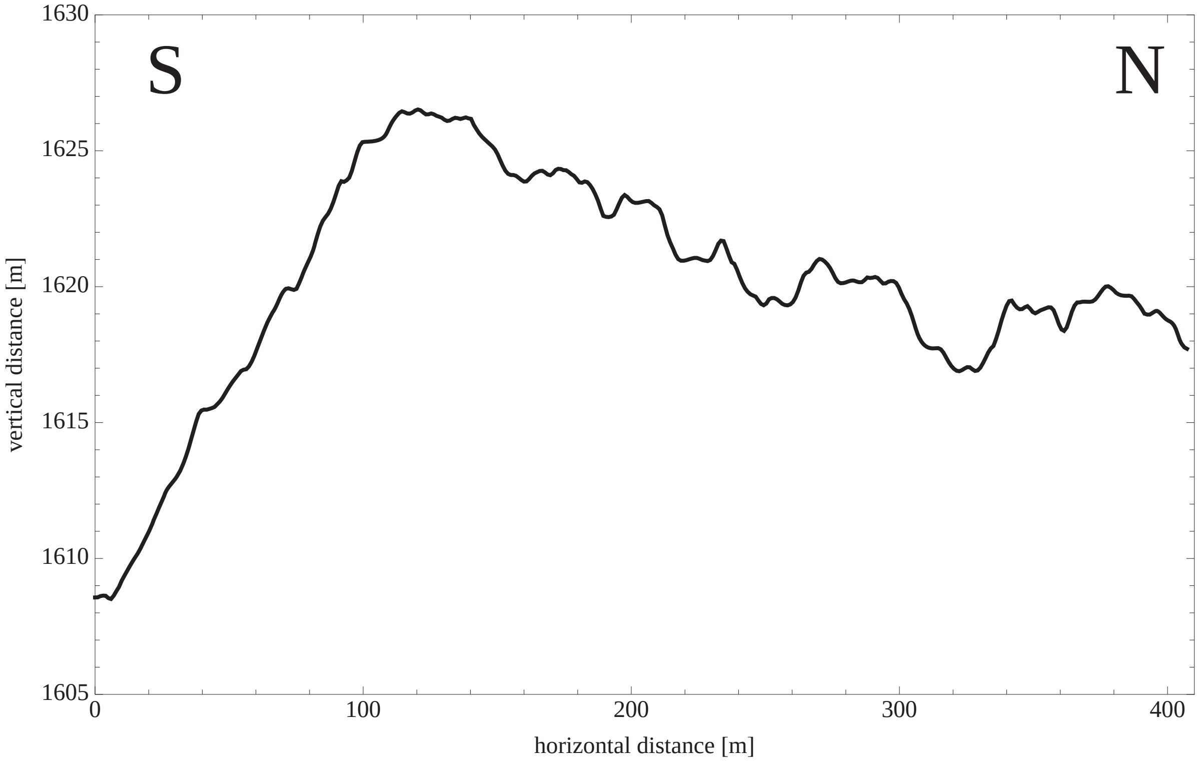

Figure 6.3.: Longitudinal Kolm-Saigurn moraine ridge (3) (see Figure 6.2).

that the Goldbergkees was not even able to regenerate at all in the basin of Kolm-Saigurn (see section 6.3), and all the ice volume can be attributed to the Pilatuskees during the last ice decay phases. More elevated and therefore older Egesen-type moraine ridges uphill to the east do not display this distinctive morphology, hence suggesting a fully developed confluence situation. Two reasons can be identified why it was possible for the Pilatuskees to extend further into the Hüttwinkl valley than the Goldbergkees during the late Younger Dryas. First, added accumulation from the north face of the Sonnblick and the flanks from the Goldzechkopf, giving the flank-type Pilatuskees (as visible today and the LIA-1850 border) a more basin-type characteristic located between the Sonnblick and the Hocharn, allowed the ELA to remain lower. During the LIA, the ELA of the Pilatuskees was generally higher than the Goldbergkees ELA (subsubsection 6.2.2.1), but a similar late Younger Dryas ELA would have allowed the Pilatuskees to transport more ice to a lower area, outmatching the Goldbergkees ice volume in the confluence area. Second, the likelihood of the Goldbergkees forming a regenerated glacier (section 6.3) at Kolm-Saigurn took momentum from the glacier. This made it possible for the Pilatuskees, which did not suffer from such an obstacle, to overrun the ice-fall and avalanches deposits before they could regenerate out of the Kolm-Saigurn basin. This situation was unique to the Lateglacial in this area. During the Egesen and later stadials, the Goldbergkees was always able to transport ice and sediments at least equally to the Pilatuskees. Whereas during the Holocene, both glaciers were never able to form a glacier confluence again, and during the LIA, the Pilatuskees, losing its advantages of a basin-type glacier, with 2.92 km^2 (see Table B.2) only amounted to 91 % of the surface area of the Goldbergkees at 3.20 km^2 (see Table B.1).

6.2. Equilibrium Line Altitudes [Reindl]

Former Equilibrium Line Altitudes (ELAs) are a good proxy for reconstructing the past climate. The concept of ELAs (the German term is *Schneegrenze*) is simple. The ELA marks the line on a glacier's surface, where the ablation balances the accumulation area (Gross et al., 1976; Sugden and John, 1976). If the climate is in favor of glacier grow, such as colder and wetter conditions, the accumulation area will grow with the glacier flowing downward, and therefore the ELA will sink to lower altitudes. Consequently, when climatic conditions are less favorable, the accumulation area will shrink and the ELA will rise to higher altitudes (see Figure 6.4). An advancing glacier produces till, and, when the climatic conditions are stable, lateral and terminal moraines. It is this sedimentary evidence that we can find today which helps us to reconstruct the former ELAs of glaciers that have long disappeared. The key factor here is that these terminal and lateral moraines are only produced when the glacier (and therefore the climate is in a stable) state. Dynamic ELAs of an advancing glacier are therefore hard to calculate. When a glacier is in retreat we are still sometimes able to calculate former ELAs, when the retreat slows down or even comes to a halt and recessional moraines can form. For the purpose of this document we will only look at these stable state ELAs, for which we can find evidence through moraines in our area.

Figure 6.5 shows the linkage between the geologic record, like moraines and basal till deposits, and the regional climate. The importance of the local topography is outlined, as it impacts both the regional climate and the glacier mass balance, as well as the glacier geometry and ice-flow dynamics. A detailed knowledge of the geologic record is therefore necessary in order to be able to reconstruct the regional climate.

A number of methods exist to estimate the former ELAs of glaciers (Benn and Lehmkuhl, 2000; Osmaston, 2005; Benn et al., 2005). They all require a specific set of input parameters, the simple methods only require a rough knowledge of the former glacier surface, while the more sophisticated rely on detailed hypsometry. All of these

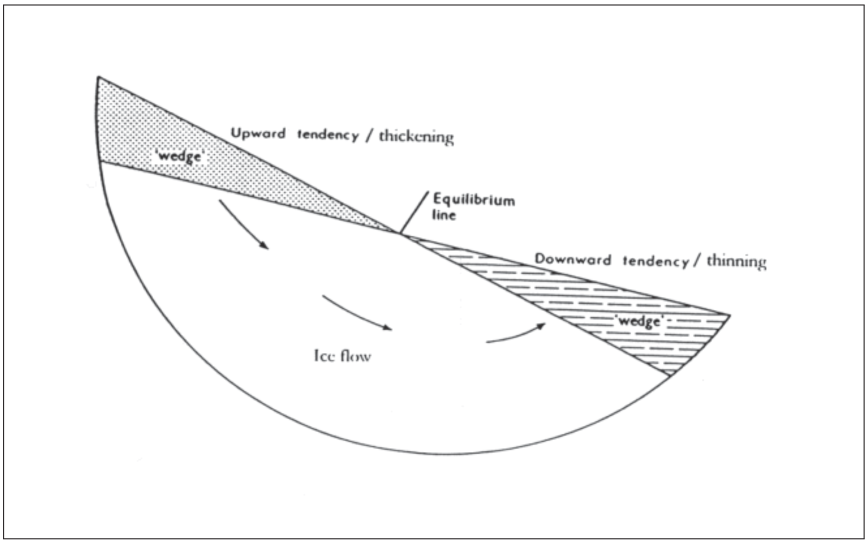

Figure 6.4.: Idealized glacier model, with the Equilibrium line separating the accumulation wedge and the ablation wedge (Sugden and John, 1976).

methods have in common that the output of each method is a number that gives the snowline (or ELA) depression in meters, relative to the LIA extent, a state often very well documented and visible in the field. It is this key number, ΔELA, that makes it possible to compare the results of the different methods, and, eventually, compare it to other published ELA depressions.

Due to the long history of research at the Sonnblick, detailed maps, photos, and documents of the historic Goldbergkees are available (Posepny, 1879). While Schöner (2009) contains a set of examples of the historic documents and gives a summary of ELA mechanics after the LIA, it is our goal to reconstruct ELAs well before the LIA.

6.2.1. Methods

Several methods for ELA calculation exist. We used the most common methods to calculate the former Egesen ELAs, as well as their depressions relative to the LIA-1850.

6.2.1.1. Maximum Elevation of Lateral Moraines

Lichtenecker (1938) suggested that the highest elevation of the onset of lateral moraine ridges give a good indication of the minimum altitude of a former ELA, because glacier ablation, and hence ice-marginal deposition, only occur below the ELA. Thus, the former ELA must lie above the highest lateral moraines (Visser et al., 1938; Andrews, 1975; Meierding, 1982). The Maximum Elevation of Lateral Moraines (MELM) method or

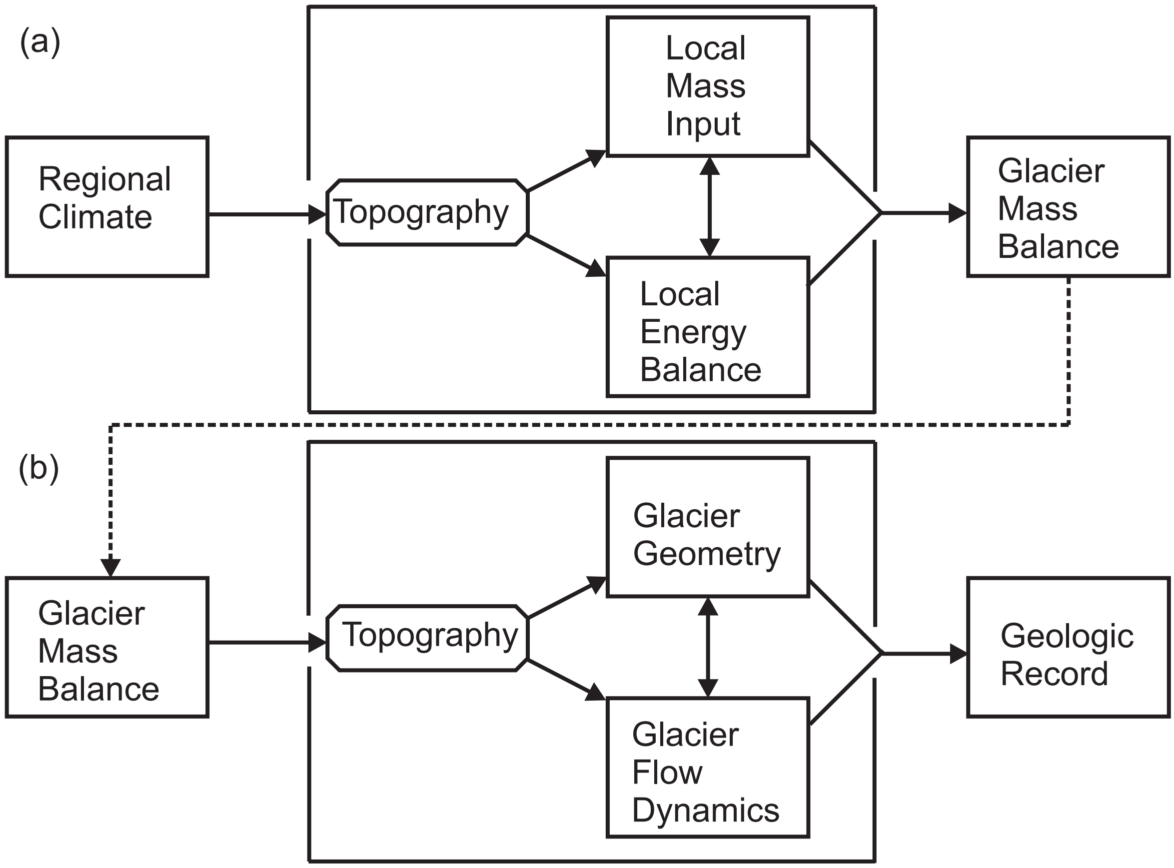

Figure 6.5.: Linkage between the regional climate and the geologic record, modified from Meier and Tangborn (1965); Andrews (1975); Furbish (1984). Generalized linkage between the regional climate and the individual glacier mass balance is shown in (a), while (b) shows the linkage between mass balance and glacier response as reflected by the geologic record. Topography influences local climate and, in part, glacier geometry and ice-flow dynamics.

Methode Lichtenecker generally gives good results with debris covered glaciers where the moraines are well established and the amount of degradation is low (Benn and Lehmkuhl, 2000). The MELM method was also successfully employed outside of the Alps (Glasser et al., 2004). For the Goldbergkees, the left lateral moraine of the LIA-1850 extent is very well documented by Lichtenecker (1935). Additionally, we were able to identify it on the Digital Elevation Model (DEM), starting at an elevation of 2556 m asl. The Egesen extent of the lateral moraine could be also identified with the parallel ridges at the Grieswiestauern (see section 4.9), with the innermost moraine starting at an elevation of 2229 m asl. This exact moraine was chosen, because the onset is easily identifiable, and the other, parallel, ridges are harder to identify. Nevertheless, the elevation of the moraine start only varies a few meters between these ridges and it is safe to use this elevation which results in a ELA depression of −327 m, with respect to the LIA-1850 ELA (see table Table 6.3).

6.2.1.2. Toe-to-Headwall Altitude Ratio

Another straightforward set of methods are the Toe-to-Headwall Altitude Ratio (THAR) method, and the similar Toe-to-Summit Altitude Method (TSAM). The THAR method assumes that the ELA lies at some fixed portion of the vertical distance between the highest and the lowest points of the glacier (Benn and Lehmkuhl, 2000). The fixed portion varies between glacier types. Debris covered glaciers have a rather high THAR ranging from 0.6 to 0.8 (Clark et al., 1994), while Porter et al. (1983) used values of 0.4–0.5 for clean ice glaciers. Charlesworth (1957) and Manley (1959) used the median elevation of glaciers (MEG), which places the ELA midway between the glacier toe and the base of the head-wall. This is equivalent to a THAR of 0.5.

Defining the upper limit of the Goldbergkees is straightforward, it is in the area just below the Sonnblick summit and we place it at 3060 m asl for this purpose. The Egesen upper limit was definitely a few meters higher, and the rocky summit was probably ice and firn covered too, so we assumed to be it at 3100 m asl. Defining the amount of debris cover on the Egesen-age Goldbergkees can be difficult. The ablation area was certainly not of the clean ice type, but a slightly debris covered area with a THAR around 0.5 (see Table 6.1 and Table 6.2). While the location of the LIA-1850 lower limit and the terminal moraine is well known at 2190 m asl (Lichtenecker, 1935), the location or existence of the terminal moraine for the Egesen and therefore the lower limit of the glacier is unknown (section 4.6 and section 4.2). Good knowledge of the glacier terminus is critical not only for the THAR method, but even more for the subsequent methods, as the glacier surface area changes significantly with a higher glacier terminus. Only lateral moraines from stable phases during glacier retreat are visible in the area of Kolm-Saigurn at an elevation of approximately 1600 m asl. The topography of the valley floor suggests the glacier extending to the Lenzanger area or even further north to the Gersteben step (section 4.2 and section 4.6). It is in this area where last traces of basal till can be found on the Durchgangwald landslide deposits. The minimum elevation and maximum extent of the Egesen advance can therefore only be assumed to be at a minimum elevation of 1400 m asl.

The TSAM method was invented to overcome difficulties in defining the upper limit of the glacier. Louis (1955) proposed that the ELA can be estimated from the arithmetical average of the altitude of the highest peak in the catchment and the terminal moraine. As the highest peak in the catchment of the Goldbergkees is the summit of the Sonnblick, the TSAM method is equivalent to the THAR method with a THAR of 0.5 and produces exactly the same result.

Combining these considerations, we calculate a maximum ELA depression for the Goldbergkees of −375 m, and a minimum ELA depression of −275 m (see also Table 6.3). The maximum value reflects the biggest advance of the Egesen glacier when climatic conditions were most favorable, while the minimum value reflects a state where the Egesen glacier was only barely able to fill the area of Kolm-Saigurn with ice, but still managed to build small lateral moraines. The ELA depressions are 44.5 m more for the Pilatuskees, peaking at −419.5 m and −319.5 m.

Table 6.1.: Equilibrium Line Altitudes for the THAR method for the Goldbergkees. As a lower estimate, the glacier terminal is assumed to be at 1400 m asl, the upper estimate is located in the basin of Kolm-Saigurn at approximately 1600 m asl.

	ELA			ΔELA max	ΔELA min
	LIA-1850	Egesen max	Egesen min		
terminal	2190 m	1400 m	1600 m		
head	3060 m	3100 m	3100 m		
THAR	0.5	0.5	0.5		
	2625 m	2250 m	2350 m	**-375 m**	**-275 m**

Table 6.2.: Equilibrium Line Altitudes for the THAR method for the Pilatuskees. The Egesen extent remains unchanged from Table 6.1.

	ELA			ΔELA max	ΔELA min
	LIA-1850	Egesen max	Egesen min		
terminal	2085 m	1400 m	1600 m		
head	3254 m	3100 m	3100 m		
THAR	0.5	0.5	0.5		
	2669.5 m	2250 m	2350 m	**-419.5 m**	**-319.5 m**

6.2.1.3. Area × Altitude

The Area × Altitude (AA) method, also termed Balance Ratio (BR) method by Furbish (1984), was first invented by Kurowski (1891) and further developed by authors such as von Drygalski (1942). The AA method relies on detailed glacier hypsometry, and therefore was often limited by the lack of reliable contour maps of glacier regions (Osmaston, 2005; Benn et al., 2005). With enough geomorphologic information and detailed elevation data available nowadays, it is possible to interpolate a glacier surface in GIS and derive a contour map for use with the AA method, and subsequently, the AAR (subsubsection 6.2.1.4) and the Area × Altitude Balance Ratio (AABR, see subsubsection 6.2.1.5) method. The AA method involves taking a trial value for the ELA (e.g. the mid-altitude), then multiplying the areas of successive contour belts by their mean altitude difference above or below the trial ELA. The algebraic sum of these indicates whether the trial ELA should be moved up or down, and the calculation is reiterated until a zero sum is obtained (Osmaston, 2005). This procedure works best when automatized, and early versions were available for download. Unfortunately, this is no longer true and we followed the method as described in Osmaston (2005) to produce ELAs for the Goldbergkees and the Pilatuskees in spreadsheets (see Table B.1, Table B.2 and Table B.3).

This method, and the subsequent AABR method requires knowledge about the contour belt area. In our case, this is the area between two 100 m interval contours. As a first step, the historic glacier surfaces of the Goldbergkees, the Pilatuskees and the maximum Egesen extent were digitized and their respective contour belt areas calculated in GIS. The LIA-1850 extent of the Goldbergkees is well documented by Lichtenecker (1935). The LIA-1850 of the Pilatuskees extent was interpolated between the well established LIA-1850 right lateral moraine and partial terminal moraines and the Hocharn summit in the north, and the Sonnblick with it's north face in the south. The total contour belt area of both LIA-1850 glaciers is comparable in size at approximately 3 km^2. The calculated ELAs of both glaciers differ by more than 100 m. While the Goldbergkees ELA is calculated to be at 2648 m, the Pilatuskees ELA is placed at 2754 m. This unlikely high difference can be attributed to the fact of a missing detailed LIA-1850 glacier map for the Pilatuskees. Such an elevated ELA value suggest an over-weighting of the size of the accumulation area in our model. But for the lack of better field evidence, we therefore choose to calculate a maximum Egesen ELA depression from the Pilatuskees LIA-1850 ELA value, and a minimum Egesen ELA depression from the Goldbergkees LIA-1850 ELA. The maximum Egesen extent was reconstructed from the field evidence presented in this work (section 4.6 and section 4.2). During most of the Younger Dryas, both glaciers were attributing to the Kolm-Saigurn glacier system (see section 6.1), which means it is possible to calculate a single Egesen ELA with this method (Table B.3).

At its maximum extent, the Kolm-Saigurn glacier system covered 11.5 km^2. Almost twice as big as the two LIA glaciers combined. The calculated ELA depression lies in the range of −375 m when the Pilatuskees LIA-1850 ELA taken as a reference, and −251 m for the Goldbergkees ELA (Table 6.3).

6.2.1.4. Accumulation Area Ratio

The Accumulation Area Ratio (AAR) method is widely used for ELA calculation. It is based on the assumption that the accumulation and the ablation area of a glacier surface are in a fixed relationship (Meier and Post, 1962; Porter, 1975; Gross et al., 1976; Torsnes et al., 1993; Benn and Lehmkuhl, 2000). For modern glaciers in the European Alps, the accumulation area is assumed to be two times higher than the ablation area (2:1). The accumulation area therefore occupies two thirds of the overall glacier surface, resulting in an AAR of 0.67. This value of course varies locally and values lower than 0.67 are reported for glaciers with debris covered snouts (Benn and Lehmkuhl, 2000). A value of 0.67 is generally also used for the reconstruction of lateglacial paleoglaciers (Gross et al., 1976; Kerschner and Ivy-Ochs, 2007; Ivy-Ochs et al., 2008).

The same input values were used for the AAR method as for the AA method. First, the total glaciated area is calculated from all contour belts, which is then multiplied by the AAR to get the size of the accumulation area. Then, the separate contour belt areas are summed up, starting at the highest point of the glacier, and therefore its accumulation area. Once the sum of the contour belt areas exceeds the calculated accumulation area the calculation is stopped. The corresponding contour belt mean altitude then approximates the real ELA. For this purpose we developed a Mathematica version (see Appendix A).

For the Goldbergkees, the AAR results in a LIA-1850 ELA of 2350 m, and for the Pilatuskees this value is at 2550 m. The calculated Egesen ELA for the Kolm-Saigurn glacier system is at 1850 m with this method.

6.2.1.5. Area × Altitude Balance Ratio

The Area × Altitude Balance Ratio (AABR) method is a refinement (Osmaston, 2005; Benn et al., 2005), based on the principle of the AA method of weighting the mass balance in areas far above or below the ELA more than those close to it. The refinement is based on the fact that the mass balance curve above and below the ELA is not linear but can still be described as different linear slopes. The AABR method provides a way to consider these non-linearity when deriving an ELA. As for the AA method (subsubsection 6.2.1.3), we use the instructions in Osmaston (2005) for the spreadsheet calculations. Being too big to include here, the full spreadsheet can be permanently found online at: `http://catai.org/~martin/Sonnblick/AABR.ods`.

The AABR method amends the AA method by the Balance Ratio (BR) factor. This factor lies between 1.5 and 3.5 for most glaciers. Clean ice glaciers tend to have a higher BR, while debris covered glaciers can have a BR as low as 1. For the Kolm-Saigurn glacier, a BR needs to be carefully chosen. Furbish (1984) used a BR = 2 for modern glaciers in Alaska, similar with respect to the size of the former Kolm-Saigurn glacier system, we therefore also used this number as a basis of our calculations. The AABR is exactly equal to the AA (subsubsection 6.2.1.3) method when the BR = 1. For each ELA trial value the belt area × *alt above ref contour* and the *area* × *alt* × *BR for contour* is then calculated and summed up. The calculation is reiterated for each trial ELA (usually the trial ELA is increased, in our case in steps of 100 m), until the total sum *area* × *alt* × *BR for contour* gets negative. The exact AABR ELA is then calculated as the ratio between the two *area* × *alt* × *BR for contour* values.

For an BR value of 1, we calculate an Egesen ELA for the Kolm-Saigurn glacier at 2397 m, which is consistent with the results from the AA method. A BR of 2 results in an Egesen ELA at 2234 m. For the LIA-1850 Goldbergkees and the Pilatuskees these numbers are at 2587 m and 2675 m, respectively (Table 6.3).

6.2.2. Comparison

6.2.2.1. ELA synthesis

We showed how five different, well established methods, can be used to calculate the ELA depression during the Younger Dryas. The results range from a maximum ΔELA of −700 m to −251 m (see Table 6.3). Reaching consent on a single value of ΔELA is difficult, but can be achieved by carefully investigating the advantages and drawbacks of each method. For the study area, this efforts are complicated by the fact that the ablation areas of the two main glaciers in the area join relatively close to the terminus, thus forming one glacier system.

Table 6.3.: Egesen ELA depressions comparison

Method	ELA				ΔELA	
	LIA-1850 PIK	LIA-1850 GOK	Egesen max	Egesen min	max	min
MELM		2556 m	2229 m		**-327 m**	
THAR	2669.5 m	2625 m	2350 m	2250 m	**-419.5 m**	**-275m**
AA	2754 m	2648 m	2397 m		**-357 m**	**-251 m**
AAR	2550 m	2350 m	1850 m		**-700 m**	**-500 m**
AABR	2675 m	2587 m	2234 m		**-441 m**	**-353 m**

Each of these methods must obey to the field evidence, as indicated by the MELM method. Luckily, we were able to employ this method both for the LIA-1850 Goldbergkees as well as the Egesen Goldbergkees. We therefore can exclude a Younger Dryas ELA lower than 2229 m, the onset of the left lateral moraine ridges at Grieswiestauern (section 4.9) and an ELA lower than 2556 m for the LIA-1850 Goldbergkees.

Interestingly, all but the AAR method calculate a higher ELA for the LIA-1850 Goldbergkees. The AABR method, gives a slightly higher, but comparable result within agreement of the MELM method (approximately 2560 m), indicating a good estimation of the LIA-1850 Goldbergkees and its Balance Ratio. The THAR and the AA methods produce values up to 92 m higher, while the AAR method produces an unlikely low value approximately 200 m below the MELM result, indicating an AAR of 0.67 does not model the LIA-1850 Goldbergkees correctly. The MELM method could not be employed for the Pilatuskees, but the four remaining methods each put the LIA-1850 ELA here generally higher than for the LIA-1850 Goldbergkees. Reconstructing the LIA-1850 Pilatuskees glacier surface proved to be difficult, but the AABR and the THAR method seem to agree on a value of around 2670 m. The AA and the AAR method differ widely, which can be attributed to the problem of defining the exact LIA-1850 glacier extent, but as the AABR method showed a good result for the LIA-1850 Goldbergkees the indicated ELA of 2670 m for the LIA-1850 Pilatuskees seems reasonable.

Finding a consensus on the Egesen ELA follows the same principles. An unlikely low ELA of 1850 m is again calculated by the AAR method, a value almost 280 m below the MELM result. The AABR result is again in accordance with the MELM result at approximately 2230 m. As the THAR method requires knowledge of the glacier terminus location, a requirement not met for the Younger Dryas, the ELA could only be estimated to lie within 2350 m and 2250 m. The latter value stems from an approximated glacier terminus at 1400 m and comes close to the MELM and AABR value. Finally, the AA method again gives the highest value of all, indicating a BR of 1 is too low for the Egesen glacier. This is also indicated by the AABR method with its results calculated with a BR of 2.

Overall, the MELM and AABR methods seem to be best situated for this study. The THAR is simple and shows surprisingly good estimations for parts of the overall picture. The AA and the AAR methods suffer from incorrect assumptions (BR=1 and AAR = 0.67). Additionally, the AAR method only works satisfactorily with uniform sloped, not too shallow valleys and no exceptional terrain drops.

Considering all these facts we can deduce a single ΔELA for the Kolm-Saigurn glacier system, albeit with limitations. Field evidence lacks the proof for terminal moraines, marking a stable state in the glacier's lifetime, and only lateral moraines of recessional stages of the glacier system are preserved. It is this fact that only allows us to estimate a maximum ELA depression during the Younger Dryas. Based on the above calculations this is at −330 m for the Kolm-Saigurn glacier system, relative to the LIA-1850 Goldbergkees. But as the field evidence shows, steady-states with ΔELAs between −200 m and −300 m were present during most of the Younger Dryas.

6.2.2.2. The Younger Dryas local climate

Kerschner and Ivy-Ochs (2007) give an overview of the relation between the Egesen-maximum ELA and the ELA depression in western Austria and Switzerland (Figure 6.6) In Kerschner (2005) is stated that research about the Lateglacial period should be extended to the Northern Alps and to areas south of the Alpine Ridge. Our study area is located well east of the areas researched in Kerschner and Ivy-Ochs (2007) and can help to fill the gaps. As the Goldberggruppe lies within the eastern part of the Hohe Tauern alpine range, south of the Northern Calcareous Alps (NCA), our ΔELA calculations can be used to further draw conclusions of the Younger Dryas local climate of the eastern Hohe Tauern alpine range.

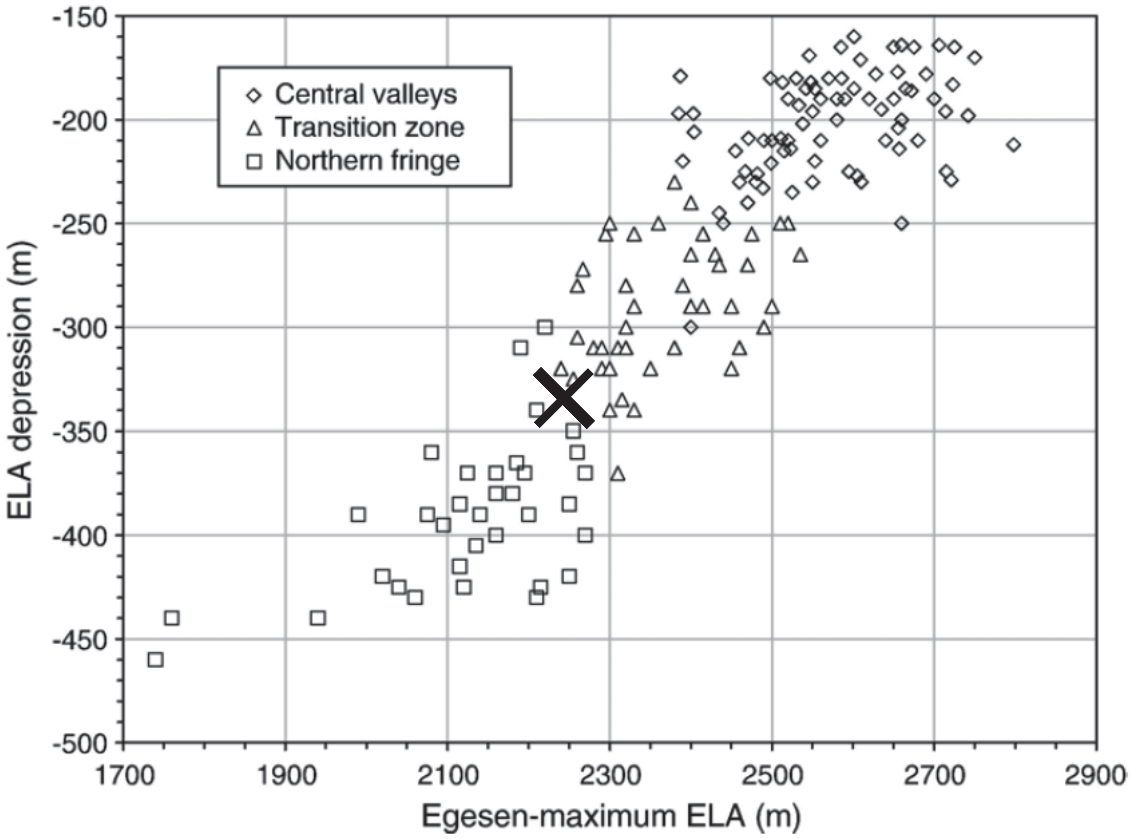

Figure 6.6.: Relation between the Egesen-maximum ELA and the ELA depression in western Austria and Switzerland. Modified after Kerschner and Ivy-Ochs (2007). The Kolm-Saigurn glacier (subsubsection 6.2.2.1) plots at the black cross

.

Kerschner and Ivy-Ochs (2007) divided the research area in western Austria into three areas, based on topographic criteria:

- The Northern Fringe, comparable to the NCA.
- The dry Central Valleys of the Alpine main ridge.
- And a transition zone between these two areas.

Clearly, from a topographic point of view, the Sonnblick and the Hüttwinkl valley fit into the second category of this model. Plotting the data from subsubsection 6.2.2.1, we see that this might not be true for the Younger Dryas local climate. The data does not plot in the *Central valleys* area, but between the data points for the *Northern fringe* glaciers with their high ΔELAs and low Egesen-maximum ELAs, and the *Transition Zone*. The study area compares badly to the central valleys of western Austria, because a higher precipitation was present during the Younger Dryas, as it is today (Figure 6.7), resulting in a glacier friendly locale climate. Two reasons could be the cause:

- The topographic conditions favored wet and cold air reaching the Sonnblick from the N and NW, similar to conditions today and similar to conditions in the NCA in western Austria.
- The Sonnblick area's distance to the water body of the Adriatic sea is much less than the Alpine central valleys of western Austria, possibly favoring wetter air masses to reach the Hohe Tauern. The calculated ELAs could therefore display an influence of some degree from the Mediterranean Sea.

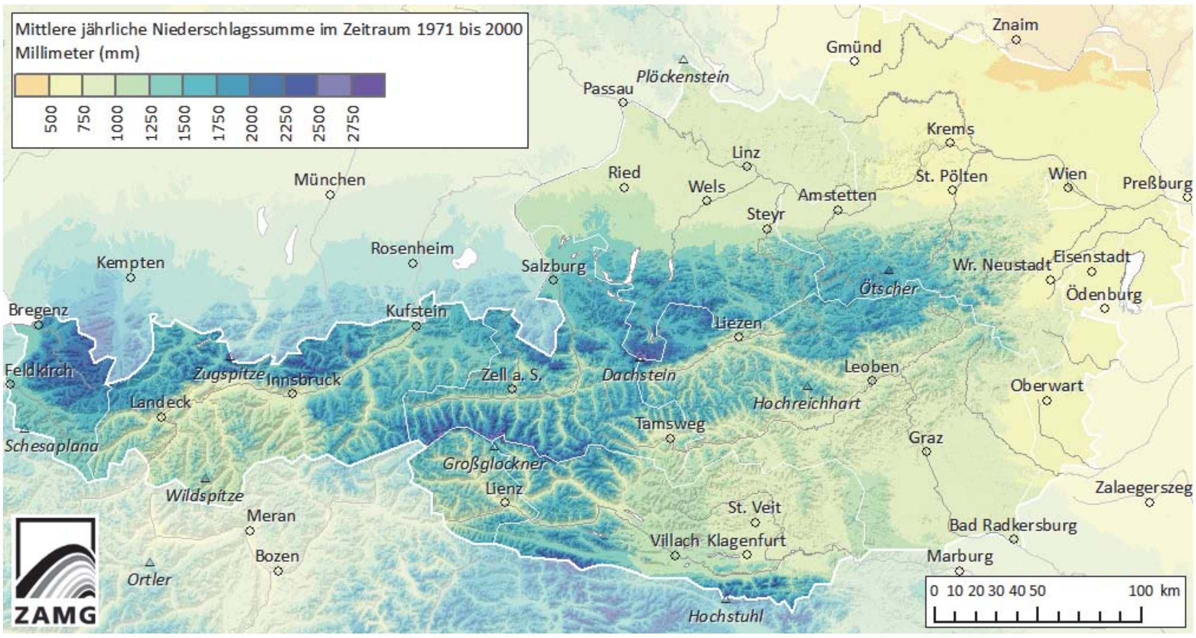

Figure 6.7.: Average annual mean total precipitation from 1971 to 2000, source: Hiebl et al. (2011). Note the N facing valleys of the Hohe Tauern Alpine range (around the Großglockner) today receive a similar amount of annual precipitation as the western NCA.

Kerschner and Ivy-Ochs (2007) also calculated the precipitation and temperature change for the early Younger Dryas (Egesen maximum) relative to the LIA (Table 6.4).

Assuming the local climate fits into the *Northern Fringe* and *Transition Zone* categories, a lower summer temperature of −3.5 K results in a +5 % (Northern Fringe) and −9 % (Transition Zone) change in precipitation, respectively. Interpolating these numbers, this can be interpreted as a solely temperature induced glacier advance under slightly drier conditions.

A much a greater impact on precipitation change is induced by a lowering of the mean summer temperature by −5 K. A drop of 20 % in precipitation is likely for the Sonnblick, with up to one third less precipitation than during the LIA. The real temperature and precipitation change is unclear and leaves room for further research, possibly by the means of the Filzenalm sediment cores (see section 4.3).

Table 6.4.: Egesen maximum (early Younger Dryas) ELA depressions relative to 1850 AD (ΔELA) and precipitation change. s: standard deviation; ΔP%, ΔP mm/a: precipitation change relative to modern values at the altitude of the modern ELA. Modified from Kerschner and Ivy-Ochs (2007). SS = Sample Size, CV = Central Valleys, TZ = Transition Zone, NF = Northern Fringe

	SS	ΔELA	s	ΔP %		ΔP mm/a	
				ΔTs=-3.5 K	ΔTs=-5 K	ΔTs=-3.5 K	ΔTs=-5 K
CV	80	-201 m	25	-24 %	-54 %	−370 mm/a	−840 mm/a
TZ	44	-290 m	32	-9 %	-36 %	−160 mm/a	−670 mm/a
NF	36	-392 m	36	+5 %	-20 %	120 mm/a	−430 mm/a

6.3. Ice thickness modelling [Reindl]

When investigating ice thickness of the former maximum extent of the Egesen glacier, the question arose if the steps of the Melcherböden south of Kolm-Saigurn up to the Neubau hut and the area of Grieswiestauern were ice covered during the Younger Dryas or the glacier forming in the basin of Kolm-Saigurn was a regenerated glacier (see Figure 6.8). A regenerated, or reconstituted, as termed by Benn and Lehmkuhl (2000), glacier has parts of his area disconnected by steep cliffs, where the lower areas are fed by the upper areas by means of avalanches and ice fall. It is even possible that these cliffs separate the accumulation area and ablation area, which puts the ELA on ice-free, possibly rocky, area. The ELA for the Egesen maximum extent of the Goldbergkees remained above these steps at any time during the Younger Dryas, although we cannot exclude it dropped to the lower lying area for very short time periods, as the calculated Egesen maximum

ELA sits just right on the edge to the aforementioned steps.

Figure 6.8.: Regenerated glacier, Morsarjökull, Iceland. The pictures gives a good idea about the former Goldbergkees, with the Glacier regenerating at Kolm-Saigurn with ice-fall and avalanches from the area of the Neubau hut and the Grieswiestauern, further continuing to flow north. Reproduced with kind permission from J. Alean (http://www.swisseduc.ch/glaciers/glossary/regenerated-glacier-en.html)

The maximum ice-coverage elevation in the basin of Kolm-Saigurn is very well known from the highest point of the till covered area which forms the right lateral extent of the former glacier area. This elevation can be estimated to be at 1770 m asl. The topography and the shallow angle at which the Hüttwinkl Transfer Tunnel (see section 2.3) cuts through the landslide deposits of the Durchgangwald suggest over-deepening in the Kolm-Saigurn basin is negligible. An assumed elevation of 1698 m asl for the basis of the glacier therefore seems reasonable. As a result, the elevation difference of approximately 180 m marks the ice thickness in this area.

Till coverage at the Melcherböden is thin, which suggests this area did not always have the same ice coverage as the areas to the north and south. To better estimate if the Goldbergkees formed a regenerated glacier in Kolm-Saigurn, we used the method described in Benn and Hulton (2010) to generate a glacier model based on geomorphologic facts. This model is based on five input parameters:

- The location of the glacier terminus.
- A longitudinal glacier bed profile, starting at the glacier terminus.
- A cross-section of the valley floor, characterized by a single parameter.
- The yield stress of the ice volume.
- Target elevations for geomorphologic field evidence for the maximum glacier extent.

First, as outlined before, the Kolm-Saigurn glacier system (see section 6.1) consisted of the two glaciers from the Hocharn (Pilatuskees) and from the Sonnblick (Goldbergkees). Therefore it is difficult to come up with a single longitudinal bed profile. As we are investigating the Goldbergkees with regard to the steps south of Kolm-Saigurn, we chose to derive a longitudinal bed profile along the flow path of the former Goldbergkees. This choice attributes all the ice volume of the glacier system to the Goldbergkees alone, but if the model indicates a regenerated glacier existed with this assumption, this would have been even more true with the ice volume missing from the Pilatuskees.

Second, no terminal moraine exists for the Kolm-Saigurn glacier system (see section 4.6 and section 4.2). This makes defining the glacier terminus difficult. But as with ELA calculations (see section 6.2), we can safely assume the lowest point of the Egesen till sediments at 1392 m asl. Like before, if the model indicates that a regenerated glacier existed, then this would have been true for even higher terminal elevations, which in turn would mean a thinner ice body at Kolm-Saigurn and, as a consequence, a higher chance of a regenerated glacier system.

The third parameter, characterizes the cross-section of the ice flow. As the ice volume has to pass different valley profiles on its flow downstream, yield stress will change. The spreadsheet method of Benn and Hulton (2010) summarizes this as one parameter, the shape factor. This shape factor is not constant along the longitudinal bed profile. In theory, it would be best to calculate the shape factor for every iteration along the longitudinal profile, but for practical reasons we chose one representative valley cross-section at the western end of the Hüttwinkl Transfer Tunnel (see section 2.3). The resulting shape factor is 0.55 (see Figure 6.9).

The target elevations are the key to empirically finding correct values for the yield stress. The yield stress has to reflect glacier conditions which correlate with the field evidence. In our case this is the maximum right lateral moraine (see Figure 6.10) and

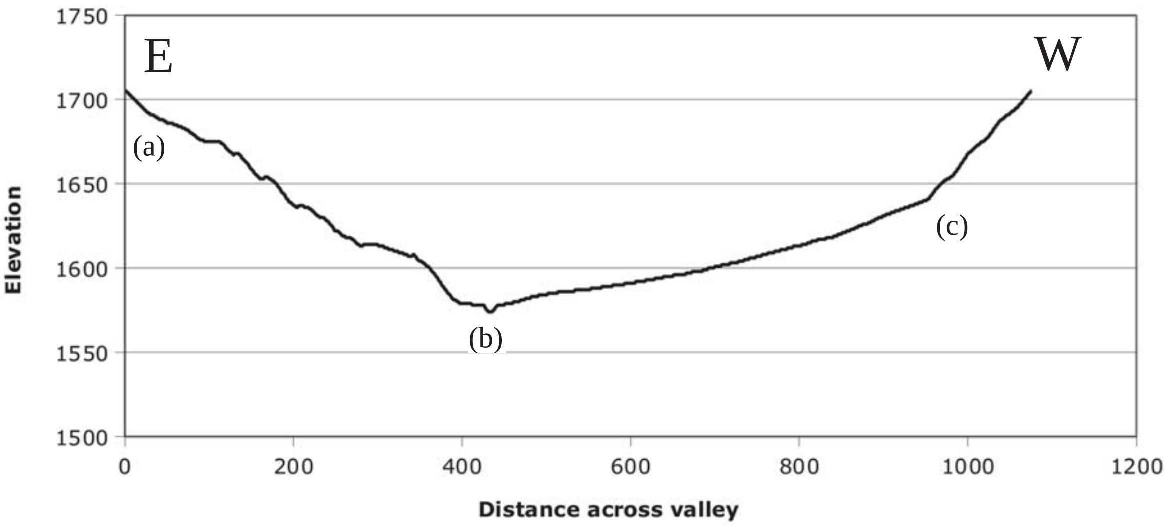

Figure 6.9.: Valley profile perpendicular to the flow direction of the former Kolm-Saigurn glacier system. Note the maximum right lateral moraine covering the Durchgangwald landslide (a), the channel formed by the Hüttwinkl creek (b), and the alluvial fans and debris flows from the valley flanks from the scarp area of the Durchgangwald landslide (c)

the glacier terminus with an target elevation of 0. It can be difficult to find the correct yield stress to cover all target elevations. We found the best fit to be around 57 kPa, as calculated with the spreadsheet method of Benn and Hulton (2010). This value is uniform over the complete longitudinal bed profile for two reasons. First, it gives good data on the expected target elevations, and second, it simplifies the model to some extent. This last point is of course a derivation from reality, as a uniform yield stress cannot be expected in a realistic glacier.

The result of this model is represented in Figure 6.10. Note that the model is calculated upstream with the start of the iterations at the terminus. The glacier surface rises from the terminus at 1392 m asl [Figure 6.10a)] over the first slope to the relatively flat area of the Lenzanger. It then continues to rise to the flat valley floor of Kolm-Saigurn with its prominent right lateral moraines [Figure 6.10c)]. The location of the western portal of the Hüttwinkl Transfer Tunnel, with the perpendicular valley profile is located approximately 1 km north of this point [Figure 6.10b)]. The ice reaches a maximum thickness here at 172 m. It then decreases rapidly as the rocky slopes gain height over the Melcherböden up to the Grieswiestauern [Figure 6.10d)]. The minimal ice thickness on the Melcherböden was therefore at a maximum value of only 15 m at the maximal extent of the Egesen glacier. This indicates a regenerated glacier for much of the time-

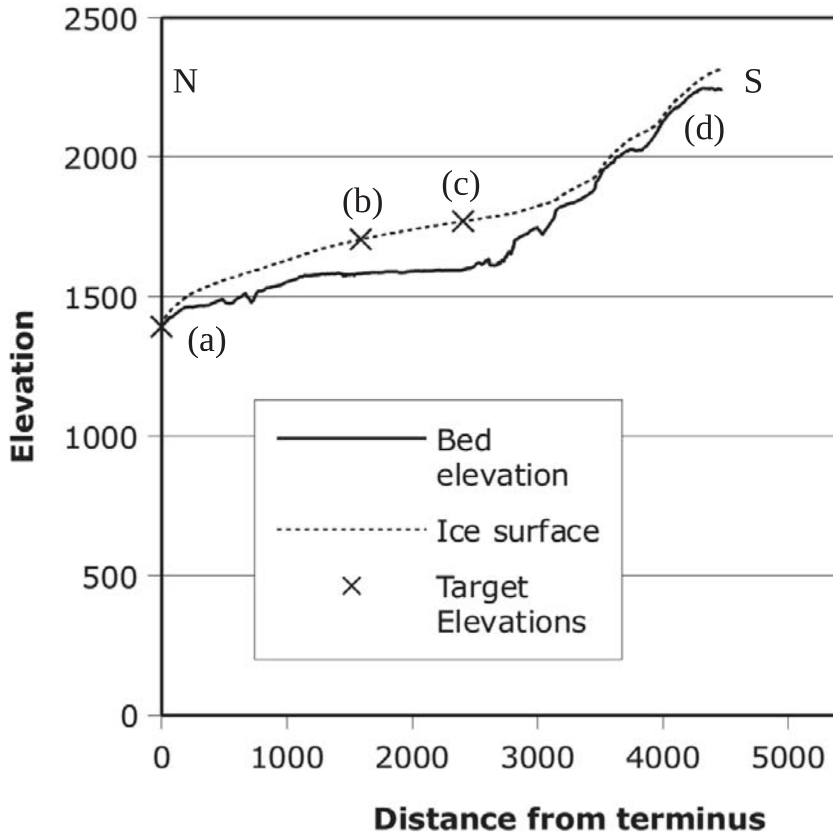

Figure 6.10.: Modeled glacier surface for the maximum extent during the Younger Dryas. The glacier terminus is located at (a), (b) marks the point of the perpendicular valley profile in Figure 6.9, (c) marks the location of Kolm-Saigurn with the maximum ice thickness of approximately 180 m. The steep area south of Kolm-Saigurn is very well visible in this model, with the modeled glacier surface reaching a minimum height of 15 m.

frame of the Younger Dryas, when the ice was either advancing or retreating and did not reach the terminus at 1392 m asl. When climatic conditions were most favorable during the Younger Dryas, it is possible that the ice masses covered much of the Melcherböden and the glacier was not by definition a regenerated glacier. But even then, the steep terrain favored mass transport in terms of avalanches and ice fall, instead of ice flow. We therefore conclude that the Goldbergkees formed a regenerated glacier in the area of Kolm-Saigurn for most of Younger Dryas.

7. Synthesis [Reindl/Bichler]

This chapter represents the synthesis of the previous chapters, and tries to reconstruct the lateglacial history of the Hüttwinkl valleyhead in detail. Figure 7.1 graphically represents the landscape evolution in the area of the Lenzanger parking space. Hillshade based visualizations of the events (Figure 7.2, Figure 7.3, and Figure 7.4) are based on the available 1 m resolution DEM and hillshade model, combined with mapping polygons in ArcGlobe 10.

7.1. Landscape Evolution [Reindl]

During the LGM, the valleyhead and the valley itself were covered by thick ice, typical for the Alpine main ridge. Primary deposits of the LGM could not be clearly identified in our working area, though remnants of it can be found in secondary moved deposits (e.g. alluvial fans of incising creeks).

In addition, no obvious traces of the phase of early Lateglacial ice decay (Reitner, 2007) were found.

As the glaciers were further decaying, ice-margin sediments formed on the north-western slopes of the Grieswiestauern (section 4.9). This was caused by an ice-filled Kolm-Saigurn basin. Although these sediments have not been dated directly, their topographic position and morphology high above the valley floor suggests deposition during the Gschnitz stadial. Their formation during Egesen can be excluded (see section 6.3). During the Gschnitz, ice from the Goldbergkees and the Pilatuskees still extensively covered the valleyhead and the confluent glaciers were free to flow downvalley.

Following the Gschnitz stadial, the Durchgangwald landslide (section 4.2) occurred during the late Bølling-Allerød interstadial at 12.82±1.1 ka BP (section 5.1, Figure 7.2). A simplified GIS model, aiming to reconstruct the former Grieswies-Schwarzkogel eastern flank, calculates the maximum landslide volume at 0.4 km^3 and a scarp surface area of 4 km^2, making it the biggest landslide in the province of Salzburg and similar in size to the Almtal landslide (approximately 0.45 km^3) in the Austrian province of Upper

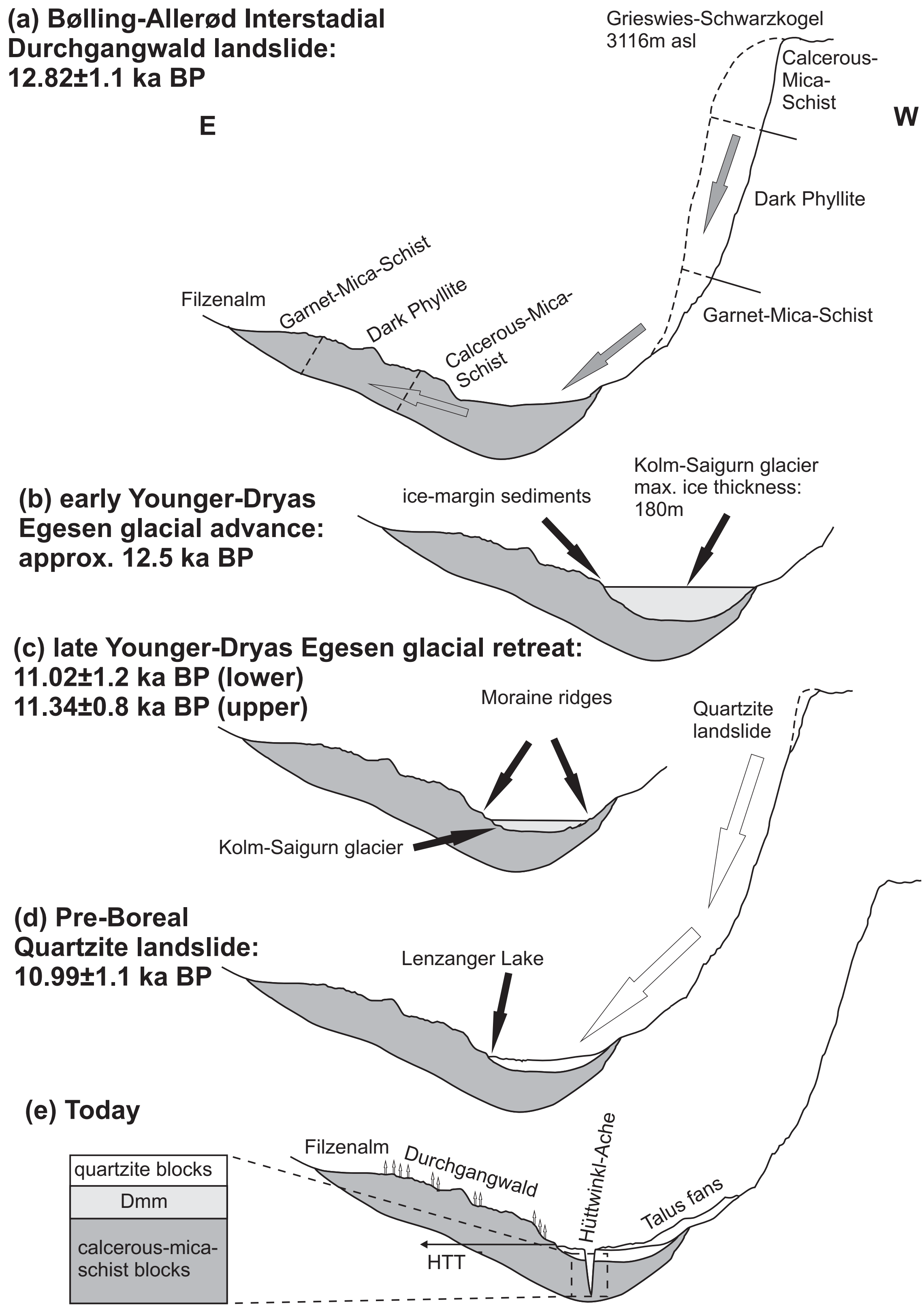

Figure 7.1.: Generalized landscape evolution sketch. Features are not to scale.

Austria (van Husen et al., 2007). These numbers are in line with the values published by von Poschinger (1986), who also excludes existing slip planes in the bedrock as a reason for the movement. Failure due to glacial oversteepening of the valley wall, followed by debuttressing (Reitner et al., 1993; van Husen, 2000; Ivy-Ochs et al., 2009b) during deglaciation is a likely cause for the Durchgangwald landslide. Originating from the Grieswies-Schwarzkogel, the 0.4 km^3 volume landslide came down on the ice-free valleyhead, filling the valley completely and rushing up to the area of what today is the Filzenalm (section 4.3). Mapping confirms the rotational-glide mechanics, due to the fact that the internal sequence of lithology in the landslide correspond with the lithology exposed on the scarp, which is in agreement with von Poschinger (1986). In the northern part, free space towards the north enabled a flow of the dynamically fragmented rock mass in this direction forming a sturzstrom (section 4.6, section 4.7). Instead, a solely W-E direction for the landslide mass between the Bodenhaus and Kolm-Saigurn, with the northern part originating from the Ritterkopf, was interpreted by von Poschinger (1986). Such a flow might have been facilitated by a pre-existing step in the valley slope. The very distal deposits of this sturzstrom, displaying the flow morphology with wave-like landforms perpendicular to the flow direction, can today be seen at the Bodenhaus inn. The area where the sturzstrom broke off from the main mass today marks the distinctive terrain step of the Gersteben (section 4.6). The landslide blocked the Hüttwinklache (section 4.1) in the area of Kolm-Saigurn and creeks at the Filzenalm (section 4.3), forming subsequent lakes. The reason for the landslide event remains unclear, but debuttressing due to glacial oversteepening during the LGM, and to some extent during the Gschnitz stadial, can be assumed to be the main cause.

During the onset of the Younger Dryas, when conditions became more favorable for glacier growth again, both the Pilatuskees (section 4.12) and the Goldbergkees (section 4.10) readvanced into the valleyhead as temperate glaciers, as documented by basal till cover on the valley floor and especially by rare sediments found uphill in the eastern corner of Kolm-Saigurn (section 4.4), towards the Durchgangriegel (section 4.15). The glacial advance peaked in a glacier system with a surface area of 10 km^2, extending to the Gersteben step reaching an elevation of 1400 m asl and covering the western areas of the Durchgangwald landslide (chapter 6, Figure 7.3). The maximum ELA depression during the advance was −330 m relative to the LIA ELA of the Goldbergkees (section 6.2). Measured from the present valley floor, maximum ice thickness in the Kolm-Saigurn basin reached at least 180 m, with possible higher values towards the north at the western parts of the Durchgangwald landslide, and the southern parts of the Grieswiesalm

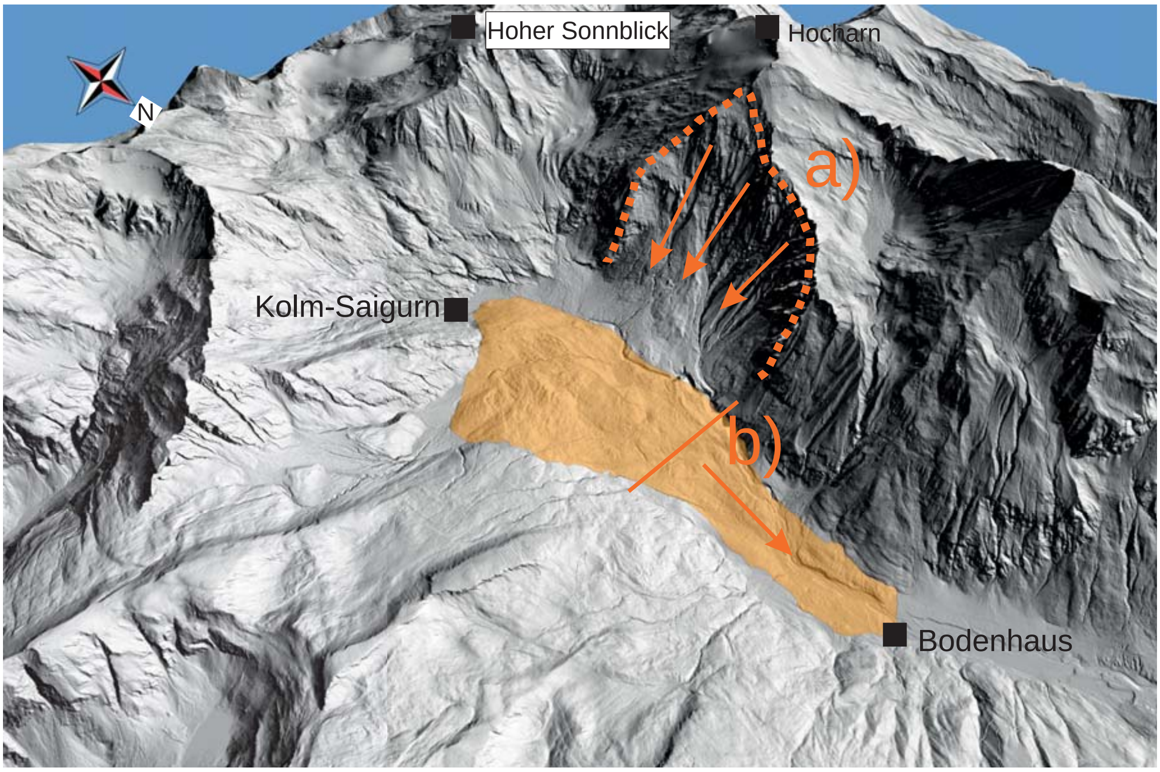

Figure 7.2.: Visualization of the extent, origin and moving direction of the Durchgangwald landslide which occurred during the Bølling-Allerød interstadial. (a) marks the scarp of the Durchgangwald landslide. (b) marks the border at a steep step where the kinematic of the landslide changed from rotational to dynamically flowing and the direction changed from E to N. Viewing direction is SW.

(section 6.3). ^{10}Be dating for one boulder (SON1) on a lateral moraine of the Grieswiestauern, supposed to be an age of almost maximum extent, yields 12.59±1.0 ka BP (section 5.2), marking a minimum age for the onset of the Younger Dryas and thus the Egesen.

Following this short and intense advance, the glacier system again decayed, with multiple retreat phases along the valley path. Stabilization during glacial retreat in the Kolm-Saigurn area is estimated to have happened at 11.02±1.18 ka BP and on the Grieswiestauern plateau at 11.34±0.78 ka BP, still putting the retreat in the Egesen stadial (section 5.2). Ice thickness modelling suggests a reconstituted glacier type for the Goldbergkees, with a dominant Pilatuskees delivering the majority of the ice volume to the valley. Only during the last phases of the ice decay, but for most of the Younger

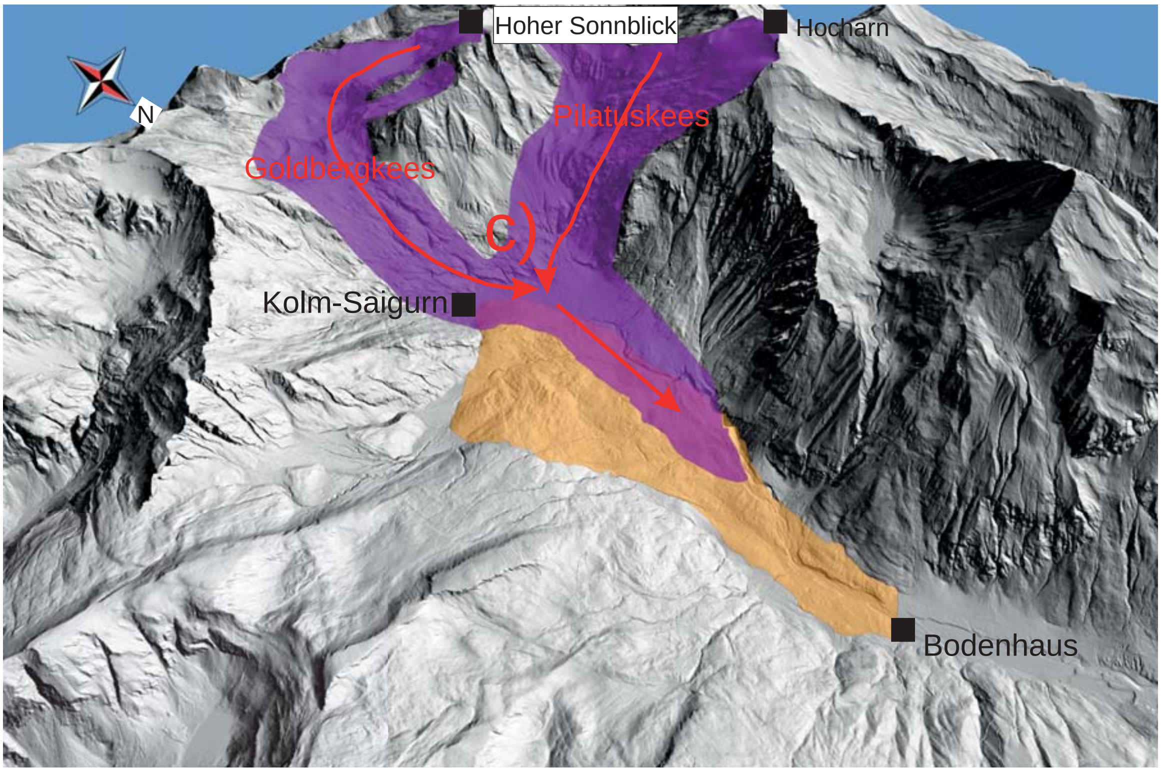

Figure 7.3.: Visualization of the maximum extent of the Egesen stadial during the Younger Dryas, topping the Durchgangwald landslide (c) marks the confluence situation of the Goldbergkees and the Pilatuskees in Kolm-Saigurn. Viewing direction is SW.

Dryas, ice-flow from the Goldbergkees and Pilatuskees was comparable. With the ice decayed further, the Melcherböden and therefore the Kolm-Saigurn basin, were ice-free by 11280±74 y cal BP (MSON2). Last remnants of the Egesen stadial can be found a few meters in front of the LIA of the Goldbergkees (SON10) and yield an age of 10.15±0.6 ka BP.

Shortly after the decaying ice uncovered the Lenzanger area, another minor landslide, mostly made up by quartzite, came down from ridges north of the Grieswies-Schwarzkogel at 10.99±1.1 ka BP (section 5.3), covering the glacial deposits and again blocking the Hüttwinklache (Figure 7.4), forming the Lenzanger Lake (section 4.5, section 4.6). During the Holocene, the Goldbergkees never extended further than during the LIA again.

Today, the area of Kolm-Saigurn is filled by deposits of the Durchgangwald (see section 4.2), fluvial sediments of the Hüttwinklache and talus fans from the western flanks

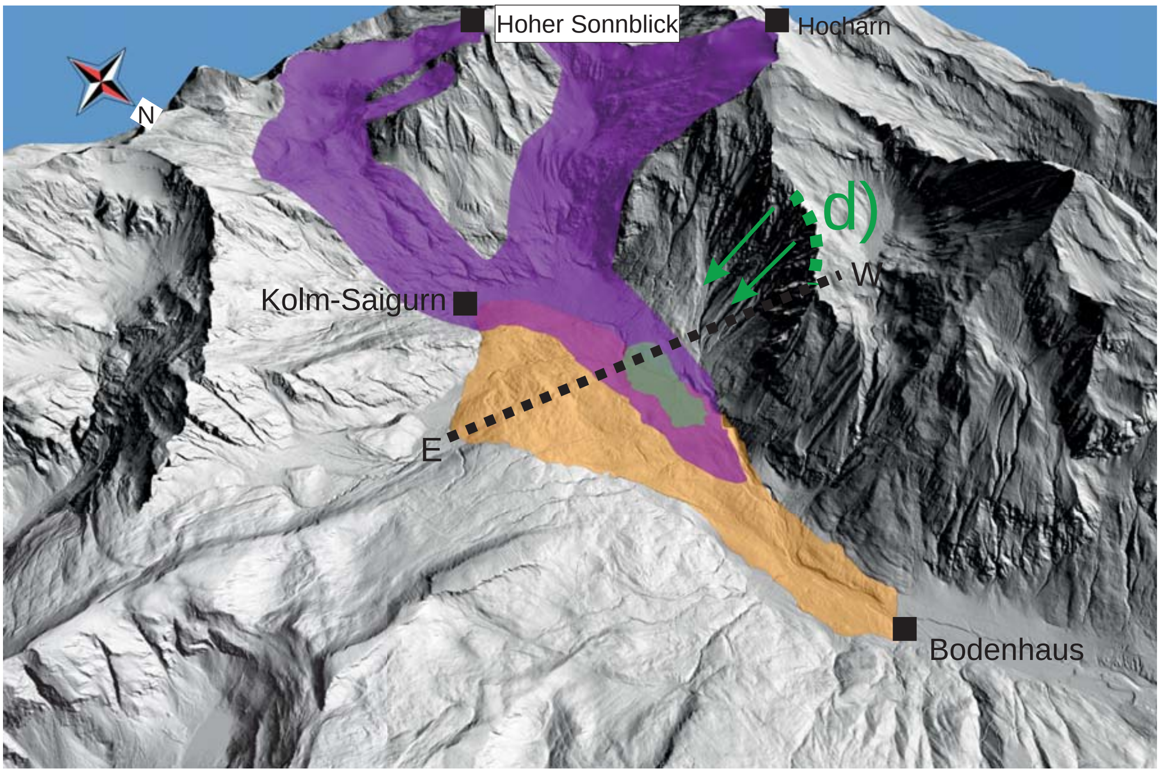

Figure 7.4.: Visualization of the Quartzite landslide, which occurred during the Preboreal to Boreal topping the Egesen till. (d) marks the supposed scarp area. The dashed line marks the approximate location of the cross-section in Figure 7.1. Viewing direction is SW.

of the valley (see section 4.1). The HTT (section 2.3) records allow us to estimate this sediment cover. As the HTT portal is located at today's valley floor, the shallow border between the bedrock and landslide mass suggest that the overdeepening in the area of Kolm-Saigurn was limited. The bedrock can therefore be conservatively estimated to lie at most 150 m below the west portal of the HTT (Figure 2.5).

7.2. Stratigraphic Correlation [Bichler]

As mentioned in section 2.2, straight forward correlations of Alpine Lateglacial stratigraphy and North European Lateglacial stratigraphy, based on high resolution climate archives in the North Atlantic region, are complicated due to multiple possible parameters influencing regional and local climates. Yet our data of moraines and glacial deposits fits those of the Egesen stadial corridor of the North Greenland Ice-core climate-curve, and thus can be correlated reasonably well (see Figure 7.5). Our oldest moraine ridge age, SON1 (12.59±1.0 ka BP), which we consider to be a good approximation for the maximum extent of the Egesen stadial, resides on the edge of the Allerød - Younger Dryas transition. In addition, our youngest age of the retreating glacier system, SON10 (10.15±0.6 ka BP) reaches far into the Preboreal.

Comparing our data with published data from the Central, Western and western Eastern Alps produces discussable uncertainties. Great care needs to taken when comparing this data, as the reproducibility of this data is not always absolutely given, when, for example different production rates of cosmogenic nuclides have been used (Balco et al., 2008; Balco, 2011, for more detail). However, so far dated sites (see section 2.2) correlate more or less well with our Egesen ages.

The Kartell stadial, in the sense of a separate stadial during Preboreal Oscillations, is itself a debatable construct. Usually, a gap concerning time or remarkable changes in climate conditions (interstadial) are needed to define two different stadials. Generally, the Kartell stadial, depending on the location and thus on topography, is defined either as a clearly delimited moraine system from the Egesen moraines, or as a more or less continuous sequence of moraine walls difficult to distinguish from the Egesen walls, but produced by remarkable re-advances during glacier retreat (Kerschner, 2009). Although some ^{10}Be samples from the Kolm-Saigurn lateral moraines and the Grieswiestauern plateau yield ages which could belong to a Kartell stadial, the continuous build-up of ridges disproves this in the first case, and morphological characteristic disprove it in the second case. The Goldbergkees on the Grieswiestauern plateau produced a set of moraines during the Egesen maximum, but the retreat-phase boulders which yield a Kartell age are not related to any moraines, which means they are products of the ice-decay from a retreating Egesen glacier. Downvalley, the Kolm-Saigurn glacier system built up a set of parallel moraine walls from its Egesen-maximum until a possible Kartell stadial. But due to the fact that from field evidence and dating, the moraine-system clearly built up continuously, a characteristic gap between Egesen and a possible Kartell is missing, and the recessional moraines do not show references of remarkable re-advancing, all the glacial deposits during the time-span from 12.59±1.0 ka BP to 10.15±0.6 ka BP are part of an Egesen-type glacier system.

Additionally, the multiple ridge-system is a crucial morphological characterization for Egesen-type systems. This is pointed out in nearby comparable regions like the Schobergruppe in the Austrian province of East Tyrol (Buchenauer, 1990), or even in larger-scale Egesen glacier systems in Scotland (Lukas and Bradwell, 2010). This

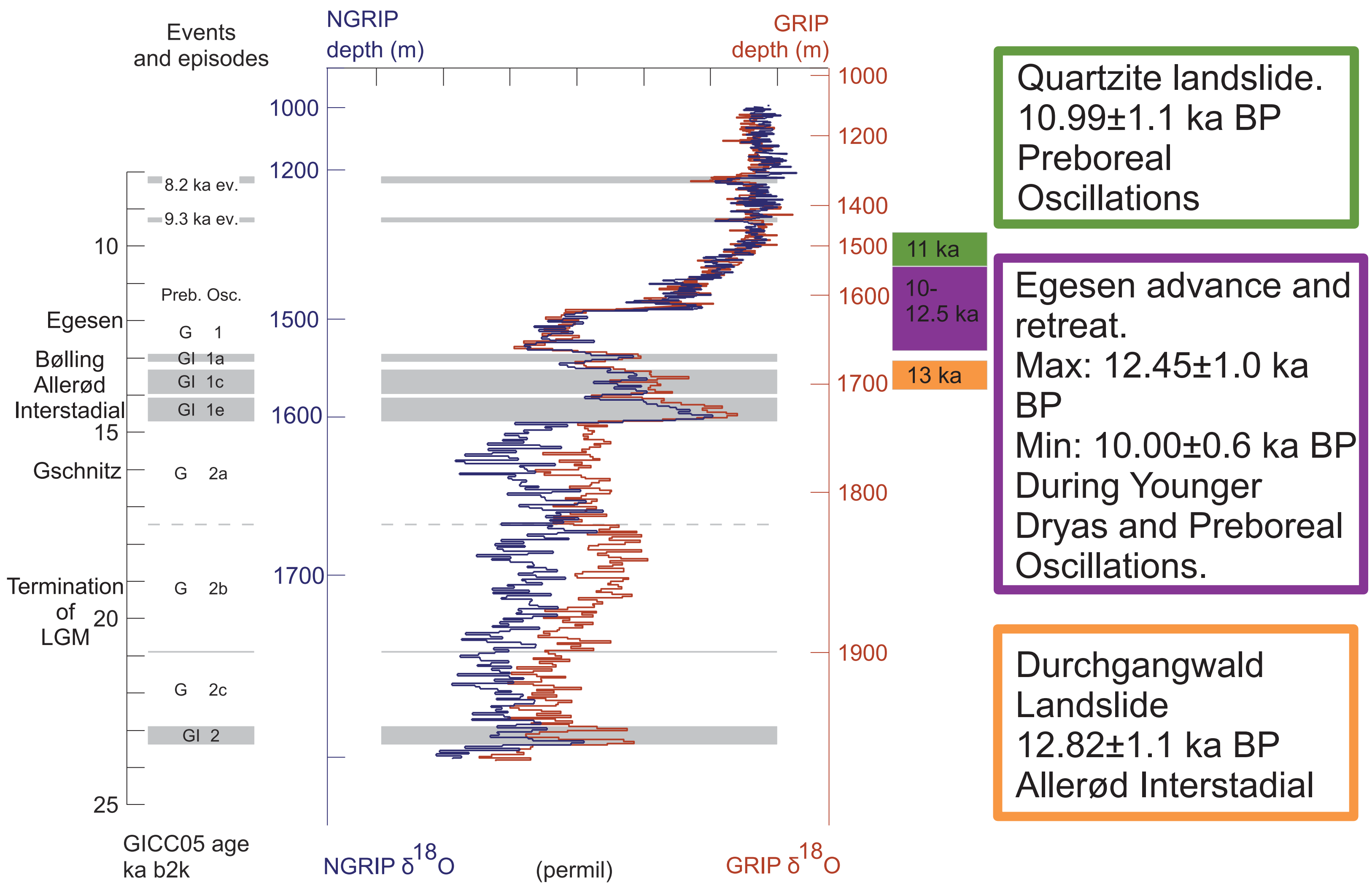

Figure 7.5.: Simplified overview of the correlation of our dating results with the Greenland Ice Core Project. Modified after Blockley et al. (2012). XXX Quartzite

means traces of the Kartell stadial, in the sense of a separated stadial during Preboreal Oscillations, could not be found in our study area. Furthermore, new refinements of production rates of cosmogenic nuclides show trends towards lower production rates. When applied to already calculated and published ages, they get older. This means earlier published Kartell ages can now reside in the Egesen.

The Kromer stadial, defined by uncertain ages in the sense of a stadial according to the 8.2 ka event, can be completely ruled out as well, as the only relevant phenomena for a Kromer age in front of the LIA from the Goldbergkees turned out to belong to the Egesen, as verified by ^{10}Be and ^{14}C dating.

8. Discussion and Conclusion [Reindl/Bichler]

This study was able to shed some light on the lateglacial dynamics in the head of the Hüttwinkl valley, but some questions remain unanswered or leave room for speculation.

The lateglacial history before the Durchgangwald landslide and the Bølling-Allerød is only scarcely documented, with the supposed Gschnitz stadial ice-margin sediments of the Grieswiestauern being the only witness of this timeframe. Estimation of Gschnitz ice-thickness and its comparison to well reconstructed Egesen is a complex task, as the Durchgangwald considerably landslide raised the valley floor between the two stadials.

It is unclear how much sediments have been deposited during the Holocene at Kolm-Saigurn. The HTT, cutting through the Durchgangwald landslide mass and any previous sediments could theoretically contain further information about the pre-Bølling-Allerød history, but remains inaccessible today. Such information could also improve knowledge on the origin of the landslide, and, whether previous creeping mass movements from the eastern flanks were gliding towards the valley floor. In general, information on the pre-Bølling-Allerød valley floor is missing and covered below the Durchgangwald sediments today. Detailed mapping was a successful tool to collect information about the mechanics of the Durchgangwald landslide. The connection of the rotational-slide part and the sturzstrom is evident, with all Durchgangwald landslide deposits belonging to one quick event. The influence of smaller landslides from the western or eastern flanks in the distal part can be excluded.

Compared to other dated regions in the Alps (see section 2.2), the Egesen stadial was a noticeable long lasting process with multiple stable phases during the glacier's recession. Additionally it is considerable that the oldest age from the Egesen is derived from a boulder on a moraine of the Goldbergkees which is not the oldest wall in the succession of this glacier system. Furthermore it is remarkable that the Pilatuskees produced a batch of recessional lateral moraines north of Kolm-Saigurn during this time, whereas the Goldbergkees just left some boulder-agglomerations higher up on a plateau.

This underlines the different behavior of the 2 glaciers as discussed in section 6.1. The maximum extent of the Egesen advance and its terminal moraine could only be deduced from the presence of basal till on the Durchgangwald landslide. In addition, no terminal moraine was found. Either the terminal moraine was eroded by the Hüttwinklache and the Trockenbach north of the Gersteben, or it never existed because of dry-calving from the Gersteben step, or it was covered by the deposits of the Quartzite landslide. A combination of all three theories is also possible, where each of the aforementioned processes was responsible for not preserving any terminal moraines of the maximum extent, nor the multiple retreat stages.

The timing of the onset of glacier advance during the Egesen is of great interest, because this still remains a big issue concerning palaeo-glacier- and climate reconstructions. For the Kolm-Saigurn glacier system the timing of the onset of advancing is up to now constrained by the age of the Durchgangwald landslide (12.82±1.1 ka BP) and by the ^{14}C age of the Melcherböden (11280±74 y cal BP, MSON2), when Kolm-Saigurn was definitely ice-free. Therefore dating the overridden ice-margin sediments succession in the eastern corner of the Kolm-Saigurn basin with ^{14}C, optically stimulated luminescence (OSL)and similar methods could be a big step forward in directly determining the timing of glacier advance.

The Durchgangwald and Quartzite landslide could only be directly measured with ^{10}Be. The nature and sensitivity of this method allows for errors which are much greater than for the radiocarbon method. Attempts to narrow down these datings with the ^{14}C method and providing minimal ages were largely unsuccessful. Further research and sampling for use with other dating methods, such as the thermoluminescence or OSL, might lead to better results, especially in the sediment core of the Filzenalm, poor in organic matter.

Combination of the ^{10}Be and ^{14}C methods worked good for reconstructing the decaying glacier, especially on the elevated areas of the Grieswiestauern and the Melcherböden. The recession of the glacier from the Kolm-Saigurn basin could only be dated with the ^{10}Be method.

When comparing the result of ^{10}Be and ^{14}C measurements, attention needs to be paid to the stated errors, which are in the 1σ range for the ^{10}Be method, and 2σ for the ^{14}C . The ^{14}C method therefore has the advantage of smaller errors and greater precision, but possesses the disadvantage of not being able to directly determine the age of a glacier deposited boulder.

It was possible to date glacially polished bedrock with ^{10}Be . On the Grieswiestauern plateau two bedrock sites and two related boulders just next to them were dated. Thinking of the method of exposure dating, all of them should yield the same age, as they were ice-free at the same time. Concerning the uncorrected ages, the boulders SON5 and SON9 (11480±770 y BP and 11480±710 y BP) and the bedrock sites SON6 and SON8 (10300±610 y BP and 10680±710 y BP) as well as their divergence to each other correlate very well and show a clear trend to slightly younger bedrock ages. By applying snow and sediment coverage correction for the bedrock ages (see chapter 5), plausible results, clustering well with the boulder ages can be gained. We therefore think exposure dating of bedrock is a promising tool at locations where boulders are missing. The relationship of our dated boulders and bedrock could serve at comparable regions and situations as an indication for the correction of bedrock ages.

No evidence was found that the Goldbergkees ever advanced again until the LIA-1850, and no traces of the Kromer stadial (Kerschner et al., 2006) were found.

9. Acknowledgments [Reindl/Bichler]

We would like to express our greatest gratitude to the people who have helped and supported us throughout our project. We are grateful to our supervisors Jürgen Reitner, Hermann Häusler, and Susan Ivy-Ochs for their continuous support for the project, from initial advice and contacts in the early stages of conceptual inception and through ongoing advice encouragement to this day.

A special thank goes to our colleagues at the ETH Zürich, Christian Wirsig, Florian Kober, Irka Hajdas and the staff of the Laboratory of Ion Beam Physics who helped us in completing the project and exchanged their interesting ideas, thoughts and made this project easy and accurate.

Great thanks to the staff of the Geologic Survey of Austria, who showed great interest in our mapping and dating work and provided funding for the ^{14}C dating and laboratory supply for ^{10}Be dating. We are especially thankful for the expertise of Dr. Ruth Drescher-Schneider, without her support, radiocarbon dating would not have been possible.

Furthermore a special thanks goes to the people at the ZAMG and the Sonnblickverein, especially Reinhard Böhm and Wolfgang Schöner, who were crucial for the starting and funding of this project.

We wish to thank our parents, families and partners, Andrea Schober, and Elena Schwaiger with Leo and Ben, for their undivided support and interest who inspired us and encouraged us to go our own way, without whom we would be unable to complete our project.

Support from the laboratories of the Department of Environmental Geosciences and the extensive use of the hydrofluoric acid workplaces is greatly appreciated, just as the help from Urs Klötzli with sample preparation.

We are grateful to the province of Salzburg, and especially Dr. Rainer Braunstingl, head of the geologic service, for supplying high resolution terrain data, greatly aiding our mapping efforts.

In addition, we wish to thank the Salzburg-AG, the Nationalpark Hohe Tauern, the Naturfreundehaus Kolm-Saigurn staff, and the municipality of Rauris for support, information and access permits in the Hüttwinkl valleyhead.

At last but not the least we want to thank our friends who appreciated us for our work and motivated us.

Our work would have not been possible without the substantial financial support by the Sonnblickverein. Additional financial support was granted by the University of Vienna Förderungsstipendium, as well as the Short-term Grants Abroad (KWA) program.

10. Abstracts [Reindl/Bichler]

10.1. Abstract

The area north of the Hoher Sonnblick, in the Austrian province of Salzburg, offers unique opportunities to study landscape forming events (glacial advances, glacial retreats and mass movements) since the Last Glacial Maximum (LGM).

The field work revealed unique relationships of cross-cutting landscape elements. These include multiple moraines and a till cover of a dominant glacial stadial overlying a giant landslide (0.4 km^3, largest in the province of Salzburg), which is then topped by a younger landslide of smaller dimension.

The landslide events (13ka BP and 10ka BP), as well as the glacial advance (12.5ka BP) and retreat (11ka BP) were dated using the ^{10}Be method. To establish an extensive chronology, six ^{10}Be samples from the landslides, twelve ^{10}Be boulder samples and two ^{10}Be polished bedrock samples related to glacier history were processed. Furthermore, ^{14}C samples were taken at suitable sites to augment the ages gained by exposure dating. The combination of the evidence found in the field, ^{14}C dating, and ^{10}Be dating made it possible to document the landscape evolution during the Lateglacial for this area.

In combination with a detailed geological map, concentrating on Quaternary features, it was possible to reconstruct the glacial chronology and the landscape evolution of the study area between 21ka BP and 1850 AD with special focus on the time between 14ka and 10ka BP.

Based on mapping and dating, we modeled the glacial dynamics of the Younger Dryas (Egesen stadial) glacier system and its relation to the prominent landslides (old: Allerød interstadial; young: Preboreal) from the onset of the ice advance to the retreat phase.

Detailed sedimentary evidence allows us to constrain the starting position of glaciers before the Younger Dryas advance, as well as reconstructing a confluence situation of the two local glaciers (Goldbergkees and Pilatuskees), producing a glacier system with a maximum surface area of 10 km^2. Furthermore, distinctive shaped moraine ridges allow us to shed some light on the glacier conditions during stabilization phases during the

retreat phases of the Egesen. In addition, surface models revealed a reconstituted glacier geometry for the Egesen-age Goldbergkees.

We employed various methods for calculating Equilibrium-Line-Altitudes (Maximum Elevation of Lateral Moraines, Toe-to-Headwall-Altitude Ratio, Area x Altitude, Area x Altitude Balance Ratio, and Accumulation Area Ratio) and compared them to already available data from western Austria and Switzerland. With this data, we are able to reconstruct temperature and precipitation change of the local climate and glacier dynamics during the maximum of the Younger Dryas in the central part of the European Eastern Alps.

With our multiple-dated Egesen (Younger Dryas) glacier system as a solid basis, we critically discuss the correlation of Lateglacial to Holocene stratigraphy with our study area and other inner-alpine areas, based on high resolution climate archives in the North Atlantic region, which have been targets of palaeoclimate research.

10.2. Zusammenfassung

Das Untersuchungsgebiet nördlich des Hohen Sonnblicks im Talschluss des Hüttwinkltals im Bundesland Salzburg bietet eine außergewöhnlich gute Möglichkeit um landschaftsprägende Ereignisse wie Gletschervorstöße, Gletscherrückzüge und Massenbewegungen seit dem letzten glazialen Maximum (Englisch: *LGM*; *Late Glacial Maximum*) zu studieren.

Erste Feldarbeiten zeigten, dass sich 3 wichtige überlagernde landschaftsformende Ereignisse unterscheiden lassen.

1. Der größte Bergsturz im Bundesland Salzburg (0.4 km^3), dessen Bergsturzlandschaft als Durchgangwald bekannt ist.

2. Dieser große Bersturz wird teilweise von einem dominanten Gletschervorstoß überlagert, der durch Grundmöranen-Bedeckung und mehreren Seitenmoränen gekennzeichnet ist.

3. Die Grundmoränen wiederum werden teilweise von einem kleineren, quarzitischen Bergsturz bedeckt.

Aufgrund dieser Abfolge war es möglich, eine solide relative Chronologie der Ereignisse als Zeitrahmen für die folgenden Altersdatierungen zu erstellen.

Sowohl die beiden Bergstürze (13ka BP und 10ka BP) als auch der Gletschervorstoß (12,5ka BP) und der Gletscherrückzug (11ka BP) wurden mit Hilfe von kosmogenen Nukliden, in unserem Fall basierend auf der ^{10}Be Methode, datiert. Um eine umfassende absolute Chronologie aufzubauen wurden 6 Proben von den Bergstürzen, 12 Proben von glazial transportierten Blöcken und 2 Proben von Gletscherschliffen bearbeitet. Zur Überprüfung der Plausibilität der absoluten Alter der ^{10}Be Datierung, wurden ^{14}C Datierungen an den Basislagen von Mooren durchgeführt. Die Bildung dieser Moore steht in direktem Zusammenhang mit den landschaftsprägenden Ereignissen (z.B. Aufstauung durch Bergsturzblöcke oder Moränen) und liefern daher ein Minimalalter für diese.

Durch die Kombination von absoluten Datierungen und einer detaillierten geologischen und geomorphologischen Kartierung war es möglich sowohl die glaziale Chronologie als auch die Landschaftsentwicklung des hinteren Hüttwinkltales seit dem LGM bis 1850 AD zu rekonstruieren. Besonderes Augenmerk wurde dabei auf den Zeitraum von 14 ka bis 10 ka gelegt.

Darauf aufbauend wurde die Gletscher Dynamik des dominanten vorgefundenen Egesen (Jüngere Dryas) Gletscher-Systems vom Beginn des Eisvorstoßes bis zu den Rückzugstadien modelliert.

Mit Hilfe von detaillierten sedimentologischen Aufnahmen gelang es uns wichtige Charakteristika des Egesen Gletschersystems wiederzugeben. Darunter die Position von Gletschern vor dem Egesen Vorstoß, eine Konfluenzsituation von den zwei wichtigsten lokalen Gletschern (Goldbergkees und Pilatuskees), die dadurch eine gesamt Gletscheroberfläche von 10 km^2 erzeugten, und die Gletscher Dynamik während der Rückzugphase. Modellierungen der Eisdicken ergaben Hinweise auf den regenerierten Charakter des Goldbergkees im Egesen.

Wir verwendeten mehrere Methoden (Maximum Elevation of Lateral Morains, auch bekannt als Methode Lichtenecker, Toe-to-Headwall-Altitude Ratio, Area x Altitude, Area x Altitude Balance Ratio, and Accumulation Area Ratio) um die Höhen der Gleichgewichtslinien (Englisch: *Equilibrium-Line-Altitudes*, *ELAs*) zu berechnen. Die Ergebnisse wurden mit bereits bestehenden Daten aus der Schweiz und West-Österreich verglichen. Dadurch war es uns möglich sowohl die Temperatur- und Niederschlagsänderungen des lokalen Klimas, als auch die Gletscher Dynamik während des Maximums des Egesen (Jüngere Dryas) in einem typischen nach Norden gerichteten Tal in den zentralen Ostalpen zu rekonstruieren.

Mit dem sehr gut erfassten und datierten Egesen Gletschersystem als Ausgangsbasis, diskutieren wir abschließend kritisch die Korrelation von spätglazialer bis holozäner Stratigraphie, basierend auf hochauflösenden Klimaarchiven im Nordatlantik, mit unserem Untersuchungsgebiet und anderen paläoklimatisch untersuchten inneralpinen Gebieten.

A. Mathematica Notebooks [Reindl]

AAR ELA calculation

```
(* this program calculates the ELA according to the AAR method *)
(* input values first *)

(* aar of 0.67 is 2:1 for accumulation:ablation area *)
aar = 0.67;

(* Excel file with columns for mean elevation of contour belts and their area:
file = "AABR.xls";
(* which sheet *)
sheet = 1;
(* column with mean elevation of contour belts *)
meancolumn = 4;
(* column with their areas *)
areacolumn = 5;

(* here we go *)
(* read the mean values *)
mean = Import[file][[sheet]][[All, meancolumn]];

(* get minimum and maximum elevation and position *)
minelevation = Min[mean][[1]];
maxelevation = Max[mean][[1]];
minposition = Position[mean, minelevation][[1]][[1]];
maxposition = Position[mean, maxelevation][[1]][[1]];

(* read the contour belt areas *)
area = Import[file][[sheet]][[minposition ;; maxposition, areacolumn]];

(* total glacier surface area *)
totalarea = Total[area];
(* size of assumed accumulation area *)
aararea = totalarea * aar;

position = maxposition - 1;
accuarea = 0;
(* loop from highest point until the accumulation
 are is greater than the value calculated above *)
While[accuarea < aararea,
 accuarea = accuarea + area[[position]];
 (* DEBUG *)
 (*Print[{position,area[[position]],accuarea}];*)
 position--]

(* print where we stopped, this is our ELA's contour belt mean elevation *)
mean[[position]]
```

Topographic shielding

```
ClearAll["Global`*"]

(* input format:
   USGS DEM works best from http://dds.cr.usgs.gov/srtm/version2_1/SRTM3/
   Choose a sufficently large area,
if close to a overlapping area, choose both HGT files *)
(* Convert the HGT files to UTM with 3DEM from http://
 freegeographytools.com/3dem_setup.exe, then save as DEM file
*)
(* 1m geotiff also works, but 90m DEM is sufficient *)
(*file="/Users/martin/Downloads/Kolm_Laserscan1.tif";
type="GeoTIFF";*)

file = "/Users/martin/Uni/Sonnblick/MasterThesis/Files/UTM_33_N_WGS84.dem";
type = "USGSDEM";

(* where are we? *)
(* input UTM coordinates of the sample point, elevation is calculated from DEM *)
(* DUR 10 *)
xin = 347 452;
yin = 5 215 381;

(* export to this XLS, for further use with http://
 hess.ess.washington.edu/math/general/skyline_input.php *)
outfile = "/Users/martin/Uni/Sonnblick/topo shading/DUR10_test.xls";

(* Import the Elevation Data *)
demdata = Transpose[Import[file, {type, "Data"}]];

(* Import upper, lower, left and right coordinates *)
xleft = Import[file, {type, "SpatialRange"}][[2, 1]];
xright = Import[file, {type, "SpatialRange"}][[2, 2]];
ylow = Import[file, {type, "SpatialRange"}][[1, 1]];
yup = Import[file, {type, "SpatialRange"}][[1, 2]];

(* How big is our matrix? *)
ydemrange = Import[file, {type, "RasterSize"}][[2]];
xdemrange = Import[file, {type, "RasterSize"}][[1]];

(* calculate the vertical and horizontal range *)
yrange = yup - ylow;
xrange = xright - xleft;

(* calculate the raster size, or raster resolution *)
(* xfactor and yfactor _should_ be the same! *)
xfactor = xrange / xdemrange;
yfactor = yrange / ydemrange;

xin = If[xin > xright, xright, xin];

(* DEM coordinates of our point *)
demx = Round[(xin - xleft) / xfactor];
demy = Round[(yin - ylow) / yfactor];

(* distance to DEM edges *)
ndist = ydemrange - demy;
sdist = -demy;
edist = xdemrange - demx;
wdist = -demx;

(* our elevation *)
elevation = demdata[[demx, demy]]
range = 20 000; (* in meters *)
steps = 2 Pi / 360; (* stepsize, smaller means more computations! *)

result = Table[{
    N[azimut / (Pi / 180)], (* print the azimut in Degrees *)
    Max[ (* take the maximum angle in the line of sight *)
     Table[{
```

```
        xvis = Round[s * Sin[azimut]]; (* Cos[azimut] means polar coordinates! *)
        yvis = Round[s * Cos[azimut]]; (* Sin[azimut] means polar coordinates! *)

        Which[
         wdist < xvis < edist, x = xvis,
         xvis < wdist, x = wdist,
         xvis > edist, x = edist
        ];
        Which[
         sdist < yvis < ndist, y = yvis,
         yvis < sdist, y = sdist,
         yvis > ndist, y = ndist
        ];
        If[yvis < sdist, y = sdist, y = yvis];

        z = (demdata[[demx + x, demy + y]] - elevation); (* delta z between points *)
        r = Sqrt[(x * xfactor)^2 + (y * yfactor)^2 + z^2];
        (* radius to calculated point *)

        90 - ArcCos[z / r] / (Pi / 180) (* 90 Degrees minus angle from zenith *)
       }, {s, 1, range / xfactor}
      ]
     ]
    }, {azimut, 0, 2 Pi - steps, steps}];

ListLinePlot[result, Frame → True, GridLines → Automatic]
Export[outfile, result];
```

B. AA and AABR Tables [Reindl]

Table B.1.: Table setup for the AA method for the LIA Goldbergkees, part of the AABR (see subsubsection 6.2.1.5) spreadsheet after Osmaston (2005). Bold entries mark the input values of the modeled glacier contours and the corresponding contour belt area. The result of the total Mean altitude × area divided by the total contour belt area equals the ELA for the LIA glacier. Also see Table B.2 and Table B.3.

Goldbergkees	Contours [m asl]	Mean belt altitude [m asl]	Contour belt area [m^2]	Mean altitude × area [m^2]
	2000	2050	**0**	0
	2100	2150	**2506**	5387900
	2200	2250	**122809**	276320250
	2300	2350	**346467**	814197450
	2400	2450	**404121**	990096450
	2500	2550	**371251**	946690050
	2600	2650	**496255**	1315075750
	2700	2750	**768621**	2113707750
	2800	2850	**359016**	1023195600
	2900	2950	**169130**	498933500
	3000	3050	**167339**	510383950
	3100	3150	**0**	0
	3200			
Totals			3207515	8493988650
LIA ELA				2648m asl

Table B.2.: Table setup for the AA method for the LIA Pilatuskees. Also see Table B.1 and Table B.3.

Pilatuskees	Contours [m asl]	Mean belt altitude [m asl]	Contour belt area [m^2]	Mean altitude × area [m^2]
	2000	2050	**27499**	56372950
	2100	2150	**49013**	105377950
	2200	2250	**151818**	341590500
	2300	2350	**163593**	384443550
	2400	2450	**201769**	494334050
	2500	2550	**138172**	352338600
	2600	2650	**148836**	394415400
	2700	2750	**651094**	1790508500
	2800	2850	**459973**	1310923050
	2900	2950	**427816**	1262057200
	3000	3050	**307310**	937295500
	3100	3150	**158783**	500166450
	3200	3250	**34194**	111130500
	3300			
Totals			2919870	8040954200
LIA ELA				2754m asl

Table B.3.: Table setup for the AA method for the Egesen extent. Also see Table B.1 and Table B.2. Note that the contour belt area values are the sums of the distinctive contour belt area of both the Goldbergkees and the Pilatuskees when they formed a glacier system during the Younger Dryas.

	Contours [m asl]	Mean belt altitude [m asl]	Contour belt area [m^2]	Mean altitude × area [m^2]
	1200	1250	**0**	0
	1300	1350	**102195**	137963250
	1400	1450	**170474**	247187300
	1500	1550	**440718**	683112900
	1600	1650	**788738**	1301417700
	1700	1750	**769470**	1346572500
	1800	1850	**786108**	1454299800
	1900	1950	**344079**	670954050
	2000	2050	**438599**	899127950
	2100	2150	**384038**	825681700
	2200	2250	**366889**	825500250
	2300	2350	**593778**	1395378300
	2400	2450	**610959**	1496849550
	2500	2550	**774193**	1974192150
	2600	2650	**580472**	1538250800
	2700	2750	**471165**	1295703750
	2800	2850	**1839734**	5243241900
	2900	2950	**742290**	2189755500
	3000	3050	**758949**	2314794450
	3100	3150	**362506**	1141893900
	3200	3250	**157743**	512664750
	3300	3350	**35227**	118010450
	3400	3450	**0**	0
	3500			
Totals			11518324	27612552900
Egesen ELA				**2397m asl**

Table B.4.: Spreadsheet excerpt for the calculation of the LIA ELAs for the Goldbergkees with the AABR method, as an extension of the table setup in Table B.1. The result appears after the second iteration. For the full spreadsheet, see http://catai.org/~martin/Sonnblick/AABR.ods.

BR	ELA trial reference contour (1)	belt area × alt above ref contour (1)	area × alt × BR for contour (1)	ELA trial reference contour (2)	belt area × alt above ref contour (2)	area × alt × BR for contour (2)	ELA trial reference contour (3)	belt area × alt above ref contour (3)	area × alt × BR for contour (3)
2	**2500**	0	0	2600	0	0	2700	0	0
		-877100	-1754200		-1127700	-2255400		-1378300	-2756600
		-30702250	-61404500		-42983150	-85966300		-55264050	-110528100
		-51970050	-103940100		-86616750	-173233500		-121263450	-242526900
		-20206050	-40412100		-60618150	-121236300		-101030250	-202060500
		18562550	18562550		-18562550	-37125100		-55687650	-111375300
		74438250	74438250		24812750	24812750		-24812750	-49625500
		192155250	192155250		115293150	115293150		38431050	38431050
		125655600	125655600		89754000	89754000		53852400	53852400
		76108500	76108500		59195500	59195500		42282500	42282500
		92036450	92036450		75302550	75302550		58568650	58568650
Totals		475201150	371445700		154449650	-55458650		-166301850	-525738300
Check =	TRUE				0			2648.1524326465	
						2587			**2611**

Table B.5.: Spreadsheet excerpt for the calculation of the LIA ELA for the Pilatuskees with the AABR method, as an extension of the table setup in Table B.2. The result appears after the third iteration. For the full spreadsheet, see `http://catai.org/~martin/Sonnblick/AABR.ods`.

BR	ELA trial reference contour (1)	belt area × alt above ref contour (1)	area × alt × BR for contour (1)	ELA trial reference contour (2)	belt area × alt above ref contour (2)	area × alt × BR for contour (2)	ELA trial reference contour (3)	belt area × alt above ref contour (3)	area × alt × BR for contour (3)
2	**2500**	0	0	2600	0	0	2700	0	0
		-12374550	-24749100		-15124450	-30248900		-17874350	-35748700
		-17154550	-34309100		-22055850	-44111700		-26957150	-53914300
		-37954500	-75909000		-53136300	-106272600		-68318100	-136636200
		-24538950	-49077900		-40898250	-81796500		-57257550	-114515100
		-10088450	-20176900		-30265350	-60530700		-50442250	-100884500
		6908600	6908600		-6908600	-13817200		-20725800	-41451600
		22325400	22325400		7441800	7441800		-7441800	-14883600
		162773500	162773500		97664100	97664100		32554700	32554700
		160990550	160990550		114993250	114993250		68995950	68995950
		192517200	192517200		149735600	149735600		106954000	106954000
		169020500	169020500		138289500	138289500		107558500	107558500
		103208950	103208950		87330650	87330650		71452350	71452350
		25645500	25645500		22226100	22226100		18806700	18806700
Totals		741279200	639168200		449292200	280903400		157305200	-91711800
Check =	TRUE								
					0			0	
						0			**2675**

Table B.6.: Spreadsheet excerpt for the calculation of the Egesen ELA with the AABR method, as an extension of the table setup in Table B.3. The result appears after the fourth iteration. For the full spreadsheet, see `http://catai.org/~martin/Sonnblick/AABR.ods`.

BR	ELA trial reference contour (1)	belt area × alt above ref contour (1)	area × alt × BR for contour (1)	ELA trial reference contour (2)	belt area × alt above ref contour (2)	area × alt × BR for contour (2)	ELA trial reference contour (3)	belt area × alt above ref contour (3)	area × alt × BR for contour (3)	ELA trial reference contour (4)	belt area × alt above ref contour (4)	area × alt × BR for contour (4)
2	2000	0	0	2100	0	0	2200	0	0	2300	0	0
		-66426750	-132853500		-76646250	-153292500		-86865750	-173731500		-97085250	-194170500
		-93760700	-187521400		-110808100	-221616200		-127855500	-255711000		-144902900	-289805800
		-198323100	-396646200		-242394900	-484789800		-286466700	-572933400		-330538500	-661077000
		-276058300	-552116600		-354932100	-709864200		-433805900	-867611800		-512679700	-1025359400
		-192367500	-384735000		-269314500	-538629000		-346261500	-692523000		-423208500	-846417000
		-117916200	-235832400		-196527000	-393054000		-275137800	-550275600		-353748600	-707497200
		-17203950	-34407900		-51611850	-103223700		-86019750	-172039500		-120427650	-240855300
		21929950	21929950		-21929950	-43859900		-65789850	-131579700		-109649750	-219299500
		57605700	57605700		19201900	19201900		-19201900	-38403800		-57605700	-115211400
		91722250	91722250		55033350	55033350		18344450	18344450		-18344450	-36688900
		207822300	207822300		148444500	148444500		89066700	89066700		29688900	29688900
		274931550	274931550		213835650	213835650		152739750	152739750		91643850	91643850
		425806150	425806150		348386850	348386850		270967550	270967550		193548250	193548250
		377306800	377306800		319259600	319259600		261212400	261212400		203165200	203165200
		353373750	353373750		306257250	306257250		259140750	259140750		212024250	212024250
		1563773900	1563773900		1379800500	1379800500		1195827100	1195827100		1011853700	1011853700
		705175500	705175500		630946500	630946500		556717500	556717500		482488500	482488500
		796896450	796896450		721001550	721001550		645106650	645106650		569211750	569211750
		416881900	416881900		380631300	380631300		344380700	344380700		308130100	308130100
		197178750	197178750		181404450	181404450		165630150	165630150		149855850	149855850
		47556450	47556450		44033750	44033750		40511050	40511050		36988350	36988350
		0	0		0	0		0	0		0	0
Totals		4575904900	3613848400		3424072500	2099907850		2272240100	544835450		1120407700	-1047783300
Check =	TRUE											
					0			0			0	
						0			0			**2234**

C. Geologic Map [Bichler]

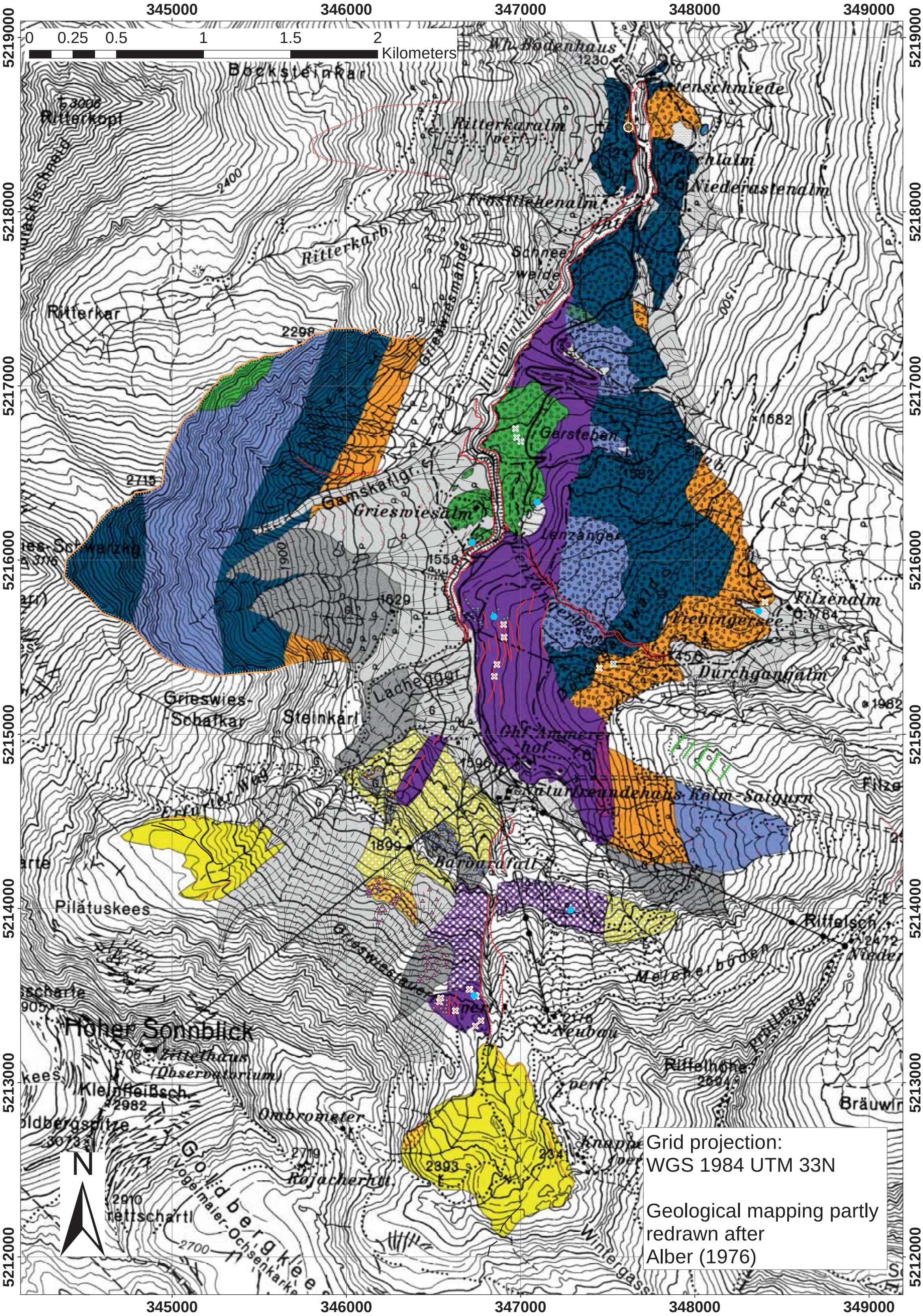
345000
346000
347000
348000
349000
5219000
5218000
5217000
5216000
5215000
5214000
5213000
5212000
0
0.25
0.5
1
1.5
2
Kilometers
Grid projection:
WGS 1984 UTM 33N
Geological mapping partly
redrawn after
Alber (1976)
N
Ritterkopf
Ritterkar
Grieswies-
Schafkar
Steinkarl
Pilatuskees
Hoher Sonnblick
Kleinfleißsch.
Goldbergkees
Ombrometer
Rojacherhtt
Gamskarlgr.
Grieswiesalm
Gersteben
Lenzanger
Filzenalm
Durchgangalm
Ritterkaralm
Wh. Bodenhaus
Fröstlhohenalm
Naturfreundehaus Kolm-Saigurn
Barbarafall
Melcherböden
Riffelsch.
Riffelhöhe
Neubau
Bräuwir
Lachegggr.

Legend

- Till (LIA or younger)
- LIA-1850 moraine ridge
- LIA-1620 moraine ridge at Knappenhaus

Little Ice Age (LIA)

- Quartzite landslide scarp
- Quartzite landslide mass

Preboreal-Boreal

- Egesen basal till
- Ice-marginal sediments in combination with Egesen till (fluviatil- and lake sediments); Egesen advance and retreat
- Egesen lateral-moraine (maximum extent and recessional moraines)
- Egesen patchy till cover

Egesen (Younger Dryas)

- Scarp Durchgangwald landslide
- Mica-schist landslide mass
- Calcareous-mica-schist landslide mass
- Serpentinit landslide mass
- Biotit-schist (Dark phyllit) landslide mass

Bølling-Allerød Interstadial

- Ice-marginal sediments at Grieswiestauern

Gschnitz (Oldest Dryas)

General geomorphological features

- Scarp
- Extensional gash
- Slipping and creeping of bedrock
- Zentralgneis block
- Calcareous-mica-schist block
- Mica-schist block
- Sinkhole

Gravitational features

- Moraine-ridge
- Ice-marginal sediments
- Patchy till cover

Glacial features

- Erosional edge
- Peat bog
- Lake (recent)
- Man-made deposits
- Alluvial deposits
- Alluvial-fan
- Debris-flow

Holocene to Lateglacial

Sampling

- 10Be samples of boulders and bedrock
- 14C samples of baselayers of peat bogs

Dating

Bedrock geology

- Calcareous-mica-schist
- Mica-schist
- Quartzite
- Biotit-schist (Dark phyllit)

Simplified bedrock modified after Alber (1976)

List of Figures

List of Tables

Bibliography

Akçar, N., Deline, P., Ivy-Ochs, S., Alfimov, V., Hajdas, I., Kubik, P. W., Christl, M., and Schlüchter, C. (2012). The AD 1717 rock avalanche deposits in the upper Ferret Valley (Italy): a dating approach with cosmogenic 10Be. *Journal of Quaternary Science*, 27(4):383–392.

Alber, J. (1976). *Seriengliederung, Metamorphose und Tektonik des Hocharngebietes – Rauristal/Salzburg*. PhD thesis, Universität Wien.

Andrews, J. (1975). *Glacial systems: an approach to glaciers and their environments*. Environmental systems. Duxbury Press.

Arnold, J. R. and Libby, W. F. (1949). Age determinations by radiocarbon content: checks with samples of known age. *Science*, 110:678–680.

Balco, G. (2011). Contributions and unrealized potential contributions of cosmogenic-nuclide exposure dating to glacier chronology, 1990–2010. *Quaternary Science Reviews*, 30(1–2):3 – 27.

Balco, G., Stone, J. O., Lifton, N. A., and Dunai, T. J. (2008). A complete and easily accessible means of calculating surface exposure ages or erosion rates from (10)Be and (26)Al measurements. *QUATERNARY GEOCHRONOLOGY*, 3(3):174–195.

Benn, D. I. and Hulton, N. R. (2010). An Excel™ spreadsheet program for reconstructing the surface profile of former mountain glaciers and ice caps. *Computers & Geosciences*, 36(5):605–610.

Benn, D. I. and Lehmkuhl, F. (2000). Mass balance and equilibrium-line altitudes of glaciers in high-mountain environments. *Quaternary International*, 65–66(0):15–29.

Benn, D. I., Owen, L. A., Osmaston, H. A., Seltzer, G. O., Porter, S. C., and Mark, B. (2005). Reconstruction of equilibrium-line altitudes for tropical and sub-tropical glaciers. *Quaternary International*, 138–139(0):8–21.

Blockley, S. P., Lane, C. S., Hardiman, M., Rasmussen, S. O., Seierstad, I. K., Steffensen, J. P., Svensson, A., Lotter, A. F., Turney, C. S., and Ramsey, C. B. (2012). Synchronisation of palaeoenvironmental records over the last 60,000 years, and an extended INTIMATE event stratigraphy to 48,000 b2k. *Quaternary Science Reviews*, 36(0):2–10.

Bortenschlager, S. and Patzelt, G. (1969). Wärmezeitliche Klima- und Gletscherschwankungen im Pollenprofil eines hochgelegenen Moores (2270m) der Venedigergruppe. *Eiszeitalter und Gegenwart*, 20:116–122.

Brandecker, H. (1981). Kraftwerkstufe Nassfeld - Böckstein, Baugeologischer Schlussbericht. Salzburg AG für Elektrizitätswirtschaft (SAFE).

Bronk Ramsey, C. (2009). Bayesian Analysis of Radiocarbon Dates. *Radiocarbon*, 51(1).

Buchenauer, H. W. (1990). Gletscher- und Blockgletschergeschichte der westlichen Schobergruppe (Osttirol). *Marburger geographische Schriften*, 117:251–270.

Cerling, T. E. and Craig, H. (1994). Geomorphology and In-Situ Cosmogenic Isotopes. *Annual Review of Earth and Planetary Sciences*, 22:273–317.

Chaline, J. and Jerz, H. (1984). Arbeitsergebnisse der Subkommission für Europäische Quartärstratigraphie Stratotypen des Würm-Glazials. *Eiszeitalter und Gegenwart*, 35:185–206.

Charlesworth, J. K. (1957). *The Quaternary era: With special reference to its glaciation*. E. Arnold (London).

Clark, D., Clark, M., and Gillespie, A. (1994). Debris-covered glaciers in the Sierra Nevada, California, and their implications for snowline reconstructions. *Quaternary Research*, 41(2):139–153.

Deplazes, G., Anselmetti, F. S., and Hajdas, I. (2007). Lake sediments deposited on the Flims rockslide mass: the key to date the largest mass movement of the Alps. *TERRA NOVA*, 19(4):252–258.

Dunai, T. (2010). *Cosmogenic Nuclides: Principles, Concepts and Applications in the Earth Surface Sciences*. Cosmogenic Nuclides: Principles, Concepts and Applications in the Earth Surface Sciences. Cambridge University Press.

Dunne, J., Elmore, D., and Muzikar, P. (1999). Scaling factors for the rates of production of cosmogenic nuclides for geometric shielding and attenuation at depth on sloped surfaces. *Geomorphology*, 27(1—2):3–11.

Exner, C. (1956). *Erläuterungen zur Geologischen Karte der Umgebung von Gastein.* Geologische Bundesanstalt, Wien.

Faupl, P. (2003). *Historische Geologie.* 2. überarbeitete Auflage.

Federmann, G. (2003). Viktor Hess und die Entdeckung der Kosmischen Strahlung. Master's thesis, Institut für Radiumforschung und Kernphysik, Universität Wien.

Fellner, D. (1993). Massenbewegungen im Bereich Bucheben im Hüttwinkeltal bei Rauris (Salzburg, Österreich). *Jahrbuch der Geologischen Bundesanstalt*, 136:307–313.

Fraedrich, R. (1979). *Spät- und postglaziale Gletscherschwankungen in der Ferwallgruppe (Tirol, Vorarlberg); mit 6 Tabellen.* Düsseldorfer geographische Schriften. Geograph. Inst. der Univ.

Furbish, D.J. Andrews, J. (1984). The use of hypsometry to indicate long term stability and response of valley glaciers to changes in mass transfer. *Journal of Glaciology*, 30:199–211.

Glasser, N. F., Harrison, S., Winchester, V., and Aniya, M. (2004). Late Pleistocene and Holocene palaeoclimate and glacier fluctuations in Patagonia. *Global and Planetary Change*, 43(1–2):79–101.

Gosse, J. C. and Phillips, F. M. (2001). Terrestrial in situ cosmogenic nuclides: theory and application. *Quaternary Science Reviews*, 20(14):1475–1560.

Gross, G., Kerschner, H., and Patzelt, G. (1976). Methodische Untersuchungen über die Schneegrenze in alpinen Gletschergebieten. *Zeitschrift für Gletscherkunde und Glazialgeologie*, 12:223–251.

Heim, A. (1932). *Bergsturz und Menschenleben.* Vierteljahrsschrift der Naturforschenden Gesellschaft in Zürich. Fretz & Wasmuth.

Hellerschmidt-Alber, J. (1998). Bericht 1997 über geologische Aufnahmen im Penninikum des Hüttwinkeltales auf Blatt 154 Rauris. *Jahrbuch der Geologischen Bundesanstalt*, 141:297–302.

Heuberger, H. (1966). Gletschergeschichtliche Untersuchungen in den Zentralalpen zwischen Sellrain und Ötztal. *Wissenschaftliche Alpenvereinshefte*, 20.

Hiebl, J., Reisenhofer, S., Auer, I., Böhm, R., and Schöner, W. (2011). Multi-methodical realisation of Austrian climate maps for 1971–2000. *Advances in Science and Research*, 6:19–26.

Holub, B. and Maschallinger, R. (1989). Die Zentralgneise im Hochalm-Ankogel-Massiv (östliches Tauernfenster), Teil I: petrographische Gliederung und Intrusionsfolge. *Mitteilung der Österreichischen Geologischen Gesellschaft*.

Hormes, A., Ivy-Ochs, S., Kubik, P. W., Ferreli, L., and Michetti, A. M. (2008). 10Be exposure ages of a rock avalanche and a late glacial moraine in Alta Valtellina, Italian Alps. *Quaternary International*, 190(1):136–145.

Hottinger, A. (1935). *Geologie der Gebirge zwischen der Sonnblick-Hocharn-Gruppe und dem Salzachtal in den östlichen Hohen Tauern*. PhD thesis, Eidgenössische Technische Hochschule Zürich.

Ivy-Ochs, S. (1996). *The dating of rock surfaces with 10Be, 26Al, and 36Cl, with examples from Antarctic and the Swiss Alps.* PhD thesis, ETH Zürich, No. 11763, 196 p.

Ivy-Ochs, S., Heuberger, H., Kubik, P., Kerschner, H., Bonani, G., Frank, M., and Schlüchter, C. (1998). The age of the Köfels event. Relative, 14C and cosmogenic isotope dating of an early Holocene landslide in the Central Alps (Tyrol, Austria). *Zeitschrift für Gletscherkunde und Glazialgeologie*, 34:57–68.

Ivy-Ochs, S., Kerschner, H., Maisch, M., Christl, M., Kubik, P. W., and Schlüchter, C. (2009a). Latest Pleistocene and Holocene glacier variations in the European Alps. *Quaternary Science Reviews*, 28(21–22):2137 –2149. Holocene and Latest Pleistocene Alpine Glacier Fluctuations: A Global Perspective.

Ivy-Ochs, S., Kerschner, H., Reuther, A., Maisch, M., Sailer, R., Schaefer, J., Kubik, P., Synal, H.-A., and Schlüchter, C. (2006). The timing of glacier advances in the northern European Alps based on surface exposure dating with cosmogenic 10Be, 26Al, 36Cl, and 21Ne. *Special Paper of the Geological Society of America*, 415:43–60. cited By (since 1996) 15.

Ivy-Ochs, S., Kerschner, H., Reuther, A., Preusser, F., Heine, K., Maisch, M., Kubik, P. W., and Schlüchter, C. (2008). Chronology of the last glacial cycle in the european alps. *Journal of Quaternary Science*, 23(6-7):559–573.

Ivy-Ochs, S., Kerschner, H., and Schlüchter, C. (2007). Cosmogenic nuclides and the dating of Lateglacial and Early Holocene glacier variations: The Alpine perspective. *Quaternary International*, 164–165(0):53–63. From the Swiss Alps to the Crimean Mountains - Alpine Quaternary stratigraphy in a European context.

Ivy Ochs, S. and Kober, F. (2008). Surface exposure dating with cosmogenic nuclides. *Quaternary Science Journals*, 57(1–2):179–209.

Ivy-Ochs, S., Poschinger, A., Synal, H.-A., and Maisch, M. (2009b). Surface exposure dating of the Flims landslide, Graubünden, Switzerland. *Geomorphology*, 103(1):104–112.

Ivy-Ochs, S., Schäfer, J., Kubik, P., Synal, H.-A., and Schlüchter, C. (2004). Timing of deglaciation on the northern Alpine foreland (Switzerland). *Eclogae Geologicae Helvetiae*, 97:47–55.

Kebede, T., Klötzli, U., Kosler, J., and Skiöld, T. (2005). Understanding the pre-variscan and variscan basement components of the central tauern window, eastern alps (austria): constraints from single zircon u-pb geochronology. *International Journal of Earth Sciences*, 94:336–353.

Keller, B. (1996). Lithofazies-Codes für die Klassifikation von Lockergesteinen. *Mitteilungen der Schweizerischen Gesellschaft für Boden- und Felsmechanik*, 132:5–12.

Kerschner, H. (2005). Glacier-climate models as palaeoclimatic information sources: Examples from the alpine younger dryas period. In Huber, U., Bugmann, H., and Reasoner, M., editors, *Global Change and Mountain Regions*, volume 23 of *Advances in Global Change Research*, pages 73–81. Springer Netherlands.

Kerschner, H. (2009). Gletscher und Klima im Alpinen Spätglazial und frühen Holozän. *In: R. Schmidt, Ch. Matulla, R. Psenner (Hsg.): Klimawandel in Österreich. Die letzten 20.000 Jahre und ein Blick voraus. (alpine space - man & environment)*, 6:5–26.

Kerschner, H., Hertl, A., Gross, G., Ivy-Ochs, S., and Kubik, P. W. (2006). Surface exposure dating of moraines in the Kromer valley (Silvretta Mountains, Austria)-evidence for glacial response to the 8.2 ka event in the Eastern Alps? *The Holocene*, 16(1):7–15.

Kerschner, H. and Ivy-Ochs, S. (2007). Palaeoclimate from glaciers: Examples from the Eastern Alps during the Alpine Lateglacial and early Holocene. *Global and Planetary Change*, 60(1–2):58–71.

Kieslinger, A. (1938). Aufnahmsberichte über Blatt Hofgastein. Verh. Geologische Bundesanstalt, Wien.

Klein, J., Middleton, R., and Q., T. H. (1982). Instrumentation of an FN tandem for the detection of ^{10}Be. *Nuclear Instruments and Methods in Physics Research*, 193:601–616.

Kubik, P. W., Ivy-Ochs, S., Masarik, J., Frank, M., and Schlüchter, C. (1998). 10Be and 26Al production rates deduced from an instantaneous event within the dendro-calibration curve, the landslide of Köfels, Ötz Valley, Austria. *Earth and Planetary Science Letters*, 161(1–4):231–241.

Kurowski, L. (1891). *Die Höhe der Schneegrenze mit besonderer Berücksichtigung der Finsteraarhorngruppe*, pages 119–160. Pencks Geographische Abhandlungen, Volume 5, Issue 1.

Lerchbaumer, L., Klötzli, U., and Pestal, G. (2010). Schists and Amphibolites of the Kleinelendtal (Ankogel-Hochalm-Gruppe/Hohe Tauern, Austria) - new insights on the Variscan basement in the eastern Tauern Window. *Austrian Journal of Earth Sciences*, 103/2:138–152.

Lichtenecker, N. (1935). Neuere Gletscherstudien in der Sonnblickgruppe. *Jahresbericht des Sonnblick-Vereines*, 44:13–37.

Lichtenecker, N. (1938). Die gegenwärtige und die eiszeitliche Schneegrenze in den Ostalpen. In Götzinger, G., editor, *Verhandlungen der III Internationalen Quartär-Conferenz, Vienna, September 1936*, pages 141–147. INQUA, Vienna, Austria, Geologische Landesanstalt.

Litt, T., Brauer, A., Goslar, T., Merkt, J., Balaga, K., Müller, H., Ralska-Jasiewiczowa, M., Stebich, M., and Negendank, J. F. (2001). Correlation and synchronisation of

Lateglacial continental sequences in northern central Europe based on annually laminated lacustrine sediments. *Quaternary Science Reviews*, 20(11):1233–1249.

Louis, H. (1955). Schneegrenze und Schneegrenzbestimmung.

Lukas, S. and Bradwell, T. (2010). Reconstruction of a Lateglacial (Younger Dryas) mountain ice field in Sutherland, northwestern Scotland, and its palaeoclimatic implications. *JOURNAL OF QUATERNARY SCIENCE*, 25(4, SI):567–580.

Malecki, G. (1972). *Zur Geologie des Silberpfennig-Gebietes, Hohe Tauern (Salzburg).* PhD thesis, University of Vienna.

Manley, G. (1959). The late-glacial climate of north-west England. *Liverpool and Manchester Geological Journal*, 2:188–215.

Matura, A. (1966). Zur Geologie des Türchlwand-Kramkogel-Gebietes: (SE Wörth im Rauristal, Salzburg). *Mitteilungen der Gesellschaft der Geologie- und Bergbaustudenten in Wien*, 17:87–126.

Mayr, F. and Heuberger, H. (1968). Type areas of late glacial and postglacial deposits in tyrol, Eastern Alps. Proceeding VII INQUA Congress, 14, University of Colorado Studies. *Series in Earth Science*, 7:143–165.

McSaveney, M. J. and Davies, T. R. H. (2006). Rapid rock mass flow with dynamic fragmentation: Inferences from the morphology and internal structure of rockslides and rock avalanches. *In: S. G. Evans, G. Scarascia-Mugnozza, A. Strom and R. L. Hermans (Eds.), Landslides from Massive Rock Slope Failure. New York: NATO Science Series: IV: Earth and Environmental Sciences*, 49:285–304.

Meier, M. and Post, A. (1962). Recent variations in mass net budgets of glaciers in western North America. *International Association of Hydrological Sciences Publication*, 58:63–77.

Meier, M. and Tangborn, W. (1965). Net budget and flow of South Cascade Glacier, Washington. *Journal of Glaciology*, 5(41):547–566.

Meierding, T. C. (1982). Late pleistocene glacial equilibrium-line altitudes in the Colorado Front Range: A comparison of methods. *Quaternary Research*, 18(3):289 – 310.

Nishiizumi, K., Imamura, M., Caffee, M. W., Southon, J. R., Finkel, R. C., and McAninch, J. (2007). Absolute calibration of 10Be AMS standards. *Nuclear Instruments and Methods in Physics Research Section B: Beam Interactions with Materials and Atoms*, 258(2):403–413.

Osmaston, H. (2005). Estimates of glacier equilibrium line altitudes by the Area x Altitude, the Area x Altitude Balance Ratio and the Area x Altitude Balance Index methods and their validation. *Quaternary International*, 138–139(0):22–31.

Patzelt, G. (1973). Die neuzeitlichen Gletscherschwankungen in der Venedigergruppe (Hohe Tauern, Ostalpen). *Zeitschrift für Gletscherkunde und Glazialgeologie*, 9:5–57.

Penck, A. (1897). Gletscherstudien im Sonnblickgebiet. *Zeitschrift des Deutschen und Österreichischen Alpenverein*, pages 52–71.

Penck, A. and Brückner, E. (1901/1909). *Die Alpen im Eiszeitalter*. Tauchnitz:Leipzig.

Plug, L. J., Gosse, J. C., McIntosh, J. J., and Bigley, R. (2007). Attenuation of cosmic ray flux in temperate forest. *J. Geophys. Res.*, 112(F2):F02022.

Porter, S., Pierce, K., and Hamilton, T. (1983). *Late Pleistocene glaciation in the western United States*, pages 71–111. In: Porter, S.C. (Ed.), Late Quaternary Environments of the United States. University of Minnesota Press, Minneapolis.

Porter, S. C. (1975). Equilibrium line altitudes of late Quaternary glaciers in the Southern Alps, New Zealand. *Quaternary Research*, 5(1):27–47.

Poscher, G. and Patzelt, G. (2000). Sink-hole Collapses in Soft Rocks: Sedimentological and hydrogeological aspects of groundwater induced erosion processes Sink-hole collapses in soft rocks. Sedimentological and hydrogeological aspects of groundwater induced erosion processes. *Felsbau, Rock and Soil Engineering*, 18(1):36–40.

Posepny, F. (1879). Die Goldbergbaue der Hohen Tauern mit besonderer Berücksichtigung des Rauriser Goldbergwerkes. Archiv für praktische Geologie 1, Wien.

Rainer, P. (1979). KW Böckstein - Stollenbautechnischer Bericht. Salzburg AG für Elektrizitätswirtschaft (SAFE).

Raisbeck, G. M., Yiou, F., Fruneau, M., and Loiseaux, J. M. (1978). Beryllium-10 Mass Spectrometry with a Cyclotron. *Science*, 202(4364):215–217.

Reimer, P., Baillie, M., Bard, E., Bayliss, A., Beck, J., Blackwell, P., Ramsey, C., Buck, C., Burr, G., Edwards, R., Friedrich, M., Grootes, P., Guilderson, T., Hajdas, I., Heaton, T., Hogg, A., Hughen, K., Kaiser, K., Kromer, B., McCormac, F., Manning, S., Reimer, R., Richards, D., Southon, J., Talamo, S., Turney, C., van der Plicht, J., and Weyhenmeyer, C. (2011). IntCal09 and Marine09 Radiocarbon Age Calibration Curves, 0–50,000 Years cal BP. *Radiocarbon*, 51(4).

Reitner, J. M. (2007). Glacial dynamics at the beginning of Termination I in the Eastern Alps and their stratigraphic implications. *Quaternary International*, 164:64–84.

Reitner, J. M., Lang, M., and van Husen, D. (1993). Deformation of high slopes in different rocks after würmian deglaciation in the Gailtal (Austria). *Quaternary International*, 18:43–51.

Sailer, R. (2002). *Späteiszeitliche Gletscherstände in der Ferwallgruppe.* PhD thesis, Universität Innsbruck.

Sanhueza-Pino, K., Korup, O., Hetzel, R., Munack, H., Weidinger, J. T., Dunning, S., Ormukov, C., and Kubik, P. W. (2011). Glacial advances constrained by 10Be exposure dating of bedrock landslides, Kyrgyz Tien Shan. *Quaternary Research*, 76(3):295–304.

Schindelwig, I., Akçar, N., Kubik, P. W., and Schlüchter, C. (2012). Lateglacial and early Holocene dynamics of adjacent valley glaciers in the Western Swiss Alps. *Journal of Quaternary Science*, 27(1):114–124.

Schmid, S. M., Fügenschuh, B., Kissling, E., and Schuster, R. (2004). Tectonic map and overall architecture of the Alpine orogen. *Eclogae Geologicae Helvetiae*, 97(1):93–117.

Schöner, W. (2009). Paläoklimainformationen aus Kenngrößen der Gletschermassenbilanz – Beispiele für die Alpen seit der ausgehenden Kleinen Eiszeit. *In: Schmidt R., Matulla C., Psenner R. (Hg.): Klimawandel in Österreich. Die letzten 20.000 Jahre…und ein Blick voraus (= alpine space – man & environment)*, 6: Klimawandel in Österreich:127–144.

Schuster, R., Pestal, G., and Reitner, J. M. (2006). Erläuterungen zu Blatt 182 Spittal an der Drau. *Geologische Karte der Republik Österreich, 1:50000.*

Starnberger, R., Rodnight, H., and Spötl, C. (2011). Chronology of the Last Glacial Maximum in the Salzach palaeoglacier area (Eastern Alps). *Journal of Quaternary Science*, 26(5):502–510.

Steinhauser, P., Brückl, E., and Aric, K. (1984). *Anwendung geophysikalischer Verfahren bei der geotechnischen Vorerkundung von Tunnelbauten*. Bundesministerium für Bauten und Technik, Bundesstraßenverwaltung.

Stone, J. O. (2000). Air pressure and cosmogenic isotope production. *Journal of Geophysical Research: Solid Earth*, 105(B10):23753–23759.

Sugden, D. E. and John, B. S. (1976). *Glaciers and landscapes: A geomorphological approach*. Edward Arnold (London).

Torsnes, I., Rye, N., and Nesje, A. (1993). Modern and Little Ice Age Equilibrium-Line Altitudes on Outlet Valley Glaciers from Jostedalsbreen, Western Norway: An Evaluation of Different Approaches to Their Calculation. *Arctic and Alpine Research*, 25(2):pp. 106–116.

van Husen, D. (1997). LGM and Late Glacial Fluctuations in the Eastern Alps. *Quaternary International*, 38:109–118.

van Husen, D. (2000). Geological Processes during the Quartenary. *Mitteilungen der Österreichischen Geologischen Gesellschaft*, 92:135–156.

van Husen, D., Ivy-Ochs, S., and Alfimov, V. (2007). Mechanism and age of late glacial landslides in the Calcareous Alps; The Almtal, Upper Austria. *Austrian Journal of Earth Sciences*, 100:114–126.

Visser, P., Visser, J., Visser-Hooft, J., and von Cvitković, J. (1938). *Wissenschaftliche Ergebnisse der Niederländischen Expeditionen in den Karakorum und die angrenzenden Gebiete in den Jahren 1922, 1925 und 1929/30*. In: Brill, E.J. (Ed.), Glaziologie. The Netherlands, Leiden, pp. 216p.

von Drygalski, E. (1942). *Gletscherkunde. Enzyklopädie der Erde*. Franz Deuticke, Vienna.

von Poschinger, A. (1986). *Instabile Talflanken in Kristallingesteinen und ihre geologischen Ursachen, dargestellt am Beispiel des oberen Hüttwinkeltales (Land Salzburg, Österreich)*. PhD thesis, Technische Universität München.

Walker, M., Björck, S., and Lowe, J. (2001). Integration of ice core, marine and terrestrial records (INTIMATE) from around the North Atlantic region: an introduction. *Quaternary Science Reviews*, 20(11):1169–1174.

Weber, F. (1971). Bericht über die refraktionsseismischen Messungen für das KW Bockhartsee und die Hüttwinkelüberleitung. Salzburg AG für Elektrizitätswirtschaft (SAFE).

Yu, Z. and Eicher, U. (2001). Three amphi-Atlantic century-scale cold events during the Bølling-Allerød warm period. *Géographie physique et Quaternaire*, 55(2):171–179.

Curriculum Vitae

Martin Reindl

Date born: 01.08.1980

Place born: Schwaz

Education

2011–2013: University of Vienna, M.Sc. Geology

2007–2011: University of Vienna, B.Sc. Earth Science

2001–2007: Technical University Vienna, Electrical Engineering, Computer Science

1995–2000: Höhere Technische Bundes Lehr- und Versuchsanstalt Innsbruck Anichstrasse, Department of Electrical Engineering

Experience

2007–2009: Developer, Sozialversicherungs-Chipkarten Betriebs- und Errichtungsgesellschaft, Austrian E-Card Project, Vienna

2003–2007: Junior Technical Analyst, Raiffeisen Zentralbank, Vienna

Activities

2009–2011: Head of the Student Council and Member of the Study Conference Earth Sciences, University of Vienna

2008–2011: Secretary, Member of the Board of Directors, Verein Funkfeuer Vienna

2004–2010: Developer, The OpenBSD project

Scientific activities

2012: February to March: Stay abroad at the Ion Beam Physics Laboratory of the ETH Zurich, Switzerland
Studying the sample preparation for measuring ^{10}Be

Publications

2011: Bachelor Thesis
LA-ICP-MS Datenanalyse mit Mathematica

Scientific conferences

2012: Oral presentation
PANGEO Austria 2012
Salzburg, Austria, 15 – 20 September 2012
Session 16: Quartärgeologie — Geoarchäologie — Paläoklimatologie: Interdisziplinäre Erforschung des regionalen und globalen Wandels

2012: Poster presentation
European Geosciences Union General Assembly 2012
Vienna , Austria , 22 – 27 April 2012
Session: GM9.2, Glacial landforms and palaeoclimatic interpretation

2011: Poster presentation
International Conference on the Occasion of the 125 Anniversary of Sonnblick Observatory
Climate Change in High Mountain Regions
From Understanding of the Past to Modelling of the Future
Salzburg, Austria, 28 August – 1 September 2011

Mathias Bichler

Date born: 16.05.1984

Place born: Radstadt

Education

2011–2013: University of Vienna, M.Sc. Geology

2008–2011: University of Vienna, B.Sc. Earth Science

1998–2003: HLW für wirtschaftliche Berufe Ried am Wolfgangsee

Experience

2010–today: Project assistant at HPC Austria GmbH, Laxenburg

2009: Project assistant at Geotechnik Tauchmann GmbH, Thalheim bei Wels

2004–2007: Purchasing agent for high-class Austrian gastronomy, Radstadt

2002–2003: Cook and waiter at the Goldener Hirsch, Salzburg

2002: Apprenticeship diploma for cook and waiter

Activities

2009–2012: Several times student assistant at the Earth-Science-Center Vienna

Scientific activities

2012: February to March: Stay abroad at the Ion Beam Physics Laboratory of the ETH Zurich, Switzerland
Studying the sample preparation for measuring ^{10}Be

Publications

2011: Bachelor Thesis
Petrographische Untersuchungen im
Bereich der Zwischenelendscharte (Maltatal/Kärnten)

Scientific conferences

2012: Oral presentation
PANGEO Austria 2012
Salzburg, Austria, 15 – 20 September 2012
Session 16: Quartärgeologie — Geoarchäologie — Paläoklimatologie: Interdisziplinäre Erforschung des regionalen und globalen Wandels

2012: Poster presentation
European Geosciences Union General Assembly 2012
Vienna , Austria , 22 – 27 April 2012
Session: GM9.2, Glacial landforms and palaeoclimatic interpretation

2011: Poster presentation
International Conference on the Occasion of the 125 Anniversary of Sonnblick Observatory
Climate Change in High Mountain Regions
From Understanding of the Past to Modelling of the Future
Salzburg, Austria, 28 August – 1 September 2011